

DOCTORAL THESIS

Modelling and Simulation of Autonomous Vehicles and Systems and Their Advanced Control Methods

Andrus Pedai

TALLINN UNIVERSITY OF TECHNOLOGY
DOCTORAL THESIS
9/2021

Modelling and Simulation of Autonomous Vehicles and Systems and Their Advanced Control Methods

ANDRUS PEDAI



TALLINN UNIVERSITY OF TECHNOLOGY

School of Engineering

Department of Mechanical and Industrial Engineering

This dissertation was accepted for the defence of the degree 25/11/2020

Supervisor:

Professor Dr. Raivo Sell
Department of Mechanical and Industrial Engineering
Tallinn University of Technology
Tallinn, Estonia

Co-supervisors:

Senior Research Scientist, Dr. Andres Udal
Department of Software Science
Tallinn University of Technology
Tallinn, Estonia

Dr. Igor Astrov
Autonomous systems independent expert

Opponents:

Dr. Libor Přeučil
Head, Intelligent and Mobile Robotic Group
Czech Technical University (CTU)
Prague, Czech Republic

Professor Dr. Timo Seppälä
School of Science
Department of Industrial Engineering and Management
Aalto University
Espoo, Finland

Associate Professor Dr. Kuldar Taveter
Faculty of Science and Technology
Institute of Computer Science
Tartu University
Tartu, Estonia

Defence of the thesis: 02/02/2021, Tallinn

Declaration:

Hereby I declare that this doctoral thesis, my original investigation and achievement, submitted for the doctoral degree at Tallinn University of Technology has not been submitted for doctoral or equivalent academic degree.

Andrus Pedai

signature

Copyright: Andrus Pedai, 2021

ISSN 2585-6898 (publication)

ISBN 978-9949-83-641-3 (publication)

ISSN 2585-6901 (PDF)

ISBN 978-9949-83-642-0 (PDF)

Printed by Auratrükk

TALLINNA TEHNIKAÜLIKOO
DOKTORITÖÖ
9/2021

Autonoomsete sõidukite ja süsteemide ning nende täiustatud juhtimismetoodikate modelleerimine ja simuleerimine

ANDRUS PEDAI



Contents

List of Publications	6
Author's contribution to the publications	7
Introduction	8
Abbreviations	10
1. Problem formulation and research questions	11
1.1 Background	11
1.2 Problem formulation.....	14
1.3 Objectives and research questions	15
1.4 Research process and organization of the thesis.....	16
2. Literature review.....	18
2.1 Levels of autonomy.....	18
2.2 Design and development of autonomous systems.....	20
2.3 State-space representation.....	21
2.4 Linear control task	22
2.5 Non-linear control task	23
2.6 Advanced control techniques	23
2.7 Multi-rate control	26
2.8 Research overview. Development of control systems for UAV's.....	27
3. Results of the research	30
3.1 Multi-rate decomposition	30
3.2 Range of autonomous vehicles and systems considered in the research	35
3.3 Flight control of a four rotor UAV	35
3.4 Three-rate neural control of UAV with ducted fan and two coaxial rotors	42
3.5 Comparison of single-rate and two-rate neural control approaches	47
3.6 Single-rate versus three-rate neural assisted control.....	50
3.7 Comparison of neural and basic tracking control for ASV	54
3.8 Flight control of small size multirotor UAV	59
3.9 Summary of different objects and control systems studied	69
4. Conclusions and further research	75
4.1 Conclusions	75
4.2 Extensions of methodology to other application fields	76
4.3 Further research	80
References	81
Acknowledgements.....	87
Abstract.....	88
Lühikokkuvõte.....	89
Appendices I-VI	91
Curriculum vitae.....	142
Elulookirjeldus.....	143

List of Publications

Main contributing publications. Thesis is based on the research work reported in the following publications.

- I. I. Astrov and A. Pedai (2011). Situational awareness based flight control of a drone. Proc. 2011 IEEE International Systems Conference (SysCon 2011, Montreal, Quebec, Canada, April 4-7, 2011), IEEE, pp. 574-578.
- II. I. Astrov and A. Pedai (2012). Three-rate neural control of TUAV with coaxial rotor and ducted fan configuration for enhanced situational awareness. Proc. 2012 International Conference on Control, Automation and Information Sciences (ICCAIS 2012, Ho Chi Minh City, Vietnam, November 26-29, 2012), IEEE, pp. 78-83.
- III. Pedai, Andrus; Astrov, Igor; Udal, Andres (2018). Comparison of single-rate and two-rate neural control approaches for coaxial rotor/ducted-fan TUAV for situational awareness applications. SISY 2018: IEEE 16th International Symposium on Intelligent Systems and Informatics, Proceedings, Subotica, Serbia, September 13-15, 2018.
- IV. Pedai, Andrus; Astrov, Igor; Udal, Andres; Sell, Raivo (2019). Single-rate versus three-rate neural assisted control approaches for coaxial rotor ducted fan TUAV for situation awareness applications. SysCon 2019: The 13th Annual IEEE International Systems Conference, April 8-11, 2019, Orlando, Florida, USA
- V. Astrov, I.; Udal, A.; Pedai, A.; Sell, R. (2019). Simulink/MATLAB based comparison of neural and basic tracking control for an autonomous surface vessel for situation awareness applications. CINTI-MACRo 2019 Proceedings: IEEE Joint 19th International Symposium on Computational Intelligence and Informatics and 7th IEEE International Conference on Recent Achievements in Mechatronics, Automation, Computer Sciences and Robotics (CINTI-MACRo 2019, Szeged, Hungary, November 14-16, 2019). IEEE, 105-110.
- VI. I. Astrov, A. Pedai (2010). Flight control of a trirotor mini-UAV for enhanced situational awareness. Volume [2010-376X] of Proceedings of World Acad. Science, Engineering and Technology (Extended papers of Int. Conf. on Aeronautical and Astronautical Engineering ICAAE 2010, Amsterdam, Netherlands), volume 70, pp. 271-277, 2010 (referenced in Scopus, www.etis.ee classification 1.1 paper).

Publications copies are enclosed in the appendix.

Author's contribution to the publications

The contribution to the papers in this thesis are:

- I. Author proposed the initial idea, developed the methodology, ran the modelling experiments, analysed the results, discussed them, made the conclusions and provided oral presentation at the IEEE SYSCON conference in Montreal, Canada.
- II. Author proposed the set of experiments with different modifications to the previously developed control systems. Author supervised the modelling experiments, helped in analysis the results and preparing the paper.
- III. Author proposed the motion control methodology for controlling coaxial rotor/ducted-fan UAV. Author carried out the experiments with selected model, helped preparing and finalizing the publication.
- IV. Author proposed the initial idea, developed the comparison methodology, ran the modelling experiments, analysed the results, discussed them, made the conclusions and provided oral presentation at the IEEE SYSCON conference in Orlando, USA.
- V. Author designed and constructed control systems and proposed approach for comparison in MATLAB/Simulink environment. Planned and conducted the modelling task.
- VI. Author developed methodology for experimentally validating theoretical model of trirotor mini-UAV. Developed experimental setup for MATLAB modelling, planned and finalized the modelling.

Introduction

Modelling and simulation of autonomous vehicles through advanced control methods.

This publications-based thesis concentrates to the summary of the recent (2018–2019) and earlier (2000–2014) research publications by the Author in the field of modelling and simulation of Control Systems for various types of Autonomous Vehicles (AVs) and smart industry systems.

Author, who’s main occupation field has been in engineering and business development, working with global technology companies (e.g. Nokia, EADS, Inmarsat, Volvo Group), has published numerous scientific publications on:

- Unmanned Vehicle Control Systems (Aerial, Surface and Underwater Vehicles).
- Smart industry, Innovation and Artificial Intelligence.

Out of the broad research scope, advanced methodology for Multi-Rate Control has been developed and applied by Author in research papers and in different AV modelling examples described in the thesis.

The main objectives of the research work will be summarized in following:

1. Development of methodology for multi-rate control via construction of target system mathematical multi-input/multi-output models and integrating them within the MATLAB/Simulink environment;
2. Testing the constructed modelling and simulation approaches, design of optimal control systems with aim of hovering flight at different heights with overshooting value of $\sigma \approx 5\%$ for nonlinear models in the case of different types of autonomous systems, e.g. from miniature one rotor helicopters to eight-rotor unmanned aerial vehicles (UAVs);
3. Introduction of several advanced approaches like parallel operation methodology and different types of neural network blocks used in the proposed multi-rate control.

The present publications-based dissertation concentrates the summary of the selected 6 main research papers. Summary of the full scope of Author’s scientific publications and research fields is described in Table 1.

Table 1 – Number of Publications by author (left) and list of the target Applications (right) based on Estonian Science Database [www.etis.ee]

Year	Number of publications	Application	Number of publications
2000	3	3 rotor UAV	1
2001	1	4 rotor UAV	6
2004	8	8 rotor UAV	4
2008	6	Coaxial rotor UAV	6
2009	6	Helicopter	4
2010	12	Experimental Airplane	8
2011	8	Fighter Airplane	2
2012	4	Missile	2
2014	4	Underwater AUV	10
2018	1	Surface ASV	1
2019	2	Supply Chain for manufacturing	3

However, in order to maintain the coherent approach, it was decided to focus in present thesis mainly only on the theme of development of smart control systems for the selected unmanned systems, thus leaving aside the other listed fields including wider philosophical discussion of the artificial intelligence problems treated in several recent publications by the Author. Exception is the multi-rate approach methodology for the control systems studied by the Author since year 2000 (when it became also hot topics in the world) and that was included as an important advanced feature in most of presented UAV simulation examples of the present thesis.

In this work Author is presenting procedures and techniques, which allows the control system designer or developer to formulate the control synthesis task to meet the requirements of selected target system.

The high level of presented work is confirmed by the positive feedback from several international conferences and by the best paper award presented in 2010 to the autonomous underwater vehicle modeling paper [International Conference on Computational Intelligence, Man-Machine Systems and Cybernetics (CIMMACS'10, Merida, Venezuela, December 14-16, 2010).

Abbreviations

AV	Autonomous Vehicle
ADALINE	Adaptive Linear Neuron, single-layer artificial neural network
AI	Artificial Intelligence
ANFIS	Adaptive Neuro Fuzzy
AS	Autonomous System
ASV	Autonomous Surface Vehicle
AUV	Autonomous Underwater Vehicle
CPS	Cyber-Physical System
DARPA	Defense Advanced Research Projects Agency
DoD	Department of Defense (US)
DOF	Degrees Of Freedom (of mechanical systems)
DSCM	Demand and Supply Chain Management
ICAO	International Civil Aviation Organization
KPI	Key Performance Indicator
LQE	Linear Quadratic Estimator
LQG	Linear Quadratic Gaussian control
LQR	Linear Quadratic Regulator
MBD	Model Based Design
NARMA	Nonlinear Autoregressive Moving Average (controller type)
NIST	National Institute of Standards and Technology
NN	Neural Network
OEM	Original Equipment Manufacturer
RCS	Real-time Control System
SA	Situational Awareness
SAE	Society of Automotive Engineers
SCM	Supply Chain Management
SMC	Sliding Mode Controller
SMI	Supplier Managed Inventory
TUAV	Tactical Unmanned Aerial Vehicle
UAS	Unmanned Aerial System
UAV	Unmanned Aerial Vehicle
UCM	User Controller Module
UGV	Unmanned Ground Vehicle
VTOL	Vertical Take-Off and Landing

1. Problem formulation and research questions

1.1 Background

Increased involvement of computers in our daily routines is highly visible. The range for computer usage is wide, from large scale information processing to managing small devices that have been introduced to support our lives. Majority of the computer usage remains well hidden in the cloud and background, supporting the embedded systems that command different interactions with physical systems. Proper control system is required to perform faultless control for the target physical system.

The design of an advanced control system for autonomous vehicles (AV) is technically challenging and an expensive task for which multiple engineering disciplines (e.g. computer science, control theory, mechanical and electrical engineering) have to align their skills and resources in order to achieve reliable system design. In this challenging field, there is strong focus on the model-based design approach [1]. It can be extended to autonomous vehicle control systems and subsystems, that provide model re-usability and possibility to replace costly live testing with simulations.

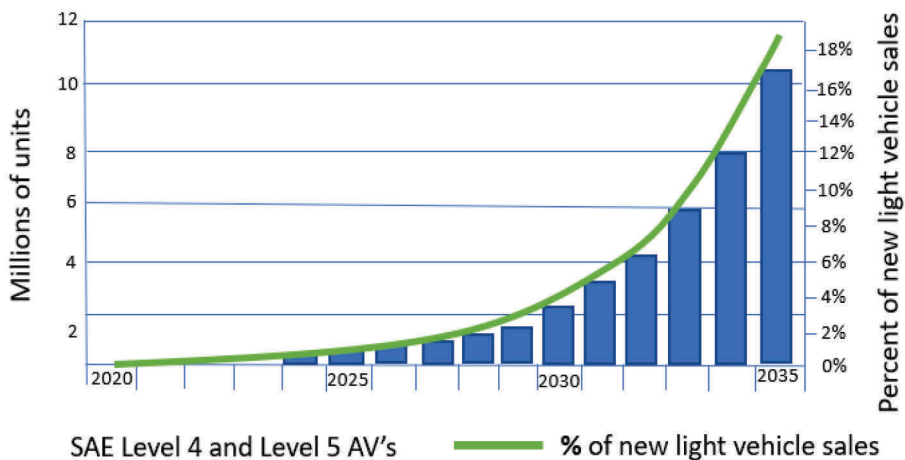


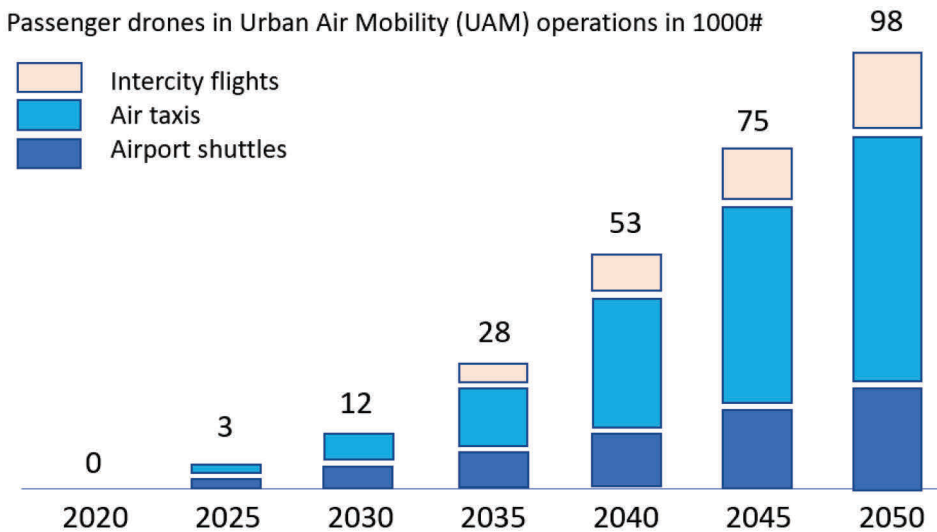
Figure 1 – Market estimate for the Autonomous Vehicle sales in units (data from [2]). With the emergence of advanced technology, AV companies are expected to grow investments in autonomous solutions. Supported by customer expectations, automation is shifting towards more comfortable and secure transportation.

New AV's and autonomous systems AS's will be equipped with advanced control systems that will enable high situational awareness and faultlessly performed trajectory path management.

Deployment of AV's and AS's has seen exponential increase in both civil and military applications since the early 2000's, the growth is only at the early stages, as illustrated on Figures 1 and 2. Depending on the operating environment, author identifies following types of AV's:

- UGV Unmanned Ground Vehicle
- USV Unmanned Surface Vehicle
- UUV Unmanned Underwater Vehicle
- UAV Unmanned Aerial Vehicle
- TUAV Tactical Unmanned Aerial Vehicle

AV's offer more options and flexibility to access hazardous environments, work at small scales, or react at speeds and scales beyond human capability. With proper design of bounded autonomous capabilities, UAV's can reduce the high cognitive load often placed on operators/supervisors. Increased autonomy can enable humans to delegate those tasks that are more effectively done by computer, including synchronizing activities between multiple unmanned systems, software agents – thus freeing humans to focus on the higher-level objectives.



Estimating that approx. 100 cities will have UAM operations by 2050

Figure 2 – Market estimate for the passenger drones (data from [3]). Market growth is driven by factors such as growing urban population coupled with rising traffic volumes, autonomous technology advancements and decline in manufacturing costs. Increasing number of participating companies is also driving the market growth.

Autonomous systems are capable of understanding intent and direction. They can decide specific course of action from multiple alternatives, without depending on human control. Although overall activity for autonomous systems can be predictable, its individual actions may not be. The system is always a composite entity [4]. In current thesis Author limits the system boundaries by the flight- or centralised control systems for the AV's.

It is also important to note that battery technology is continuously improving. By meeting necessary regulations, air taxis, ambulances, services will be safely enabled. That is supported by improvements in machine learning that has enabled dramatic cost reductions in automatic flight, as illustrated on Figure 3.

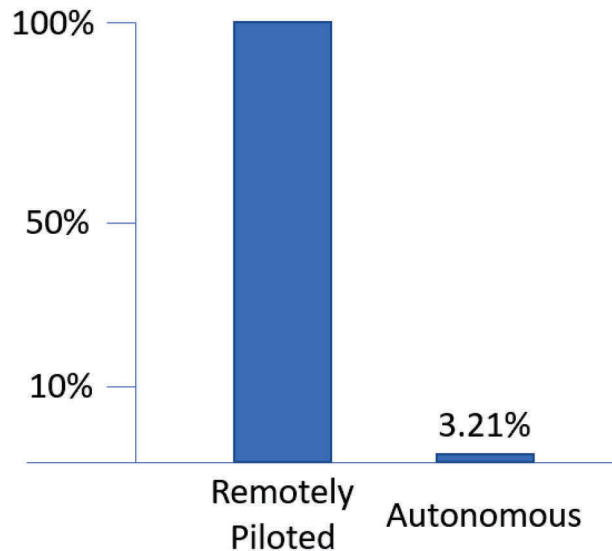


Figure 3 – Estimated cost for autonomous air taxi service (data from [5]). Growing need for cheaper, faster and cleaner transport is supporting the investments in AV technology. Advanced technologies that reduce emissions, offer higher energy efficiency and improved safety play a key role in the passenger drone market growth.

Note that prices indicated on Figure 3 are estimates for the future when each technology reaches scale. We could estimate commercialized drone deliveries in the next 5–10 years, although it depends on available technology and regulatory approvals [5].

Autonomous flight is a challenging but important task for UAV's to secure a high level of autonomy under adverse conditions. The fundamental requirement for autonomous flight is the knowledge of the height above the ground, and a properly designed controller to govern the process.

The characteristics of an UAV motion depend on the mode of manoeuvring, forward speed, and outside appendages such as measuring instruments. In addition, the small UAV's are sensitive to many factors during the flight, such as mechanical vibration caused by engines, unexpected roll, yaw, and pitch due to atmospheric turbulence. Due to these reasons, the appropriate controllers are needed to control UAV motions. Some controllers, such as NARMA-L2 controllers, adaptive neural network controllers, neural network predictive controllers, LQG controllers, and model reference hybrid controllers have been successfully implemented by my simulation experiments.

In order to improve the quality for the autonomous systems control process, current thesis focuses on the design and modelling of the control systems that are required to operate different types of autonomous vehicles: UAV, UAS and other AS.

1.2 Problem formulation

Since early 2000's the development of control systems that support AV's has been in the focus of extensive research. This drive is supported by the growing number of applications where AV's outperform traditional 'human operated' systems and devices.

Concerning UAV's, high number of control approaches has been proposed for movement control and trajectory planning. According to [6] traditional methods include:

1. Kinematic model of the vehicle. Applied for control at relatively lower speeds.
 - PID control;
 - Feedback linearization;
 - Model predictive control

In principle these linear control systems are using negative feedback to produce a control signal to maintain the controlled process variable at the desired setpoint.

2. Full dynamic model of the vehicle. Needed while operating at higher speeds.
 - Nonlinear control;
 - Model predictive control;
 - Feedback-feedforward control

Nonlinear control covers wider class of systems that do not follow the superposition principle of linear control. It applies to real world systems, the control systems are nonlinear and they are governed by nonlinear differential equations.

During the long-term work with control systems for various types of AV's, Author has noticed that traditional methods of movement and trajectory control provided simulation results that are 'good enough' but clearly leaving room for further improvements. In current thesis Author is focusing on several advanced options to improve the control system performance and receive improved parameters for the AV's control and motion planning compared to the traditional control approaches.

AV's control systems are often described by set of complex equations, requesting computing power that could be limited to support Real-time Control System (RCS) e.g. due to the rapid speed of AV's manoeuvring. Novel decomposition approach has been proposed by Author to break down the initial high-order control system to leaner multi-rate control approach.

In order to improve the process behaviour for the AV's control and motion planning, several advanced options are proposed by Author and discussed in current thesis:

- Multi-rate control;
- Multi-rate Neural assisted control;
- Single rate vs Multi-rate comparisons.

Concerning the high development cost related to AV's control and motion planning, Author has been focusing in re-usability for proposed methods and AV control approaches. Proposed solutions for centralised controller decomposition and re-usability of multi-rate control approaches will enable faster development time and reduced cost for the introduction of upcoming AV platforms.

1.3 Objectives and research questions

Current thesis is targeting to develop and test advanced control systems for AV's propulsion and motion control. Developed control systems and -approaches are tested in MATLAB/Simulink environment, providing confirmation for the possible real-life adaptation and re-usability. Specific planning to reach this target is including following:

- To research required control task for AV's trajectory and motion;
- To research required control task for AS's key performance indicators (KPI's);
- To propose and test re-usable methods for advanced control systems development.

The dissertation is targeting to provide researchers, control system developers and manufacturers, design and test methodology, including proposed approaches for advanced control system development in fast and cost controlled way. Proposed approaches can be utilized not only for AV's motion trajectory control. Variety of time critical environments can be considered. Specific examples are provided for the supply chain management in the electronics manufacturing industry.

Following research questions (RQ's) are answered in this work:

RQ1: How to develop flight control for the autonomous vertical flight for a nontrivial nonlinear model of the tactical unmanned aerial vehicle?

RQ2: How to make multi-rate decomposition of the control system and replace initial control system with three-rate neural control for the coaxial rotor and ducted fan UAV?

RQ3: How to perform control system decomposition and quantitative comparison of the UAV's initial control system with proposed two-rate neural control approach?

RQ4: How to compare UAV's initial control system with specifically designed three-rate neural control approach?

RQ5: Provide evidence on the advantages of NN supported trajectory control over the basic trajectory control for the ASV.

RQ6 How to develop flight control system for the small multi-rotor UAVs that are sensitive to many factors during the flight, such as mechanical vibration caused by engines, unexpected roll, yaw, and pitch due to atmospheric turbulence?

RQ7: Explore the alternative fields of implementation for the proposed advanced and multi-rate control.

The research questions are answered in the 6 contributing publications to current Thesis:

Publication 1 is a study that is focusing on the RQ1. In this publication the research technique is proposed using control system modelling and simulation based on equations of motion for the centre of mass of TUAV drone for fast SA.

Publication 2 is a study that is focusing on the RQ2. In this publication three-rate decomposition is performed for the initial high-order control system for the TUAV. Successful implementation for the new advanced control system is verified in the Matlab/Simulink environment.

Publication 3 is a study that is focusing on the RQ3. Decomposition for the TUAV's initial high-order control system into two-rate neural control and specific comparison for the take-off and hovering characteristics for both control systems.

Publication 4 is the study that is focusing on the RQ4. Decomposition for initial high-order control system for coaxial unmanned helicopter with ducted fan configuration into three-rate neural control. Specific comparison is performed for the UAV's take-off and hovering characteristics with both control systems.

Publication 5 is the study that is focusing on the RQ5. Development of methodology of model-based modelling and simulation of cyber-physical nonlinear system of ASV in Simulink/MATLAB environment. The comparison between predictive NN control and basic tracking feedback control is been presented for two specific manoeuvres.

Publication 6 is the study that is focusing on the RQ6. Flight controller is designed for the small trirotor UAV that is sensitive to mechanical vibration caused by engines, unexpected roll, yaw, and pitch due to atmospheric turbulence.

Chapter 4 will provide response to RQ7. Alternative field of implementation is discussed and presented for the proposed control approaches. Further implementation alternatives are described under 'Extensions of methodology to other application fields.'

1.4 Research process and organization of the thesis

Framework for the current thesis combines selected results from the long-term research. Introduction to the background of AV's motion control task is followed by the results from research experiments and development concepts. These are supported by the literature review and specific references.

Framework for the research was created through an extensive development task, starting with defining the multi-rate control and proceeding with advanced control systems development for various types of AV's.

The results of the dissertation have been presented at several international conferences and journals. The main platforms for publishing were the IEEE International Systems Conference (by IEEE Systems Council), International Conference on Control, Automation and Information Sciences (by International Information and Engineering Association) and IEEE International Conference on Recent Achievements in Mechatronics, Automation, Computer Sciences and Robotics (by IEEE Robotics and Automation Society).

Figure 4 illustrates the structure of the chapters in the dissertation.

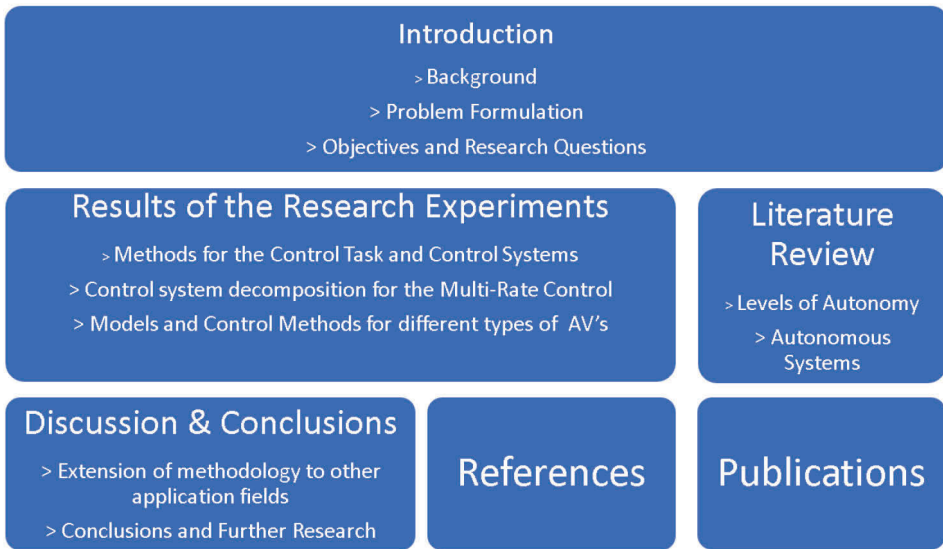


Figure 4 – Explaining the framework of the dissertation

2. Literature review

2.1 Levels of autonomy

Reason for creating levels of autonomy is originated by military requirements. It was important to track the progress of defence technology programmers and determine whether targets for increased autonomy had been met [7]. In the literature we can find four distinct ways to explain the levels of autonomy:

1. Categorical linear scales (e.g. Sheradin, Clough, NIAG [7]).
Autonomous Systems, by NATO Industrial Advisory Group.
 - Level 1: Remotely controlled system (non-autonomous);
 - Level 2: Automated system (pre-programmed system);
 - Level 3: Autonomous non-learning system;
 - Level 4: Autonomous learning system.
2. Multidimensional scales (e.g. Parasurman, Proud, Clough[8]).
Autonomous Systems, by NASA Johnson Space Centre.
 - Level 1 Human alone can execute decision;
 - Level 2 Human is the prime executor, supported by computer for contingencies;
 - Level 3 Computer is the prime executor, supported by human for contingencies;
 - Level 4 Computer allows human to veto its execution, during pre-programmed time;
 - Level 5 Computer allows context-dependent veto by human before the execution;
 - Level 6 Automatic execution by computer, informs the human. Human has over-ride ability after execution;
 - Level 7 Computer executes automatically and informs human only if required by context. Human over-ride possible;
 - Level 8 Computer executes decisions automatically and does not allow any human interaction.
3. Contextual scales, by NIST, DoD.
Autonomous Systems are defined by their ability to achieve mission goals. The more complex the goal is, the higher is its level of autonomy.
4. Levels of Autonomy in Automotive industry, by SAE.
Although Automated Driving is not directly addressed in current thesis, the levels of Driving Automation provide good comparison for autonomy in road vehicles and autonomous systems.

Society of Automotive Engineers (SAE) has launched the standard J3016 “Levels of Driving Automation” [9] SAE is defining J3016 as living document, that continues to evolve gradually as the industry and technical standard J3016 itself evolves.

SEA J3016 defines level of driving automation in following 6 levels:

- Level 0 Human is driving and constantly supervising. Features provide warnings and momentary assistance;
- Level 1 Human is driving and constantly supervising. Features provide steering OR brake/acceleration assistance;
- Level 2 Human is driving and constantly supervising. Features provide steering AND brake/acceleration support;
- Level 3 Human is not driving when automated driving features are engaged. When feature requires, human must drive;
- Level 4 Human is not driving when automated driving features are engaged. Features will not require human to take over driving;
- Level 5 Human is not driving when automated driving features are engaged. Feature can drive the vehicle in all conditions.

Autonomous Systems. Civilian and Military Implications.

Recent and upcoming progress in the field of civilian Autonomous Vehicle technology will have strong impact to the future of military operations.

Research and development in AV technology can be seen in 3 stages [4]:

- Stage 1, from 1980 to 2003, mostly university research, focused on:
 - o Automated highways were ‘passive’ vehicles rely on the advanced highway infrastructure;
 - o AV for off-road driving.
- Stage 2, from 2003 to 2007, DARPA [10] and its “Grand Challenges” provided strong leaps forward in AV technology. The initial DARPA Grand Challenge was created to spur the development of technologies needed to create the first fully autonomous ground vehicles capable of completing a substantial off-road course within a limited time.
- Stage 3. Recent private company advancements in AV technology. Development is driven by global technology companies e.g. Google (facilitating sharing, increase the car utilization), major automotive OEM’s and Universities (e.g. TalTech’s ISEAUTO project).

2.2 Design and development of autonomous systems

In the report of the High-Level Group on Aviation Research “Flightpath 2050 Europe’s Vision for Aviation” [11] objective is set for seamless operation of the European air transport system through interoperable and networked systems that are allowing manned and unmanned aerial vehicles to safely operate in the same airspace. Important target is to develop advances for unmanned systems in a way that is efficiently considering the total cost of development task. The design of unmanned aerial systems can follow structured approach were autonomous capabilities of the vehicle are based on the previously defined models, simulated scenarios and on real-time calculations.

Modelling and Simulation provides powerful toolset in the industry for systems design and evaluation, also prototyping. It is proposed [12] that integration of modelling and simulation to the product development lifecycle will support the total cost reduction targets while extending UAV’s role to the management of autonomous capabilities of the vehicle that is based on the previously simulated scenario and on real-time calculation, to adopt the behaviour of the vehicle on the real operational scenario. In addition, the well performing models and simulation results are essential since the actual UV’s will perform their missions in critical and potentially violent environments e.g. military operations, nuclear facilities.

Adding Neural Networks (NN) to the AV control systems.

Recent developments in hardware and software have reduced the cost to train neural networks by 100x in about 2 years [5]. That is resulting extended artificial intelligence (AI) capabilities as specific models are trained with 10x increased computing power each year, as illustrated on Figure 5.

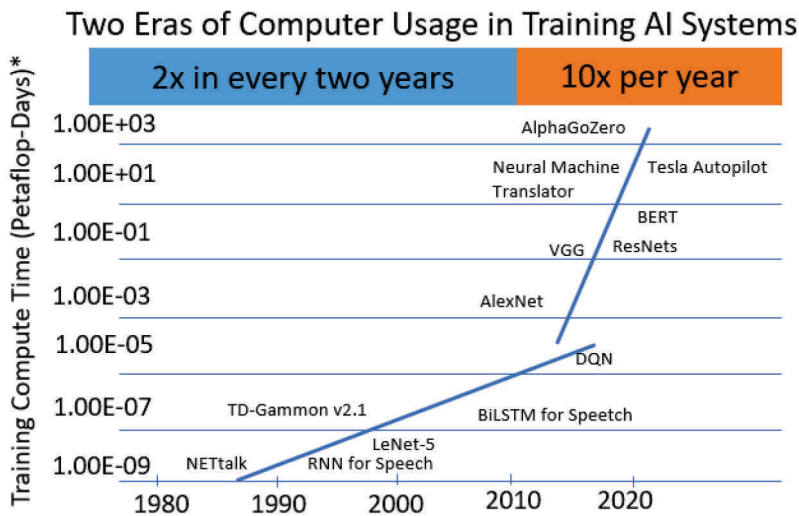


Figure 5 – Increase in available computing power for AI trained NN (data from [12]). A “Petaflop-Day” refers to performing a quadrillion operations per second for a day.

2.3 State-space representation

In control engineering, a state-space representation [13] is a mathematical model of a physical system as a set of input, output and state variables related by first-order differential equations or difference equations.

- State variables are variables whose values evolve through time in a way that depends on the values they have at any given time and also depends on the externally imposed values of input variables;
- Output variables' values depend on the values of the state variables;
- The "state space" is the Euclidean space in which the variables on the axes are the state variables.

The state of the system can be represented as a vector within that space.

- The internal state variables are the smallest possible subset of system variables that can represent the entire state of the system at any given time [14];
- The minimum number of state variables required to represent a given system, is usually equal to the order of the system's defining differential equation, but not necessarily;
- If the system is represented in transfer function form, the minimum number of state variables is equal to the order of the transfer function's denominator after it has been reduced to a proper fraction.

It is important to understand that converting a state-space realization to a transfer function form may lose some internal information about the system and may provide a description of a system which is stable, when the state-space realization is unstable at certain points.

In electric circuits, the number of state variables is often, though not always, the same as the number of energy storage elements in the circuit such as capacitors and inductors. The state variables defined must be linearly independent, i.e., no state variable can be written as a linear combination of the other state variables or the system will not be able to be solved.

A state-space representation for linear time-invariant system has the following general form [15]:

$$\frac{dX_n}{dt} = A_{n \times n} \times X_n + B_{n \times p} \times U_p \quad , \quad (1)$$

$$Y_q = C_{q \times n} \times X_n + D_{q \times p} \times U_p$$

where:

X_n is the state vector of dimension n ,

$A_{n \times n}$ is the system (dynamics) matrix of dimension $n \times n$,

$B_{n \times p}$ is the control matrix of dimension $n \times p$,

U_p is the control vector of dimension p ,

Y_q is the output vector of dimension q ,

$C_{q \times n}$ is the output matrix of dimension $q \times n$,

$D_{q \times p}$ is the feed-forward matrix of dimension $q \times p$.

Note that for every fixed moment of time the system remains linear.

The state-space representation is described in [16]:

$$\begin{aligned}\dot{x}(t) &= Ax(t) + Bu(t) , \\ y(t) &= Cx(t) + Du(t) , \\ x(t_0) &= x_0 .\end{aligned}\tag{2}$$

In which $\dot{x}(t)$ is the n -dimensional state vector:

$$x(t) = \begin{pmatrix} x_1(t) \\ x_2(t) \\ \vdots \\ x_n(t) \end{pmatrix}\tag{3}$$

where n scalar components are called state variables. The same way m -dimensional input vector and p -dimensional output vectors are given:

$$u(t) = \begin{pmatrix} u_1(t) \\ u_2(t) \\ \vdots \\ u_m(t) \end{pmatrix}, \quad y(t) = \begin{pmatrix} y_1(t) \\ y_2(t) \\ \vdots \\ y_p(t) \end{pmatrix}.\tag{4}$$

Differentiation with respect to time of a time-varying vector quantity is performed on component level, the time-derivative on the left-hand side of equation (2) is representing

$$\dot{x}(t) = \begin{pmatrix} \dot{x}_1(t) \\ \dot{x}_2(t) \\ \vdots \\ \dot{x}_n(t) \end{pmatrix}.\tag{5}$$

For a specified initial time t_0 , the initial state $x(t_0) = x_0$ is a specified, constant, n -dimensional vector.

2.4 Linear control task

Linear control systems [17] are based on linear differential equations. Typical linear control systems provide accurate system models over wide range of applications but there are limits:

- The principle of superposition is applicable to the system. The response to several inputs can be obtained by considering one input at a time and then algebraically adding the individual results;
- Linear differential equation is describing the system, having its coefficients as constants;
- In practice the control output varies linearly with the input.

Most of the real-life systems have non-linear behaviour, the systems are inherently nonlinear. Linear relationships can be obtained by restricting system variables to sufficiently small deviations. Linear model is obtained in the neighbourhood of each operating point and linear control is used along with gain scheduling [18]. There is great practical value in implementing linear models since often control systems are designed to maintain narrow control range e.g. autopilot control systems for aircraft, spacecrafts.

Other examples include missile control, process control. Linearized models in most cases provide good first approximation for the behaviour of the actual process. Simulation and modelling for AV's motion control often involves random parameters in input, state and output parameters. In these cases, stochastic systems are defined in order to manage prediction, stochastic control, modelling and estimation of systems dynamics and simultaneous performance of all these tasks [19].

2.5 Non-linear control task

While the properties of linear systems provide powerful design and analysis tools, the behaviour of nonlinear system enables to consider also natural nonlinear effects that are discontinuous and response from these effects can not be approximated by linear functions [20]. Even a simple one degree of freedom positioning system contains nonlinearity in its model. Nonlinear models describe also motions for more complex AV systems. In order to reach precise positioning for the AV, all nonlinearities have to be taken into consideration during controller design phase [21] Specific attention is needed on the development of control systems that compensate the nonlinearities on the motion of AV's. As stated earlier, linear systems are special cases of nonlinear systems.

Nonlinear control systems have to be tested before applied to target application. During these simulations real systems are replaced by their models.

2.6 Advanced control techniques

In practice controller design for the AV's and AS's often provides results that are satisfactory in one operating regime but unsatisfactory in the other. Concerning AV's, we need hybrid, or advanced controllers that have to be designed. In complex controller structure we can combine different controller types, and secure target control characteristics for the new hybrid controller. Joining neural network and fuzzy logic blocks to the control scheme provides solution to minimize unwanted influence of stochastic noises.

- Fuzzy logic control can be easily combined with traditional controllers to maximize the control for nonlinear processes [22], as shown in Figure 6.

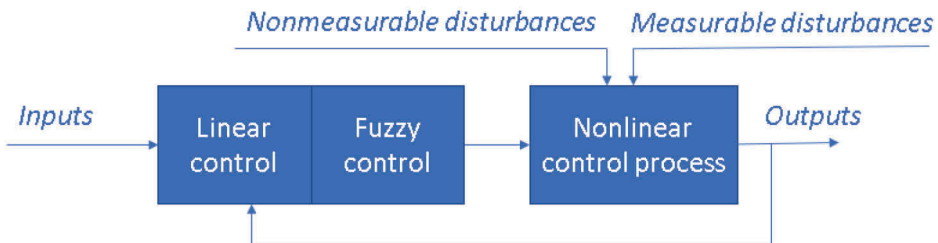


Figure 6 – Hybrid controller with linear + fuzzy control for the nonlinear process control. Fuzzy logic control can be considered as intelligent technique that allows the translation of logic statements to support a nonlinear system behaviour (data from [22]).

- Predictive NN prepares model of the controlled process used to predict the future plant outputs/states based on the past and current outputs/states as well as future control signals. It is attractive to consider predictive control algorithms since they have capability to take into account the process and technological

constraints imposed on input, output or state variables [23]. The first phase in model predictive control is to determine the NN plant model. In second phase the plant model is used by the controller to predict future performance, Figures 7a and 7b. Model predictive control starts with training NN to represent the forward dynamics of the plant. Prediction error between the plant output Y_p and the NN output Y_m is used as the NN training signal, presented in Figure 7a. u is the control signal.

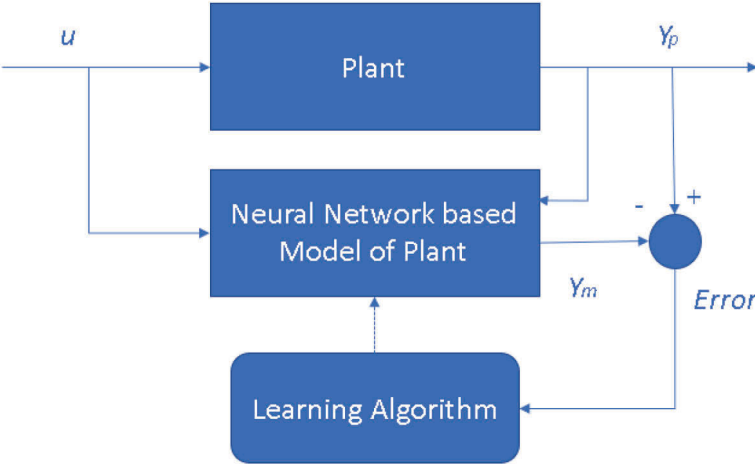


Figure 7a – Model predictive NN control. Description of training of NN based model of plant (data from [23]).

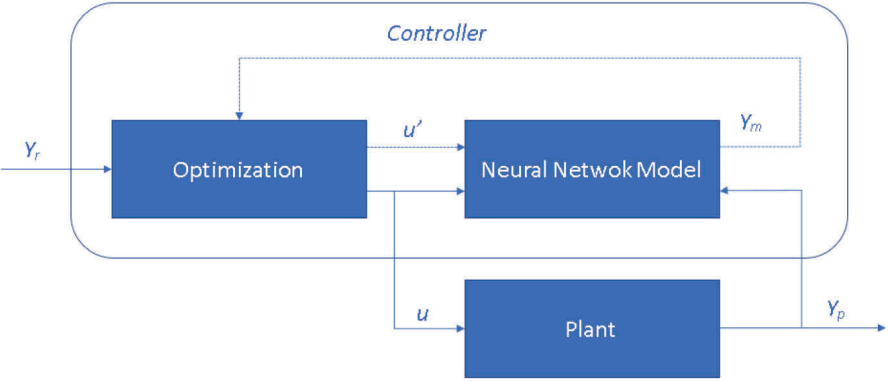


Figure 7b – Model predictive control process. The controller consists of the NN plant model and the optimization block. The optimization block determines the values of u' and then the optimal u is input to the plant. The u' variable is the tentative control signal, Y_r is the desired response, and Y_m is the network model response. The p value determines the contribution that the sum of the squares of the control increments has on the performance index [data from 23].

- Adaptive Linear Element, single-layer artificial neural network (ADALINE NN). The adaptive filter is based on the Adaline NN that is similar to the perceptron but having transfer function that is linear rather than hard-limiting. This allows ADALINE output to have any value, whereas the perceptron output is limited to either 0 or 1. ADALINE enables design of adaptive linear system that responds to the changes in its environment as it is operating [24]. Adaptive filtering used for noise cancellation is one of the major application areas for ADALIN. Specific studies confirm that ADALINE is performing better in noise cancellations than comparable techniques [25].

Figure 8 provides example for engine noise cancellation in airplane pilots microphone [26].

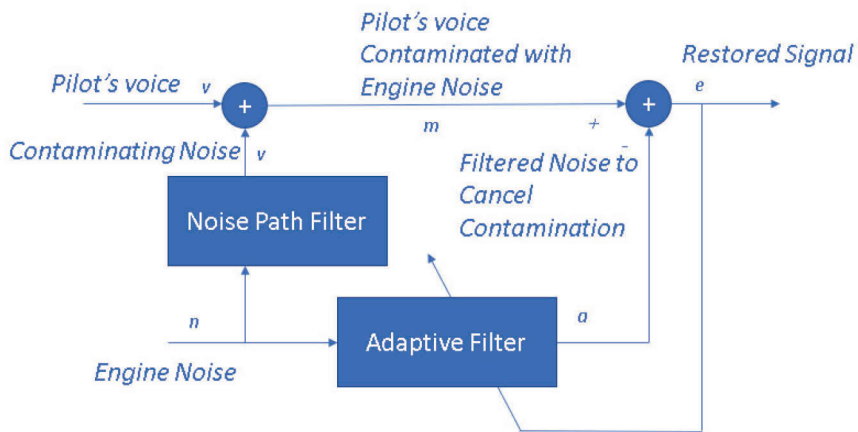


Figure 8 – Adaptive filter to remove engine noise from the contaminated signal, leaving the pilots voice as the “Error” [data from 24]. Neural linear network is adaptively trained to predict the combined pilot/engine signal m from an engine signal n . The engine signal n does not tell the adaptive network anything about the pilot's voice signal contained in m . However, the engine signal n does give the network information it can use to predict the engine's contribution to the pilot/engine signal m (data from [26]).

- Adaptive Neuro Fuzzy (ANFIS) technique provides further improvements for the AV's navigation control in unknown environment. In [27] the control results confirmed the validity of ANFIS approach by creating collision free path for the mobile robot. ANFIS controllers were also successfully used in [28] for the UGV to avoid obstacles safely and reaching target with feasible and smooth online generated path between the initial and target points. However, as discussed in [29] the ANFIS controller used for flight control task demonstrated inferior performance compared with well-tuned PI and Fuzzy controllers.
- Neural controllers can be designed also with Feedback linearization (FL) control or as NARMA-L2. FL provides ways of transforming original system models into equivalent models of simpler form [30]. Key approach with FL enables algebraical transformation of nonlinear system dynamics in to (fully or partly) linear ones, making possible to apply linear control techniques. It is referred to as NARMA-L2 control when the plant model can be approximated by the same form. NARMA-L2 Control block is available in the MATLAB Command toolbox, Figure 9 is illustrating the NARMA-L2 controller working principle.

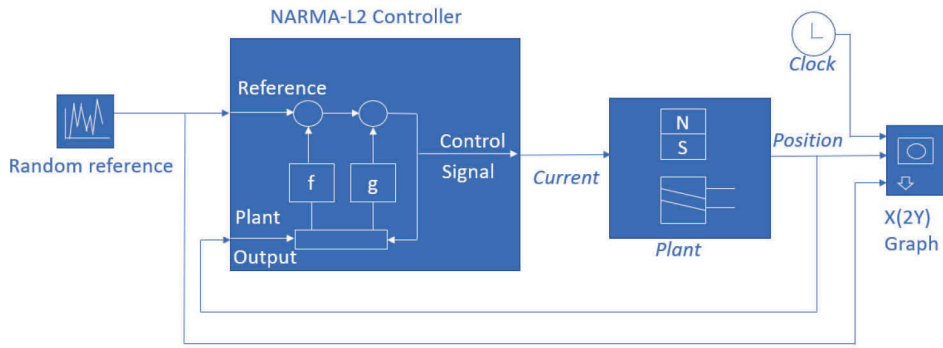


Figure 9 – NARMA 2 controller training in the MATLAB [data from 26]. The central idea of this type of control is to transform nonlinear system dynamics into linear dynamics by cancelling the nonlinearities [30].

2.7 Multi-rate control

Multi-rate control enables time-division treatment for control and sensor signals. In control engineering this has considerable practical advantages since limits in technology restrict controllers to individually treat the inputs and calculated output values. Especially with large multivariable systems having multi-rate controllers will improve the control quality and performance. It is discussed in [31] that multi-rate controllers can achieve simultaneous stabilization, gain margin improvements and distributed control that are impossible for the single-rate controllers.

Multi-rate controller design is explained and supported also in [28] for the fast motion and trajectory control in mechatronic systems. Mechatronics is present in systems with dynamical motion, its an integrated methodology for motion control including the variety of sensors, processors, actuators and machines to control the dynamics and motion.

Figure 10 provides example of Multi-Rate Controller, described in [32].

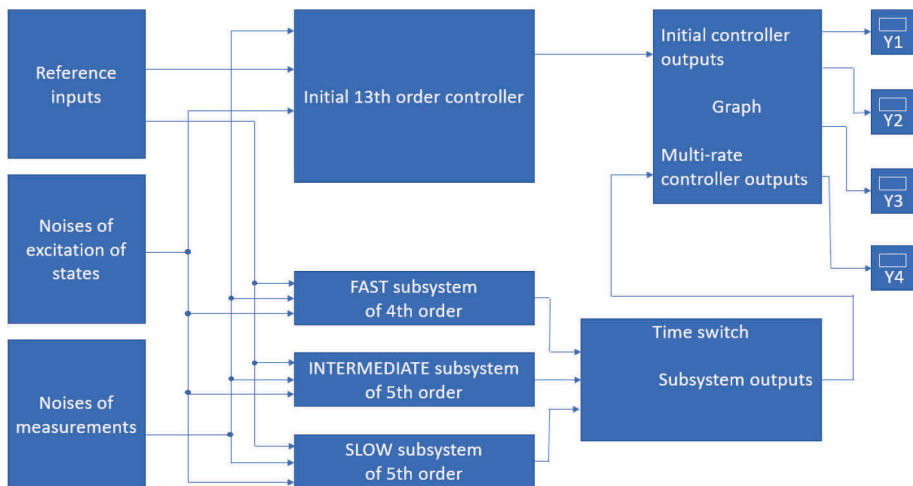


Figure 10 – Example of multi-rate controller implementation. In MATLAB comparison the control performance of initial high order controller is compared to the performance of reduced order multi-rate controller (data from [32]).

2.8 Research overview. Development of control systems for UAV's

Progress behind the development of UAV control systems has been based on the recent advancements in nonlinear control theory. The possibility to transform complex nonlinear systems sequentially to simpler prototypes has introduced new technologies for UAV control. Listed below are selected research approaches that focus on the similar research on control systems development for unmanned systems.

- Nonlinear control of robots and unmanned aerial vehicles, an integrated approach [33]. The ability to transform complex nonlinear systems sequentially to simpler prototypes, which can be controlled by the application of Lyapunov's second method, has led to the development of some novel techniques for controlling both robot manipulators and autonomous vehicles without the need for approximations. Specific methods are described in this research approach for designing nonlinear UAV controllers. Design for UAV's motion control and dynamics is presented thru combination of Lagrangian dynamics, feedback linearization (Figure 11) and Lyapunov based methods.

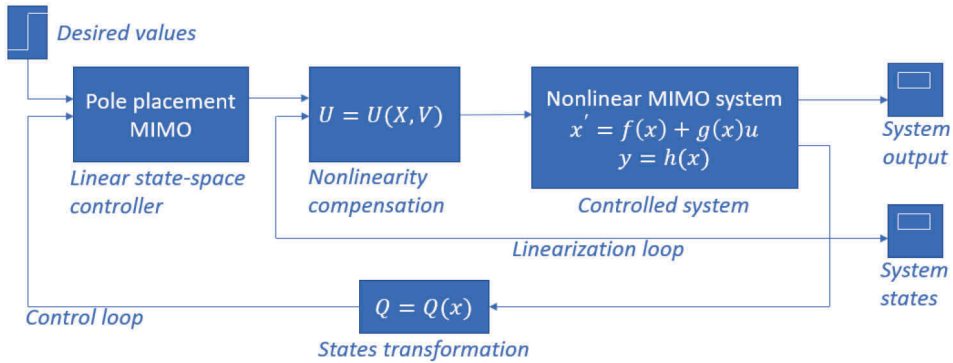


Figure 11 – Feedback linearization (data from [33]). This approach algebraically transforms the nonlinear system dynamics into a fully or partially linearized system so that the feedback control techniques could be applied.

The objective of the feedback linearization is to control nonlinear system:

$$\dot{x} = f(x) + g(x)u , \quad (6)$$

$$y = h(x) \quad (7)$$

by turning it into linear and controllable one, so that it can be described by linear state space equations:

$$\dot{q} = Aq + Bv , \quad (8)$$

$$y = Cq \quad (9)$$

via states transformation $q = q(x)$ and nonlinear state feedback $u = u(x, v)$ where $x = (x_1, x_2, \dots, x_N)^T$ is the states vector of the nonlinear system, $u = (u_1, u_2, \dots, u_P)^T$ and $y = (y_1, y_2, \dots, y_P)^T$ input and output vector of the system, respectively; vector

$q = (q_1, q_2, \dots, q_N)^T$ is the states vector and $v = (v_1, v_2, \dots, v_p)^T$ the input of the linear system resulting from the transformation.

Research described in the main publications attached to current thesis has added feasible approaches to solve the nonlinearization task by successfully introducing approximations to the nonlinear autoregressive moving average. Author also proposes novel multi-rate predictive control method, where controller is using NN model to predict future plant responses to potential control signals. It is shown that the problem of noise reducing without additional filtering can be decided using appropriate design strategies with these NN controllers.

- Unmanned aerial vehicles: breakthroughs in research and practice [34]. The research approach is providing comprehensive study on UAV's linear and nonlinear control algorithms. The mathematical model of a quadrotor UAV is developed. Four control techniques are applied and synthesized: a linear proportional-integral-derivative controller, a Gain Scheduling based PD controller, a nonlinear Sliding Mode Controller (SMC) and a nonlinear Back-stepping controller. Simulation is performed using MATLAB/Simulink environment, results are presented on Figure 12.

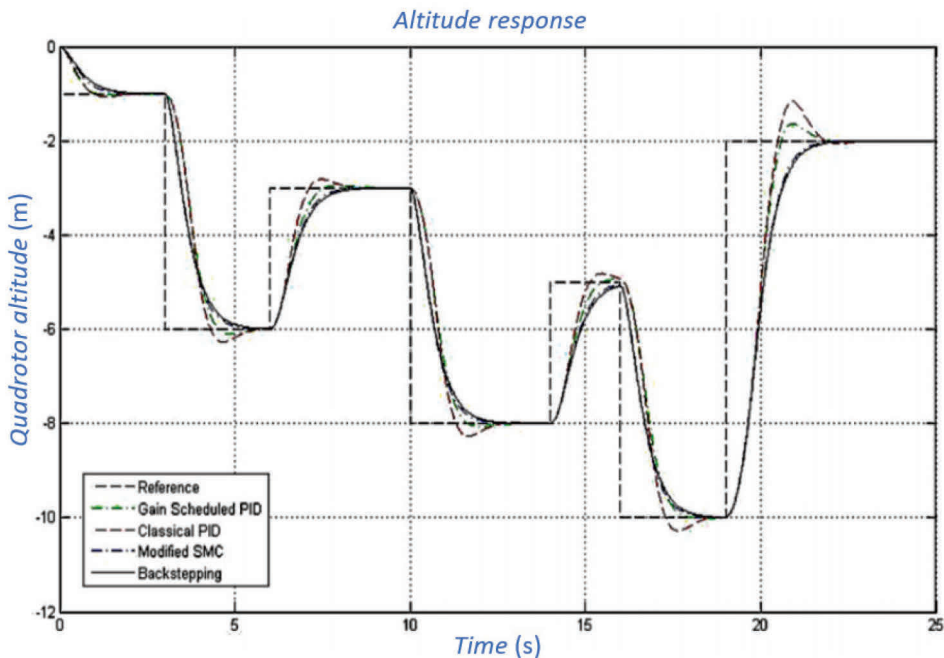


Figure 12 – Comparison of four control technologies response for quadrotor UAV altitude control (data from [34]).

It is shown that choice of the controller depends on the target application. Following approach is proposed for quadrotor:

- Hovering mode, PID controller is sufficient;
- Manoeuvring tasks, SMC or Backstepping controls

Balancing disturbances, PID and Backstepping controllers multi rate control joined with predictive NN control methods that is described in the main

publications attached to current thesis provides further improvements to the trajectory and height control for the quadrotor's control system.

- Model-based design for effective control system development [35]. The book provides close insight to the field of model-based design (MBD). By using a model of control system, simulation and testing can be done earlier compared to the design from scratch approach, where testing and simulations can only be done late in the development phase of the real process. MBD saves the time and cost of possible re-design loops, it also reduces risk of making design errors in the development, therefore significantly bringing down total cost related to development task. During the research work with current thesis, specific control system models were designed that meet the requirements and the final product functions to fit potential customer needs. Author agrees with [35] that by using model-based design options the productivity for development process can be increased by automatically generating production code from the pre-defined models and efficiently managing the control system development by using modelling and simulation tools.

Control systems modelling task that is described in the main publications attached to current thesis was done in the Simulink. Concerning MBD, it is important to note that Simulink provides tools for running simulation-based tests of models, generated code and simulated hardware. There is functionality for back-to back testing, including software in the loop, hardware in the loop and processor in the loop.

After the model has fulfilled its requirements, production code can be automatically generated from the model. Code verification is performed by previously mentioned software in the loop and processor in the loop tests. Simplified model in the loop process is described on Figure 13.

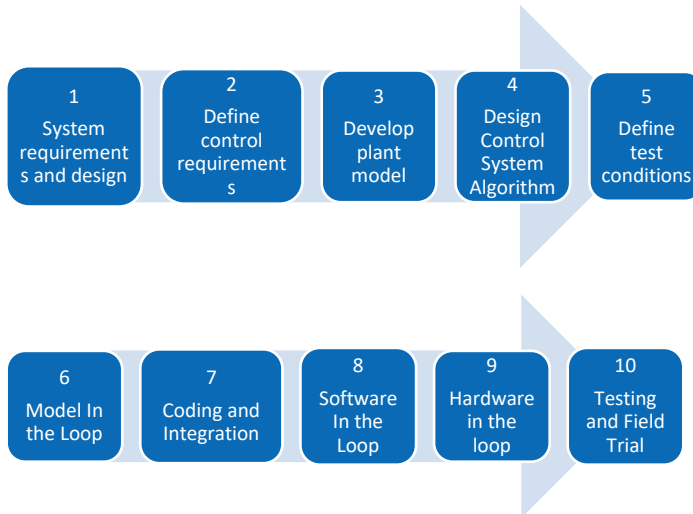


Figure 13 – Model Based Design process flow (data from [35]). The process is composed of ten steps and can be applied for the design of an entire control system or specific part like a single control algorithm.

3. Results of the research

3.1 Multi-rate decomposition

A decomposition framework was developed [32] to solve the problem of partitioning a centralised controller into a decentralised hierarchical structure suitable for autonomous system control implementation. The resulting subsystem controllers are closely matching the performance properties of the original high order closed – loop system with the centralised controller while maintaining the desired controller partitioning structure.

Author took short take-off and landing (STOL) aircraft in the approach to landing task situation where the forces and moments generated by the propulsion system provide control and manoeuvring capabilities for the aircraft at low speeds thus creating the need for integrated flight/propulsion control (IFPC) system design. Generic approach to IFPC design is to design a centralised controller considering the integrated airframe and propulsion system with all its interconnections as the design plant. Although such an approach yields an optimal design since it accounts for all subsystem interactions, it results in a high-order controller, which is difficult to implement and validate. In [32] simple decomposition was proposed, that lead to reduced order subcontrollers that match the closed-loop command tracking and decoupling performance achieved by a high order centralised controller.

Centralised controller partitioning structure is shown in Figure 14 with reference to an integrated flight/propulsion system. In this figure, the subscript c refers to commanded quantities.

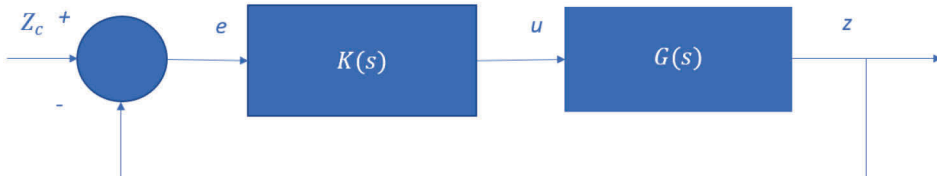


Figure 14 – Control loop for the centralised controller partitioning. Structure for engine and airframe subsystems for short take-off and landing aircraft. The transfer matrix for the plant is $G(s)$ and for the centralised controller is $K(s)$.

The centralised controller is of 13th order and has the form [32]:

$$u = K(s)e \quad (10)$$

where s denotes Laplace transform s -domain argument variable used for generalised analysis of frequency-depend properties of a system. The error vector e consisting of errors:

$$e = [e_V, e_q, e_{N2}, e_{EPR}]^T \quad (11)$$

- e_V velocity (v m/s),
- e_q pitch variable ($e_q = q + 0.1\theta$ where q is the pitch rate in deg/s and θ is the pitch attitude in deg),

- e_{N2} engine fan speed (N2 rpm),
- e_{EPR} engine pressure ratio (EPR, a dimensionless ratio).

The control input vector u consists of following rates:

$$u = [\dot{\delta TF}, \dot{WF}, \dot{A78}, \dot{A8}] \quad (12)$$

- $\dot{\delta TF}$ change of thrust vectoring angle (deg),
- \dot{WF} fuel flow (m^3/s),
- $\dot{A78}$ thrust reverser port area (m^2),
- $\dot{A8}$ nozzle throat area (m^2).

Note that u consists of rates because integrators were appended to the control inputs during the process of centralised control design to achieve zero steady-state error for step commands.

The centralised controller state-space matrices are listed in [32] the work done by the author. The plant state variables are described accordingly. Note that the plant and controller inputs and outputs were normalised prior to applying the controller partitioning procedure to account for the differences in measurement units for the various quantities [36]. The state-space matrices listed in the [32] correspond to the normalized systems.

The structure of the centralised controller partitioning is shown in Figure 15.

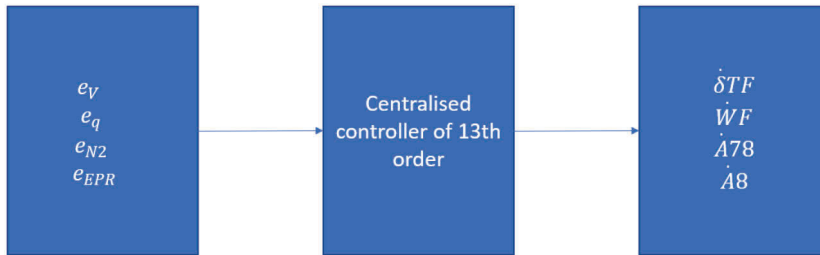


Figure 15 – Structure of high order centralised controller, showing the error and the control input vectors.

Decomposition of stochastic continuous-time control systems. Transformations of the state equations. We have linear, stochastic, continuous-time control system [37] described by the state and output equations:

$$\dot{x}(\tau) = Ax(\tau) + Bu(\tau) + v(\tau) , \quad (13)$$

$$y(\tau) = Cx(\tau) + w(\tau) \quad (14)$$

where $x(\tau) \in R^n, u(\tau) \in R^m, y(\tau) \in R^p, v(\tau) \in R^n, w(\tau) \in R^p$

are the $x(\tau)$ state, $u(\tau)$ control input, $y(\tau)$ output, $v(\tau)$ white noise of excitation of states and $w(\tau)$ white noise of measurements vectors, respectively. These noises are such that:

$$E[w] = E[v] = 0, E[ww^T] = Q, E[vv^T] = R, E[wv^T] = 0.$$

We consider the linear transformation $q(t) = Tx(t)$, where T is a non-singular $n \times n$ matrix. It is easy to see that (13)–(14) are transformed into the equations:

$$\dot{q}(\tau) = J_c q(\tau) + \tilde{B}u(\tau) + Tv(\tau), \quad (15)$$

$$y(\tau) = \tilde{C}q(\tau) + w(\tau) \quad (16)$$

where $J_c = TAT^{-1}$, $\tilde{B} = TB$, $\tilde{T} = T$, $C = CT^{-1}$.

Equations (14),(15) can be written in terms of submatrices as:

$$\dot{z}_1(\tau) = A_1 z_1(\tau) + B_1 u(\tau) + T_1 \vartheta(\tau), \quad (17)$$

$$\dot{z}_2(\tau) = A_2 z_2(\tau) + B_2 u(\tau) + T_2 \vartheta(\tau), \quad (18)$$

$$\dot{z}_3(\tau) = A_3 z_3(\tau) + B_3 u(\tau) + T_3 \vartheta(\tau), \quad (19)$$

$$y(\tau) = C_1 z_1(\tau) + C_2 z_2(\tau) + C_3 z_3(\tau) + w(\tau) \quad (20)$$

where:

small eigenvalues of a matrix A_1 $|\lambda(A_1)| < \gamma_{s_{\max}}$,

intermediate eigenvalues of a matrix A_2 $\gamma_{i_{\min}} < |\lambda(A_2)| < \gamma_{i_{\max}}$,

large eigenvalues of a matrix A_3 $|\lambda(A_3)| > \gamma_{f_{\min}}$,

and matrices containing submatrices

$$J_c = \begin{bmatrix} A_1 & 0 & 0 \\ 0 & A_2 & 0 \\ 0 & 0 & A_3 \end{bmatrix}, \tilde{B} = \begin{bmatrix} B_1 \\ B_2 \\ B_3 \end{bmatrix}, \tilde{C} = [C_1 \quad C_2 \quad C_3], T = \begin{bmatrix} T_1 \\ T_2 \\ T_3 \end{bmatrix}, q(\tau) = \begin{bmatrix} z_1(\tau) \\ z_2(\tau) \\ z_3(\tau) \end{bmatrix}.$$

State equations for three-rate stochastic subsystems

Definition (1):

A function with a large derivative, that is quickly decreasing, is said to be “fast” function;

A function with a small derivative, that is slowly decreasing, is said to be “slow” function;

A function is said to be an intermediate function if the derivative of this function is intermediate between small and large values.

We look the first the time interval mentioned above: $0 < \tau_f \leq \tau_{fi}$. The equation (17) can be rewritten as:

$$\dot{z}_1(\tau) = F(z_1(\tau), u(\tau), v(\tau)). \quad (21)$$

Euler method is used and the solution (20) on a considered interval is given by

$$z_1(\tau_f) = z_1(0) + \tau_f F(z_1(0), u(0), v(0)) . \quad (22)$$

According to definition (1) variables u, v can be considered as “slow” functions of time on this interval. Assuming that $\dot{z}_1(0) = (0)$, we find from (17) and (22):

$$z_1 \approx \tau_f B_1 u(\tau_f) + \tau_f T_1 v(\tau_f) . \quad (23)$$

The same way we apply Euler method to (7) and assuming that $\dot{z}_2(0) = (0)$, we find

$$z_2 \approx \tau_f B_2 u(\tau_f) + \tau_f T_2 v(\tau_f) . \quad (24)$$

From (18), (19), (23) and (24), we find that the state equations for a “fast” subsystem may be written as

$$\dot{z}_f(\tau_f) = A_f z_f(\tau_f) + B_f u_f(\tau_f) + T_f v_f(\tau_f) , \quad (25)$$

$$y_f(\tau_f) = C_f z_f(\tau_f) + D_f u_f(\tau_f) + w_f(\tau_f) \quad (26)$$

where

$$A_f = a_3 , \quad B_f = b_3 , \quad T_f = T_3 , \quad C_f = C_3 ,$$

$$D_f = \tau_f (C_1 B_1 + C_2 B_2) , \quad V_f = \tau_f (C_1 T_1 + C_2 T_2) ,$$

$$z_f(\tau_f) = z_3(\tau_f) , \quad u_f(\tau_f) = u(\tau_f) , \quad v_f(\tau_f) = v(\tau_f) , \quad y_f(\tau_f) = y(\tau_f) ,$$

$$W_f(\tau_f) = w(\tau_f) + V_f v(\tau_f) .$$

Let us look the second time interval mentioned above: $\tau_{fi} < \tau_i \leq \tau_{is}$. According to the definition (1), variable z_3 can be considered as a “fast” function of time. Hence, assuming that $\dot{z}_3(\tau_f) \approx 0$, we find from (18)

$$z_3 \approx -A_3^{-1} B_3 u(\tau_i) - A_3^{-1} T_3 v(\tau_i) . \quad (27)$$

The implicit Euler formula for \dot{z}_1 from (17) can be written as

$$\dot{z}_1(\tau_i) = (z_1(\tau_i) - z_1(0)) / \tau_i . \quad (28)$$

If we now substitute (28) into (17) and assuming that $z_1(0) = 0$, we find that

$$z_1(\tau_i) \approx \tau_i [I - \tau_i A_1]^{-1} B_1 u(\tau_i) + \tau_i [I - \tau_i A_1]^{-1} T_1 v(\tau_i) . \quad (29)$$

From (18), (20), (27) and (29), we find that the state equations for an “intermediate” subsystem may be written as

$$\dot{z}_i(\tau_i) = A_i z_i(\tau_i) + B_i u_i(\tau_i) + T_i v_i(\tau_i) , \quad (30)$$

$$y_i(\tau_i) = C_i z_i(\tau_i) + D_i u_i(\tau_i) + w_i(\tau_i) \quad (31)$$

where

$$\begin{aligned}
A_i &= a_2, \quad B_i = b_2, \quad T_i = T_2, \quad C_i = C_2, \\
D_i &= \tau_i C_1 [I - \tau_i A_1]^{-1} B_1 - C_3 A_3^{-1} C_3, \quad V_i = \tau_i C_1 [I - \tau_i A_1]^{-1} T_1 - C_3 A_3^{-1} T_3, \\
z_i(\tau_i) &= z_2(\tau_i), \quad u_i(\tau_i) = u(\tau_i), \quad v_i(\tau_i) = v(\tau_i), \quad y_i(\tau_i) = y(\tau_i), \\
W_i(\tau_i) &= w(\tau_i) + V_i v(\tau_i).
\end{aligned}$$

We will now proceed to the third time interval mentioned above $\tau_s > \tau_{is}$. According to definition (1), variable z_2 can be considered as an “intermediate” function of time. Hence, assuming that $\dot{z}_2(\tau_s) \approx 0$, we find from (18)

$$z_2(\tau_s) \approx -A_2^{-1} B_3 u(\tau_s) - A_3^{-1} T_3 v(\tau_s). \quad (32)$$

According to the definition (1), variable z_3 can be considered as a “fast” function of time. Hence, assuming that $\dot{z}_3(\tau_s) \approx 0$, we find from (9)

$$z_3(\tau_s) \approx -A_3^{-1} B_3 u(\tau_s) - A_3^{-1} T_3 v(\tau_s). \quad (33)$$

From (17), (20), (32) and (33), we find that the state equations for a “slow” subsystem may be written as:

$$\dot{z}_s(\tau_s) = A_s z_s(\tau_s) + B_s u_s(\tau_s) + T_s v_s(\tau_s), \quad (34)$$

$$y_s(\tau_s) = C_s z_s(\tau_s) + D_s u_s(\tau_s) + w_s(\tau_s) \quad (35)$$

where

$$\begin{aligned}
A_s &= a_1, \quad B_s = b_1, \quad T_s = T_1, \quad C_s = C_1, \\
D_s &= -C_2 A_2^{-1} B_2 - C_3 A_3^{-1} B_3, \quad V_s = -C_2 A_2^{-1} T_2 - C_3 A_3^{-1} T_3, \\
z_s(\tau_s) &= z_2(\tau_s), \quad u_s(\tau_s) = u(\tau_s), \quad v_s(\tau_s) = v(\tau_s), \quad y_s(\tau_s) = y(\tau_s), \\
W_s(\tau_s) &= w(\tau_s) + V_s v(\tau_s).
\end{aligned}$$

By following the proposed decomposition technique, the high order initial centralised controller of 13th order (described in [32]) can be replaced with multi-rate controller with lean 4th order fast subsystem, 5th order intermediate subsystem and 4th order slow subsystem.

3.2 Range of autonomous vehicles and systems considered in the research

Current thesis is based on the long-term research for the control of unmanned and autonomous systems. My research scope has involved variety of unmanned vehicles and complex systems. Illustrative summary about different research applications that author has used for simulation and modelling is presented below on Figure 16. Only selection from the extensive work is discussed in current thesis.

Applications used by the author for the control systems modelling and simulation. Specific tasks were including control of motion, trajectory, behavior, performance.

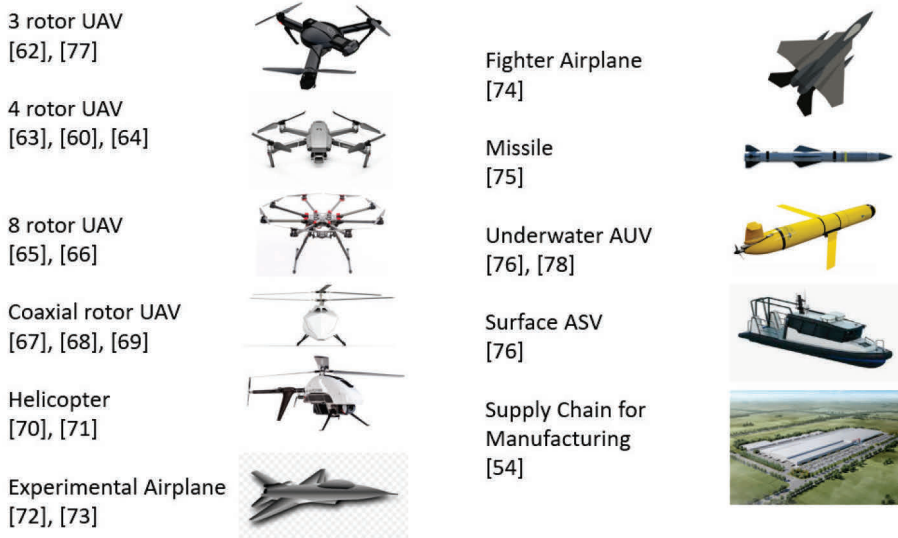


Figure 16 – Illustrated range of autonomous vehicles and complex systems studied by the author under the research theme of modelling and simulation the control systems. References to author’s publications related to specific type of autonomous vehicles or systems are shown.

3.3 Flight control of a four rotor UAV

Contributing publication 1 [93] provides answer to the RQ1 of current thesis: How to develop flight control for the autonomous vertical flight for the nontrivial nonlinear model of the tactical unmanned aerial vehicle? Publication keeps also attention on a critical component of the situational awareness (SA), the control of autonomous vertical flight for a four rotor UAV. A rotorcraft or rotary-wing aircraft is a heavier-than-air flying machine that uses lift generated by wings, called rotary wings or rotor blades, that revolve around a mast. Several rotor blades mounted on a single mast are referred to as a rotor. The International Civil Aviation Organization (ICAO) defines a rotorcraft as “supported in flight by the reactions of the air on one or more rotors” [38]. Rotorcraft generally include those aircraft where one or more rotors are required to provide lift throughout the entire flight. A helicopter is a rotorcraft whose rotors are driven by the

engine(s) throughout the flight to allow the helicopter to take off vertically, hover, fly forwards, backwards and laterally, as well as to land vertically. Helicopters have several different configurations of one or more main rotors.

Multi-rotor UAV's have more than two rotors. An advantage of multirotor aircraft is the simpler rotor mechanics required for flight control. Unlike single- and double-rotor helicopters which use complex variable pitch rotors whose pitch varies as the blade rotates for flight stability and control, multi-rotors often use fixed-pitch blades; control of vehicle motion is achieved by varying the relative speed of each rotor to change the thrust and torque produced by each. There are a wide variety of Multi-Rotor UAV shapes, sizes and configurations.

Due to their ease of both construction and control, multi-rotor aircraft are frequently used as radio control UAVs in which the names tricopter, quadcopter, hexacopter and octocopter are frequently used to refer to 3-, 4-, 6- and 8-rotor helicopters, respectively.

A multi-rotor UAV offers many advantages, including low cost, relative invisibility, the ability to fly within a narrow space and the unique hovering and vertical take-off and landing (VTOL) flying characteristics.

The characteristics of a multi-rotor UAV motion depend on mode of manoeuvring, speed, and outside appendages such as measuring instruments. In addition, the small Multi-rotor UAVs are sensitive to many factors during the flight, such as mechanical vibration caused by engines, unexpected roll, yaw, and pitch due to atmospheric turbulence. Due to these reasons, the appropriate controllers are needed to control Multi-rotor UAV flightpath and motions.

In the contributing publication 1 author proposed a two-stage flight control procedure to address the dynamics variation and performance requirement difference in initial and final stages of flight trajectory for a nontrivial nonlinear model of four-rotor helicopter robot called drone. This control strategy for chosen drone model has been verified by simulation of hovering manoeuvres using software package Simulink and demonstrated good performance for fast stabilization of engines in hovering, consequently, fast SA with economy in energy of batteries can be asserted during the flight.

A mathematical model of a four rotor UAV. The drone is equipped with four rotors where two are directional. Compared to quadrotors, the drone has some advantages: given that two rotors 3 and 4 rotate counter clockwise while the other two (1 and 2) rotate clockwise, gyroscopic effects and aerodynamic torques tend, in trimmed flight, to cancel. The main feature of the presented drone in comparison with the existing quadrotors, is the swivelling of the actuators supports rotors 1 and 3 around the pitching axis. This permits a more stabilized horizontal flight and a suitable cornering.

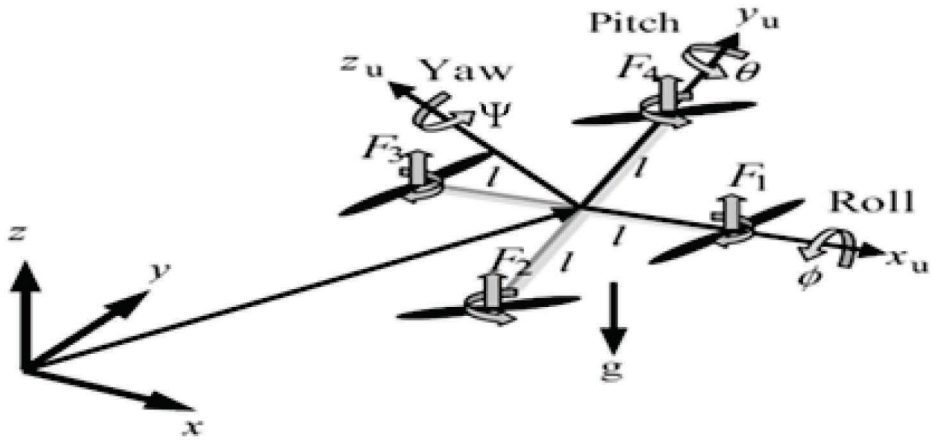


Figure 17 – Illustrative example for quadrotor UAV. Two diagonal motors are running in the same direction whereas the others run in the opposite direction to eliminate anti-torque.

If the four-rotor helicopter (see Figure 17) is assumed to move at low speed, the dynamical equations of motion have the following form [37]

$$\ddot{x} = \frac{(\sin \psi \sin \phi + \cos \psi \sin \theta \cos \phi)u_1}{m}, \quad (36)$$

$$\ddot{y} = \frac{(\sin \psi \sin \theta \cos \phi - \cos \psi \sin \phi)u_1}{m}, \quad (37)$$

$$\ddot{z} = \frac{(\cos \phi \cos \theta)u_1}{m} - g, \quad (38)$$

$$\ddot{\phi} = \frac{lu_3}{I_x}, \quad (39)$$

$$\ddot{\theta} = \frac{lu_2}{I_y}, \quad (40)$$

$$\ddot{\psi} = \frac{Cu_4}{I_z} \quad (41)$$

where:

x, y, z are coordinates of center of mass in the earth-frame;

ϕ, θ, ψ are roll, pitch and yaw angles;

I_x, I_y, I_z are moments of inertia along x, y, z directions;

C is the force to moment scaling factor;

l is the distance from the center of mass to the rotors;

g is the gravity constant;

m is the mass of the drone;

$u_i (i = 1, \dots, 4)$ is the control input i .

Note that the constraints as external perturbations and the gyroscopic torques are neglected in this model.

For convenience of calculations, the inputs in (36)–(41) are defined as

$$u_1 = f_1 + f_2 + f_3 + f_4, \quad (42)$$

$$u_2 = f_4 - f_2, \quad (43)$$

$$u_3 = f_3 - f_1, \quad (44)$$

$$u_4 = f_1 - f_2 + f_3 - f_4 \quad (45)$$

where $f_i (i = 1, \dots, 4)$ is the thrust force of rotor i .

The thrust forces in (42)–(45) then can be represented in matrix form as

$$\begin{bmatrix} f_1 \\ f_2 \\ f_3 \\ f_4 \end{bmatrix} = \begin{bmatrix} 0.25 & 0 & -0.5 & 0.25 \\ 0.25 & -0.5 & 0 & -0.25 \\ 0.25 & 0 & 0.5 & 0.25 \\ 0.25 & 0.5 & 0 & -0.25 \end{bmatrix} \begin{bmatrix} u_1 \\ u_2 \\ u_3 \\ u_4 \end{bmatrix}. \quad (46)$$

The thrust forces of each rotor can be expressed in the form [39]

$$f_i = K_T \omega_i^2 \quad (47)$$

where

ω_i is the angular speed of rotor i and coefficient $K_T = 10^{-5} N s^2$.

It may be now seen that the angular speed ω_i of rotor i simplifies to:

$$\omega_i = 2\pi \frac{n_{m_i}}{60} \approx \frac{n_{m_i}}{10} \quad (48)$$

where n_{m_i} (rpm) is the number of revolutions per minute of rotor i .

Combining (47) and (48), we have

$$n_{m_i} \approx 10 \sqrt{\frac{f_i}{K_T}} . \quad (49)$$

From (34)–(43), we can see that the attitude vector $(x, y, z)^T$ for given model of four-rotor UAV can be computed.

The numerical values for parameters of (36)–(41) for a case of small elevation above sea level are given by [40]:

$$\begin{aligned} m &= 2,5 \text{ kg}, \quad l = 0,23 \text{ m}, \quad I_x = 0,0224931 \text{ kgm}^2, \\ I_y &= 0,0222611 \text{ kgm}^2, \quad I_z = 0,0325130 \text{ kgm}^2, \\ K_T &= 10^{-5} \text{ Ns}^2, \quad K_M = 9 \times 10^{-6} \text{ Nms}^2, \quad g = 9,81 \frac{\text{m}}{\text{s}^2}. \end{aligned}$$

Control system with control of collective thrust. Note that the inputs in (42)–(45) then can be represented in matrix form as

$$\begin{bmatrix} u_1 \\ u_2 \\ u_3 \\ u_4 \end{bmatrix} = \begin{bmatrix} 1 & 1 & 1 & 1 \\ 0 & -1 & 0 & 1 \\ -1 & 0 & 1 & 0 \\ 1 & -1 & 1 & -1 \end{bmatrix} \begin{bmatrix} f_1 \\ f_2 \\ f_3 \\ f_4 \end{bmatrix} . \quad (50)$$

It is possible to consider the control inputs u_2 and u_4 in (50) as zero functions. Hence, we have

$$u_2(t) = 0, \quad (51)$$

$$u_4(t) = 0. \quad (52)$$

With selection of (51)–(52), control problem is now turned into a hybrid constrained control problem with using only control input u_1 for controlling the coordinate z of altitude with respect to reference input z^0 and with using control input u_3 for controlling the roll ϕ of attitude with respect to reference input ϕ^0 .

The main equation defining the control system to regulate the input variable u_1 can be specified in the following form

$$\dot{u}_1 = K(t_1(z^0 - z) - t_2\dot{z} - \ddot{z}) \quad (53)$$

where t_1, t_2 are constants to be determined. This idea was proposed by author in [32].

It is possible to consider the variable u_1 as a “fast” function of time. Hence, assuming that $\dot{u}_1 \approx 0$, from (53), we find

$$\ddot{z} + t_2 \dot{z} + t_1 z = t_1 z^0 . \quad (54)$$

The following coefficients of (54) are obtained from [36], for overshooting with value of $\sigma \approx 5\%$

$$t_1 \approx \frac{9}{t_{dz}^2}, \quad t_2 \approx 3 \sqrt{\frac{2}{t_{dz}}} \quad (55)$$

where t_{dz} is desired transition time of coordinate z .

For a hovering flight, angles of roll, pitch, and yaw must be zeros. Therefore, (37) becomes

$$\ddot{z}(t) = bu_1(t) - g, \quad (56)$$

where $b \approx \frac{1}{m}$.

Differentiating both sides of (56) with respect to time, we obtain

$$\ddot{z}(t) = b\dot{u}_1(t) . \quad (57)$$

Combining (53) and (57), we have

$$\ddot{z}(t) = bK(i_3(t) - \ddot{z}(t)), \quad (58)$$

where $i_3(t) = t_1(z^0 - z(t)) - t_2 \dot{z}(t)$.

Defining $\ddot{z}(t) = a(t)$, (56) can be expressed as

$$\dot{a}(t) = -bKa(t) + bKi_3(t) . \quad (59)$$

The variable $a(t)$ in (59) can be described in a common way through next expression

$$a(t) = (a_0 + \int_0^t e^{-A(\tau)} bKi_3(\tau) d\tau) e^{A(t)} , \quad (60)$$

where $A(t) = -\int_0^t bK d\tau$.

Let us consider the behavior of the considered control system for time t of time interval $t \geq t_{dz}$ during the hovering.

Hence, assuming that $a_0 = 0$, $z^0 - z(t) \approx \Delta z^0$, $\Delta = 0.005$, $\dot{z}(t) \approx 0$, $i_3(t) \approx t_1 \Delta z^0 \approx const$, from (60), we find

$$a(t) = i_3(1 - e^{-bKt}). \quad (61)$$

Assume now that for the desired transition time for control of acceleration $a(t)$ lies in the zone of overshooting with value of $\sigma \approx 5\%$, then, from (59), it follows that

$$t_{d_z} = -\frac{\ln(\Delta)}{bK}. \quad (62)$$

Therefore, using (60), and that $b \approx \frac{1}{m}$, $\ln(\Delta) \approx -3$, and the ratio of coordinate-to-acceleration transition times $N = \frac{t_{d_z}}{t_{d_{\ddot{z}}}}$, we obtain

$$K \approx \frac{3Nm}{t_{dz}}. \quad (63)$$

Note that the structure of control system using control input u_3 for controlling the roll ϕ is similar to the control structure for controlling the coordinate z , which was described above.

Simulation results for control system with control of collective thrust. In the main Publication 1, Author presents numerical example to evaluate the proposed technique [41] in scenario involving control of the considered maneuver.

Control of quadrotor helicopter model (36)–(41) was considered for the case of take-off and hovering maneuvers by hybrid constrained system of three control subsystems.

The goal for the following simulations was twofold:

- First, I verify that these control subsystems are able to control the take-off and hovering trajectories;
- Second, I observed the effect of enhancing SA because the variety of such trajectory parameters as desired transition times, ratios of coordinate-to-acceleration transition times and heights of hovering easily can be changed the possible take-off and hovering trajectories of quadrotor helicopter.

Specific advantages of proposed approach could be summarized:

- Smooth trajectory of flight with possibility of lag in two different selected height positions;
- Using of two simple control subsystems to control the take-off and hovering trajectories of the quadrotor UAV flight;
- Possibility to consider terrain specific restrictions in the places of hovering.

3.4 Three-rate neural control of UAV with ducted fan and two coaxial rotors

Contributing publication 2 [82] provides answer to the RQ2 of the current thesis. It explains how to make initial control system decomposition and replace the original control system with three-rate neural control for the coaxial rotor and ducted fan UAV. Research is done on a multi-rate control of a ducted fan UAV with two coaxial rotors. In comparison with conventional main and tail rotor configuration, the coaxial rotors design with ducted fan configuration provides more lift and move easily in any direction [83], during take-off and landing. These design features not only increase the manoeuvrability of unmanned helicopter but also increases its stability making it easier to fly especially in narrow and bumpy take-off and landing sites.

A mathematical model of an UAV. In [42], a model of prototype coaxial unmanned helicopter with ducted fan configuration (see Figure 18) was proposed.

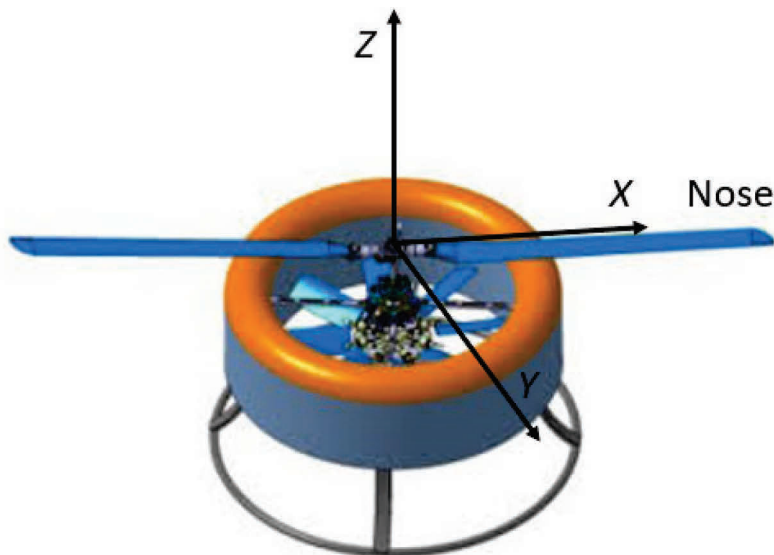


Figure 18 – Illustrative example for unmanned helicopter with two coaxial rotors, having second auxiliary fan mounted in ducted configuration [42].

With this publication I focus on the model of prototype unmanned helicopter. It is a vertical take-off and landing (VTOL) aircraft that includes a fuselage with toroidal portion and coaxial rotors. A duct is formed through the fuselage and extends from the top to the bottom of the fuselage. A propeller assembly is mounted to the top portion of the fuselage with a main rotor of diameter. A ducted rotor assembly is installed in fuselage compensating the propeller antitorque besides providing some fraction of lift. The coaxial rotors, main and ducted, rotate at in opposite directions. The main rotor provides about 80% of lift, drag, pitch and roll movements of unmanned helicopter and the ducted rotor provides about 20% of lift and yaw movements [42].

By following the proposed methodology in 3.1 of current thesis, the original UAV control system model is decomposed into three subsystems: the “fast” subsystem used in the initial phase of trajectory (take-off), the “intermediate” subsystem used in the middle phase of trajectory (approach), and the “slow” subsystem used in the final phase of trajectory (hovering).

The dynamic model for control yields the general form of state equations for the prototype unmanned helicopter [42]:

$$\dot{x}(\tau) = Ax(\tau) + Bu(\tau) + v(\tau), \quad (64)$$

$$y(\tau) = Cx(\tau) + w(\tau) \quad (65)$$

where $x(\tau)$ is the state, $u(\tau)$ is the control input, $y(\tau)$ is the output, $v(\tau)$ is the process noise and $w(\tau)$ is the measurement noise vectors, respectively.

The variables of this model are:

$$x = \begin{bmatrix} V_x \\ V_y \\ V_z \\ \omega_x \\ \omega_y \\ \omega_z \\ \phi \\ \theta \\ \psi \end{bmatrix},$$

$$u = \begin{bmatrix} \delta_{mr} \\ \delta_{lat} \\ \delta_{lon} \\ \delta_{fan} \end{bmatrix}, \quad (66)$$

where V_x, V_y, V_z are forward, lateral and vertical velocities; $\omega_x, \omega_y, \omega_z$ are roll, pitch and yaw rates; ϕ, θ, ψ are roll, pitch and yaw angles; $\delta_{mr}, \delta_{lat}, \delta_{lon}, \delta_{fan}$ are main rotor collective, lateral cyclic, longitudinal cyclic and fan collective pitches.

Notice that the velocities from (66) can be expressed in the form

$$V_x = \dot{x}_c, V_y = \dot{y}_c, V_z = \dot{z}_c \quad (67)$$

where x_c, y_c, z_c are coordinates of center of mass of UAV in the earth-frame.

Combining (66) and (67), we have

$$x = \begin{bmatrix} \dot{x}_c \\ \dot{y}_c \\ \dot{z}_c \\ \omega_x \\ \omega_y \\ \omega_z \\ \phi \\ \theta \\ \psi \end{bmatrix},$$

$$u = \begin{bmatrix} \delta_{mr} \\ \delta_{lat} \\ \delta_{lon} \\ \delta_{fan} \end{bmatrix}. \quad (68)$$

The matrix structure of A, B, C for the state-space model of system (64)–(65) is given by

$$A = \begin{bmatrix} a_1 & a_2 & 0 & a_3 & a_4 & 0 & 0 & a_5 & 0 \\ a_6 & a_7 & 0 & a_8 & a_9 & 0 & a_{10} & 0 & 0 \\ 0 & 0 & a_{11} & 0 & 0 & a_{12} & 0 & 0 & 0 \\ a_{13} & a_{14} & 0 & a_{15} & a_{16} & 0 & 0 & 0 & 0 \\ a_{17} & a_{18} & 0 & a_{19} & a_{20} & 0 & 0 & 0 & 0 \\ 0 & 0 & a_{21} & 0 & 0 & a_{22} & 0 & 0 & 0 \\ 0 & 0 & 0 & 1 & 0 & 0 & 0 & 0 & 0 \\ 0 & 0 & 0 & 0 & 1 & 0 & 0 & 0 & 0 \\ 0 & 0 & 0 & 0 & 0 & 1 & 0 & 0 & 0 \end{bmatrix},$$

$$B = \begin{bmatrix} 0 & b_1 & b_2 & 0 \\ 0 & b_3 & b_4 & 0 \\ b_5 & 0 & 0 & b_6 \\ 0 & b_7 & b_8 & 0 \\ 0 & b_9 & b_{10} & 0 \\ b_{11} & 0 & 0 & b_{12} \\ 0 & 0 & 0 & 0 \\ 0 & 0 & 0 & 0 \\ 0 & 0 & 0 & 0 \end{bmatrix},$$

$$C = \begin{bmatrix} 1 & 0 & 0 & 0 & 0 & 0 & 0 & 0 & 0 \\ 0 & 1 & 0 & 0 & 0 & 0 & 0 & 0 & 0 \\ 0 & 0 & 1 & 0 & 0 & 0 & 0 & 0 & 0 \\ 0 & 0 & 0 & 1 & 0 & 0 & 0 & 0 & 0 \\ 0 & 0 & 0 & 0 & 1 & 0 & 0 & 0 & 0 \\ 0 & 0 & 0 & 0 & 0 & 1 & 0 & 0 & 0 \\ 0 & 0 & 0 & 0 & 0 & 0 & 1 & 0 & 0 \\ 0 & 0 & 0 & 0 & 0 & 0 & 0 & 1 & 0 \\ 0 & 0 & 0 & 0 & 0 & 0 & 0 & 0 & 1 \end{bmatrix}, \quad (69)$$

The parameters a_1 through a_{22} and parameters b_1 through b_{12} in (69) are given by:

$$\begin{aligned} a_1 &= 0.0058, a_2 = 0.0017, a_3 = 0.0081, \\ a_4 &= 0.0329, a_5 = -9.8000, a_6 = -0.0015, \\ a_7 &= -0.0058, a_8 = -0.0329, a_9 = 0.0081, \\ a_{10} &= 9.8000, a_{11} = -0.9816, a_{12} = 0.0794, \\ a_{13} &= -0.0072, a_{14} = -0.0154, a_{15} = -0.0867, \\ a_{16} &= 0.0153, a_{17} = 0.0106, a_{18} = -0.0049, \\ a_{19} &= -0.0106, a_{20} = -0.0697, a_{21} = -0.0416, \\ a_{22} &= -0.1691, \\ b_1 &= -0.1294, b_2 = -2.8845, b_3 = 2.8845, \\ b_4 &= -0.1294, b_5 = 122.0518, b_6 = 11.8688, \\ b_7 &= 7.5964, b_8 = -0.9077, b_9 = 0.8578, \\ b_{10} &= 7.2260, b_{11} = -26.0034, b_{12} = 10.7727. \end{aligned}$$

Then, we have

$$x_c(\tau) = \int_0^\tau \dot{x}_c(t)dt, y_c(\tau) = \int_0^\tau \dot{y}_c(t)dt, z_c(\tau) = \int_0^\tau \dot{z}_c(t)dt, \quad (70)$$

where $x_c(0) = 0, y_c(0) = 0, z_c(0) = 0$.

From (64)–(65), (68)–(69) can be seen that the attitude vector $(x_c, y_c, z_c)^T$ for given model of UAV can be computed.

In [43], is offered the approach to design of decomposed multi-rate stochastic linear systems, which consist of naturally grouped entrance and target signals that are caused by their characteristic frequencies. The three-rate control system for the given model of UAV was generated accordingly.

Simulation results. Maneuvering task was given to the three-rate TUAV model with coaxial rotor and ducted fan configuration for the take-off, approach and hovering. Initial conditions and desired height were chosen to be:

$$x(0) = y(0) = z(0), z_1^0 = 30 \text{ m}.$$

Target height of 30 m was chosen based on EU regulations [44]. These regulations are risk-based and divide the operations, whether commercial or recreational, in a low risk category (open category) and a medium risk category (specific category). The high-risk operations remain in the (manned) aviation domain under the certified category. Current commercial drone operations are possible in this open category as long as they do not take place over or near (30m) people.

In [45], the two approximations to the nonlinear autoregressive moving average (NARMA) model called the NARMA-L1 and the NARMA-L2 are proposed. From a practical stand-point, the NARMA-L2 model is found to be simpler to realize than the NARMA-L1 model. The neurocontroller used in this section was based only on the NARMA-L2 approximate model. The Simulink block scheme with three control subsystems is shown in Figure 19.

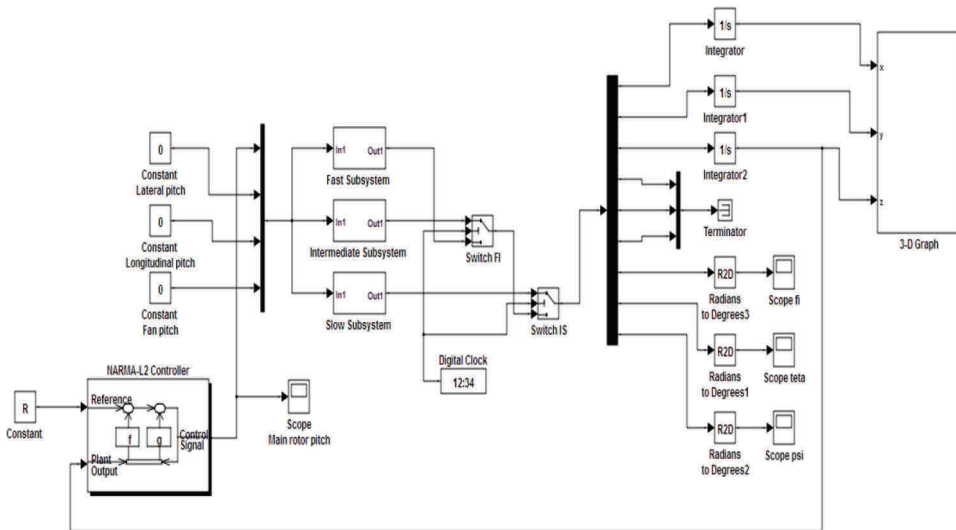


Figure 19 – Block diagram of three-rate control system supported by NARMA L2 neurocontroller.

In the simulation results, the trajectory tracking display forms provide a control system designer an immediate view of given TUAV motion with a range of such parameter as main rotor collective pitch. This allows to investigate the sensitivity of the three-rate control system, providing a medium for such development and evaluation and enhancing the control system designer's understanding of flight manoeuvres.

3.5 Comparison of single-rate and two-rate neural control approaches

The 3rd contributing research paper [81] provides answer to the RQ3 of current thesis on how to compare UAV's initial control system with proposed two-rate neural control approach? Publication also discusses the modelling and control methodologies of a UAV of coaxial rotor type with ducted fan via introduction of two-rate control and neural network methods in order to achieve more stabilized flight control. The effectiveness of the proposed two-rate control strategy versus original single rate control is illustrated and confirmed by numerical simulations of flight manoeuvres using software package MATLAB/Simulink.

Single-rate UAV control model

The aerodynamic parameters of VTOL type UAVs are often difficult and expensive to define precisely. In [46], the dynamics of a VTOL aircraft, such as a Harrier around hover, is described. It is shown that a simple choice of control Lyapunov function, i.e., the one obtained from Jacobian linearization of the dynamics at hover, will achieve a good performance. In [42], a reliable model of coaxial rotor/ducted-fan TUAV with parameters measured in wind tunnel is described.

Two-rate UAV control model

The methodology of multi-rate decomposition is discussed closely in [47] and more systematically in [48]. Following this methodology, in the present UAV case the below described fast and slow subsystem models were constructed.

In [47], such basic heuristic reception in the theory of dynamic systems as frequency-response separation of motions, that is, the separation of motions on "fast" and "slow" motions in a given case, is developed.

The offered block scheme (see Figure 20) allows us to compare the following outputs:

- the original system's outputs and the "fast" system's outputs;
- the original system's outputs and the "slow" system's outputs.

It was obtained that it is possible to accept 15 s as a border of the temporary division of the "fast" and "slow" control subsystems

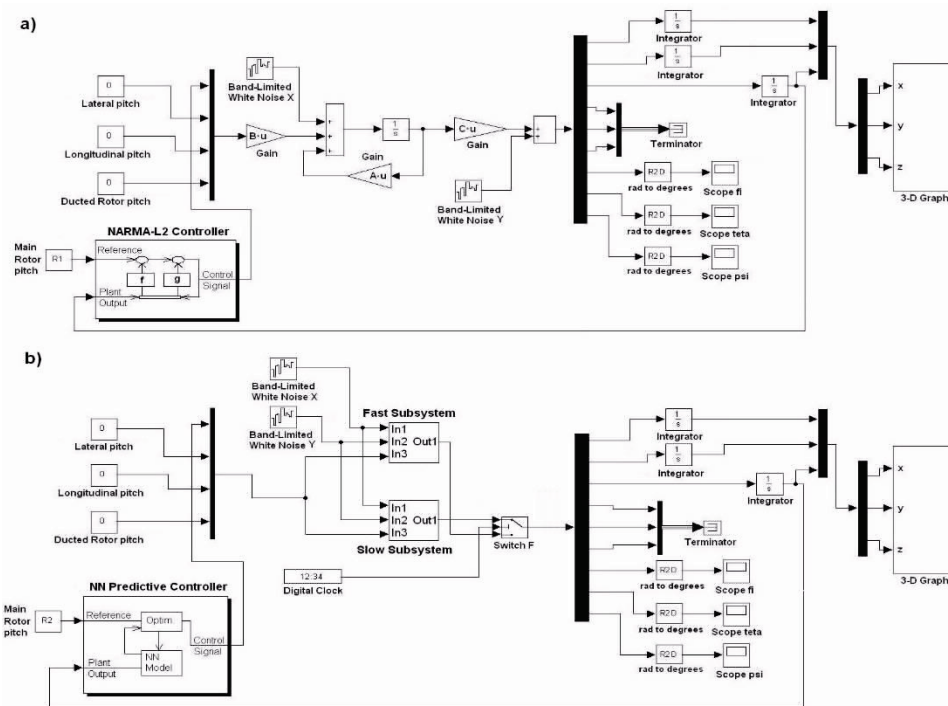


Figure 20 – Simulink style block diagrams of single-rate (a) and two-rate control systems (b). Control systems are supported by NARMA-L2 (a) and Predictive (b) neurocontrollers available in MATLAB/Simulink environment.

Simulation results. Requested trajectory for UAV motion simulation a take-off, approach and hovering flight manoeuvres were defined using the above described single rate and two-rate control system variants. Initial and desired final height for simulation example were specified as:

$$x(0) = y(0) = z(0) = 0 \text{ m}, z_1^0 = 20 \text{ m}.$$

Before running the models, I had to assign numerical values to each of the variables used in the models through MATLAB. Simulink was used to simulate the complete control system.

The simulation results and comparison of the offered block schemes with one control system or two control subsystems are shown in Figures 21–23.

Figure 21 presents straightforward comparison of two-rate system take-off and hovering ability with original single-rate system. The main observations from the simulation results are summarized in Table 2.

Table 2 – Comparison of control system performance parameters for single-rate and three-rate control systems

Systems	Control System Performance Parameters			
	Rise Time (t_r)	Time to First Peak (t_p)	Settling Time (t_s)	Overshoot (O)
Single-Rate System	2.12s	5s	20s	5.5%
Two-Rate System	4.79s	10s	10s	1.05%

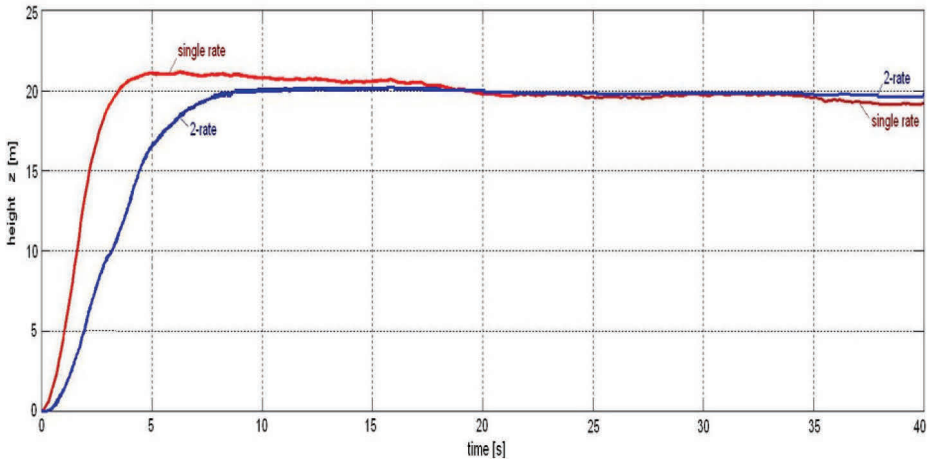


Figure 21 – Comparison of UAV take-off and hovering trajectories at height 20 m in the case of single-rate and two-rate control systems (UAV centre of mass plotted). Small height oscillations on the hovering part of flight are missing in the case of two-rate control.

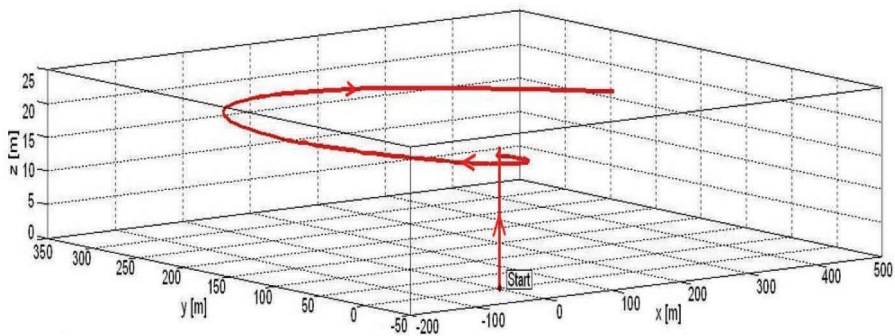


Figure 22 – 3D presentation of take-off and hovering trajectory at height 20 m in the case of single-rate TUAV control.

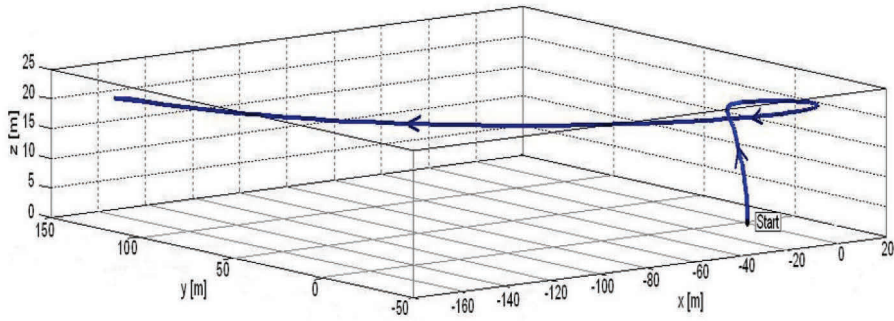


Figure 23 – 3D presentation of take-off and hovering trajectory at height 20 m in the case of two-rate TUAV control.

Conclusions:

- Using the pre-defined methodology, decomposition was performed for the original control system of 9th order, resulting the “fast” subsystem of 7th order used in the initial phase of trajectory (take-off and approach motions) and the “slow” subsystem of 2nd order used in the final phase of trajectory (hovering motion);
- The effectiveness of the proposed control strategy was verified by simulation tests for the chosen model of TUAV. From the applications viewpoint, the modelled and simulated flight control strategy that was proposed, offers a reasonable possibility to improve VTOL class UAVs flight characteristics needed for information collection in sophisticated conditions.

3.6 Single-rate versus three-rate neural assisted control

The 4th contributing research paper [67] provides answer to the RQ4 of current thesis on how to compare UAV’s initial control system with proposed three-rate neural control approach? Publication also discusses the modelling and control methodologies of a UAV of coaxial rotor type with ducted fan via introduction of three-rate control and neural network methods in order to achieve more stabilized flight control. The effectiveness of the proposed three-rate control strategy versus original single rate control is illustrated and confirmed by numerical simulations of flight manoeuvres using software package MATLAB/Simulink.

Single-rate UAV control model was described in 3.5.

Three-rate UAV control model. The methodology of multi-rate decomposition is discussed by current thesis under 3.1. It is also processes in [47] and in [48]. Following the proposed decomposition methodology for the present UAV case the below described fast, intermediate and slow subsystem models were constructed. Via the system properties analysis [48], the borders of temporary division of the “fast”, “intermediate” and “slow” control subsystems were defined. It was obtained that it is possible to accept 15 and 35 seconds, respectively, as a border of temporary division of the “fast” and “intermediate” control subsystems and as a border of temporary division of the “intermediate” and “slow” control subsystems.

The block schemes for single-rate and three-rate UAV control systems realization are presented in Figure 24.

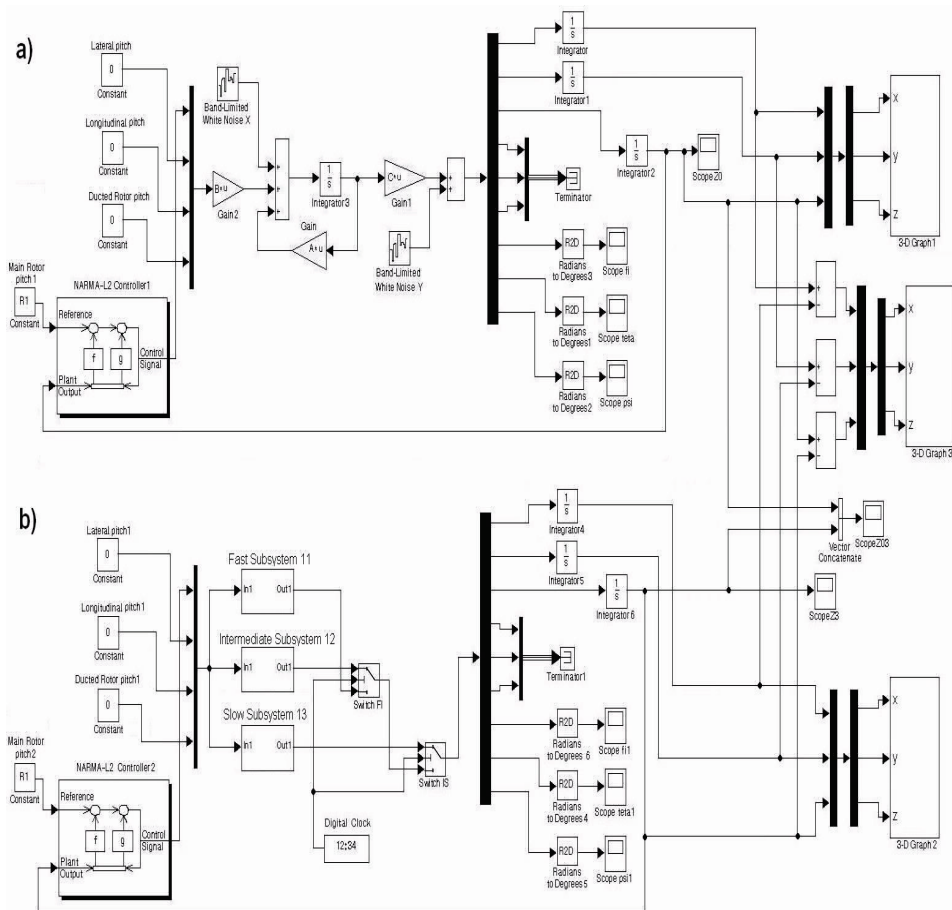


Figure 24 – Block diagrams of single-rate (part a) and three-rate (part b) control systems. Both control systems are supported by NARMA-L2 neurocontrollers.

Simulation Results. Requested trajectory for UAV motion simulation a take-off, approach and hovering flight manoeuvres were defined using the above described single rate and three-rate control system variants. Initial and desired final height for simulation example were specified as:

$$x(0) = y(0) = z(0) = 0 \text{ m}, z_1^0 = 25 \text{ m}.$$

Before running the models, we had to assign numerical values to each of the variables used in the models through MATLAB. Simulink was used to simulate the complete control system.

The simulation results and comparison of the offered block schemes with one control system or three control subsystems are shown in Figures 25–28. The main observations from the simulation results are summarized in Table 3.

Table 3 – Comparison of control system performance parameters for single-rate and three-rate control systems

Systems	Control System Performance Parameters			
	Rise Time (t_r)	Time to First Peak (t_p)	Settling Time (t_s)	Overshoot (O)
Single-Rate System	2.25s	6.20s	47.0s	11.6%
Three-Rate System	2.73s	8.85s	21.2s	4.0%

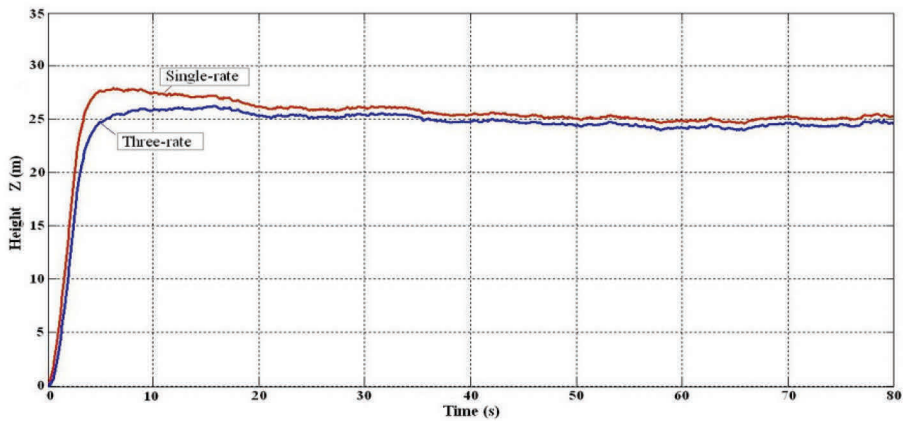


Figure 25 – Comparison of UAV take-off and hovering trajectories at height 25 m in the case of single-rate (red) and three-rate (blue) control systems (UAV centre of mass z-coordinate plotted).

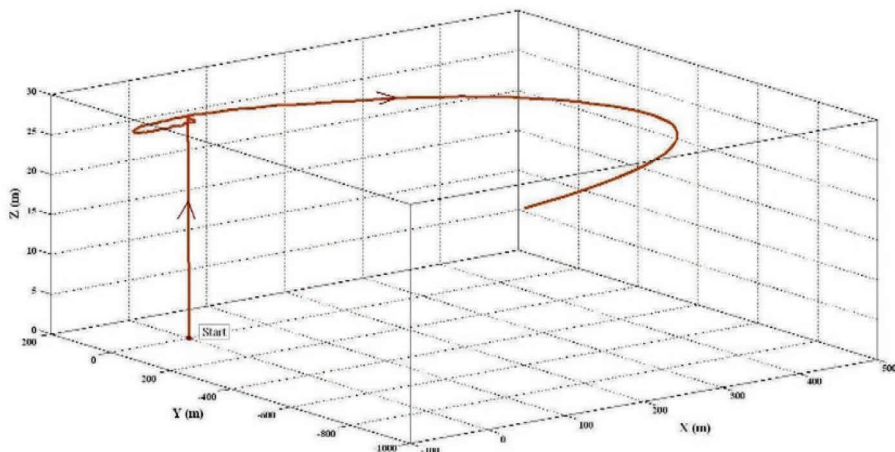


Figure 26 – 3D presentation of take-off and hovering trajectory at height 25 m in the case of single-rate UAV control.

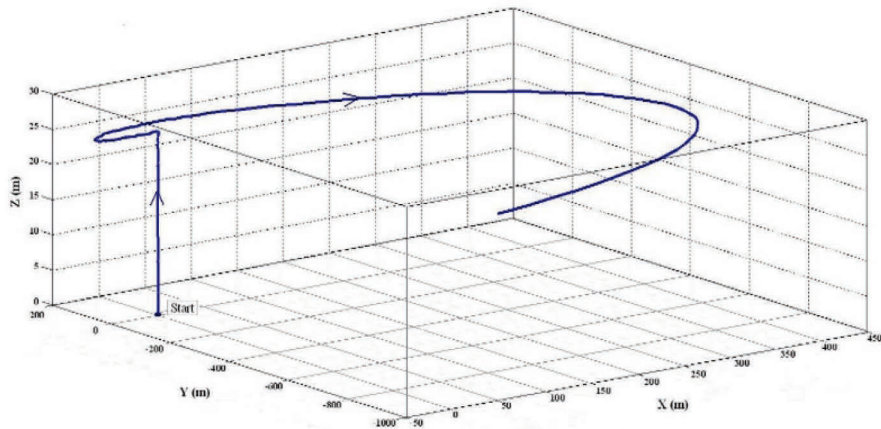


Figure 27 – 3D-presentation of take-off and hovering trajectory at the height of 25 m in the case of three-rate TUAV control.

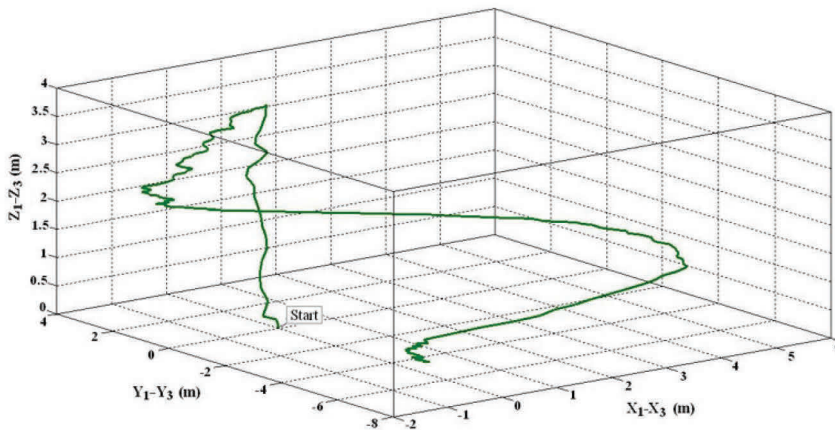


Figure 28 – 3D-presentation of the trajectories difference between the cases of single-rate and three-rate TUAV control.

Conclusions:

- For the stable and smooth flight manoeuvres a three-rate decomposition was performed for the initial control system. By following the proposed methodology, the TUAV model of 9th order was decomposed into three subsystems: the “fast” subsystem of 3rd order used in the initial phase of trajectory (take-off motion), the “intermediate” subsystem of 4th order used in the middle phase of trajectory (approach motion), and the “slow” subsystem of 2nd order used in the final phase of trajectory (hovering motion);
- The effectiveness of the proposed multi-rate control strategy was verified by simulation tests for the TUAV model using realistic simulator of Math Works software. Simulation results confirm the effectiveness of the three-rate control over the single-rate control yielding the higher accuracy of the tracking and correspondingly better energy efficiency indicators. In particular, the settling

time is reduced by the factor of 2.2 and the height overshoot by factor of 2.9. From the applications viewpoint, I believe that the modelled and simulated flight control strategy may offer a reasonable possibility to improve VTOL class UAVs flight characteristics.

3.7 Comparison of neural and basic tracking control for ASV

Contributing publication 5 [79] provides answer to the RQ5 of current thesis. It is presenting the comparison between predictive NN control and basic tracking feedback control for two specific manoeuvres. Publication 5 also explores the alternative fields of implementation for the proposed advanced control methods. As discussed in the Preface of current thesis, Author has been working with control systems for wide range of unmanned vehicles. Current chapter provides insight to the control systems development for unmanned surface vehicles that are moving on water. Moving of an Autonomous Surface Vessel (ASV) to the desired area of sea is a challenging task to achieve high level of autonomy under adverse conditions. Current main contributing publication focuses on the development of methodology of model-based modelling and simulation of cyber-physical nonlinear system of ASV in MATLAB/Simulink software environment. The comparison between predictive neural control and basic tracking feedback control is presented for two manoeuvres: the turn at different angles and the circular motion at final destination. Simulation results confirm the necessity and superiority of neural controller approach.

UAV control system development is moving towards smarter cyber physical systems (CPS), further integrating the AI elements and, in particular, the neural network control blocks [49], [50], [51]. Reason for this is that often the traditional proportional or proportional-integral-derivative (PID) feedback tracking controller technologies cannot yield the desired control quality and more sophisticated controller realizations that consider also information about the physical model of the vehicle under control are needed. To accomplish this advanced control system development task, the proposed approach is application of model-based methodology in design environment like MATLAB/Simulink where different options for neural network controllers and sophisticated possibilities description of linear or nonlinear physical object models are available for developers. Hereby Author demonstrates definition of an Autonomous Surface Vessel neural network assisted control modelling task in MATLAB/Simulink environment and study of control quality via specific simulation of different trajectory control tasks. This study used some ideas offered in [61] for an under actuated unmanned surface vehicle: a practical adaptive sliding mode control scheme applying backstepping technique; sliding mode control; radial basis neural network and auxiliary dynamic system.

Model of ASV. We consider the model of an ASV (see Figure 29). The vessel has two propellers which are responsible for the surge force and the yaw control torque. Figure 29 shows the system variable definitions where heading angle ψ represents the orientation of the vessel's body-fixed frame relative to the North-East-Down (NED) frame. The instantaneous vessel heading angle ψ , is measured in anticlockwise direction from the global X axis.

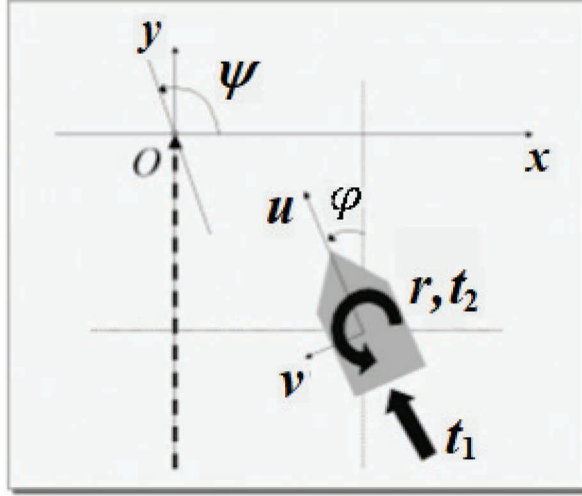


Figure 29 – Coordinate and system variable definitions of the studied ASV. Heading angle ψ represents the orientation of the vessel's body-fixed frame relative to the north-east-down frame. This is a 3 DOF (degrees of freedom) task.

Angle φ is connected to the angle ψ by $\varphi = \psi - \frac{\pi}{2}$.

The kinematics of this system can be presented as [50]

$$\begin{bmatrix} \dot{x} \\ \dot{y} \\ \dot{\psi} \end{bmatrix} = \begin{bmatrix} \cos \psi & -\sin \psi & 0 \\ \sin \psi & \cos \psi & 0 \\ 0 & 0 & 1 \end{bmatrix} \begin{bmatrix} u \\ v \\ r \end{bmatrix} \quad (71)$$

where (x, y) denote the coordinates of the center of mass of the vessel in the earth-fixed frame, ψ is the heading angle of the vessel, and u, v, r are the velocities of surge, sway and yaw, respectively.

Concerning ASV, following assumptions are made:

- the disturbing environment forces due to wind, currents and waves can be neglected;
- the inertia matrices added mass matrices and hydrodynamic damping matrices are diagonal.

The simplified mechanical model for of the analyzed ASV can be presented by the following equations [51]

$$\dot{u} = \frac{m_{22}}{m_{11}} vr - \frac{d_{11}}{m_{11}} u + \frac{1}{m_{11}} t_1, \quad (72)$$

$$\dot{v} = -\frac{m_{11}}{m_{22}} ur - \frac{d_{22}}{m_{22}} v, \quad (73)$$

$$\dot{r} = \frac{m_{11} - m_{22}}{m_{33}} uv - \frac{d_{33}}{m_{33}} r + \frac{1}{m_{33}} t_2 \quad (74)$$

where $m_{ii} > 0, i=1,2,3$ model the vessel inertia and the added mass effects, $d_{ii} > 0, i=1,2,3$ describe the hydrodynamic damping, m_{ii} and d_{ii} are assumed to be constant, and t_1, t_2 specify the surge control force and the yaw control moment, respectively.

The parameters m_{11} through m_{33} and d_{11} through d_{33} in (72)-(74) have the following values [49]:

$$m_{11} = 200 \text{ kg}, m_{22} = 250 \text{ kg}, m_{33} = 80 \text{ kg},$$

$$d_{11} = 70 \text{ kg}, d_{22} = 100 \frac{\text{kg}}{\text{s}}, d_{33} = 50 \frac{\text{kg}}{\text{s}}.$$

Next, the center of mass coordinates and heading angle are obtained by the integration

$$x(\tau) = \int_0^\tau \dot{x}(t) dt, y(\tau) = \int_0^\tau \dot{y}(t) dt, \Psi(\tau) = \int_0^\tau \dot{\Psi}(t) dt \quad (75)$$

where initial state $x(0) = 0, y(0) = 0, \Psi(0) = 0$.

We can see from (71)-(75) that the position coordinates and the heading angle of the ASV $(x, y, \Psi)^T$ can be computed on the basis of given set of equations and initial conditions. The non-linear object description and control task is described in Figure 30.

Simulation results

The Simulink block-scheme, allowing simultaneously compare the predictive neural control and simple proportional feedback control methods, is presented in Figure 31. For the initial parts of trajectories the constant surge control force $t_1 = 50 \text{ N}$ and feedback-controlled control moment t_2 were applied in order to achieve the desired heading angle.

For the final circular motion phases the constant yaw control moment $t_{21} = 5 \text{ Nm}$ was applied.

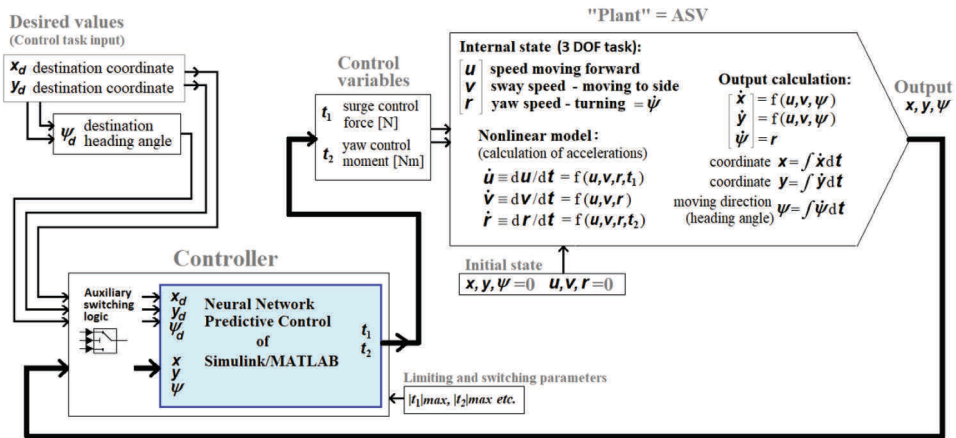


Figure 30 – Description of autonomous surface vehicle task; non-linear mathematical model with three main variables and three secondary output variables and the control block that uses pretrained NN Predictive controller.

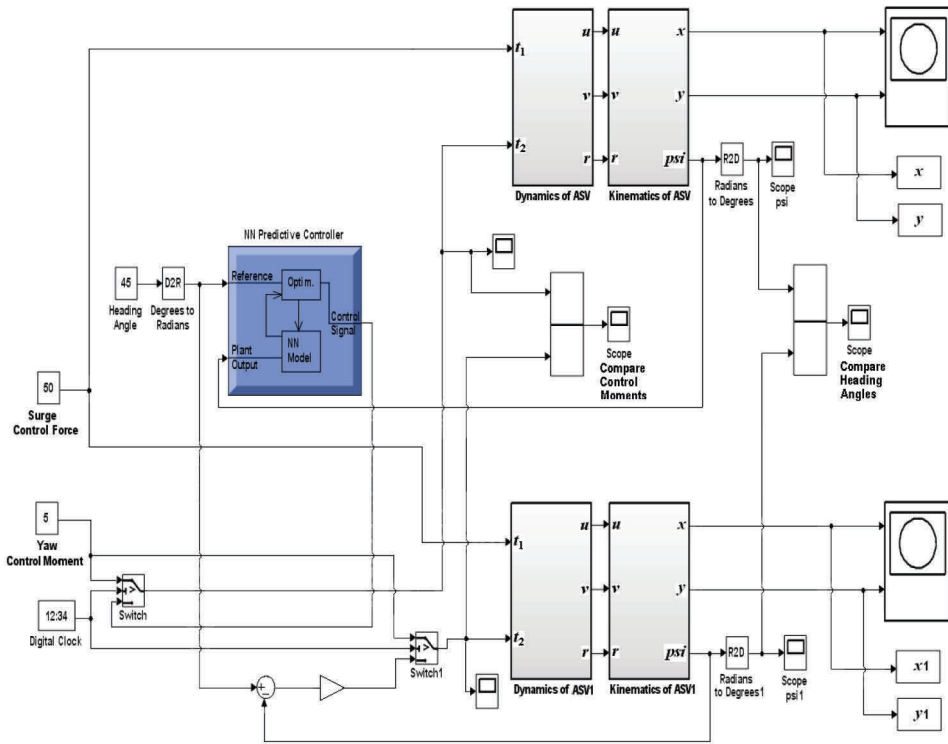


Figure 31 – Simulink block diagram for simultaneous behavior analysis for ASV with predictive neural controller (upper part) and with simple proportional tracking controller (lower part) in the feedback loop.

Simulation results provide comparison for the two control methods. The resulting trajectories of ASV for two control methods and two heading angles can be also analyzed. The main control quality parameters for basic and advanced control methods are summarized in Tables 4, 5 and Figures 32, 33.

Table 4 – Comparison of control system performance parameters for simple proportional feedback and neural control approaches at 45-degree heading angle

Systems	Rise Time (t_r)	Time to First Peak (t_p)	Settling Time (t_s)	Overshoot (O)	Decay Ratio (DR)
Feedback Control	23 s	45 s	670 s	78%	77%
Neural Control	17 s	25 s	100 s	33%	26%

Table 5 – Comparison of control system performance parameters for simple proportional feedback and neural control approaches at 135-degree heading angle

Systems	Rise Time (t_r)	Time to First Peak (t_p)	Settling Time (t_s)	Overshoot (O)	Decay Ratio (DR)
Feedback Control	27 s	46 s	580 s	44%	61%
Neural Control	31 s	45 s	120 s	20%	18%

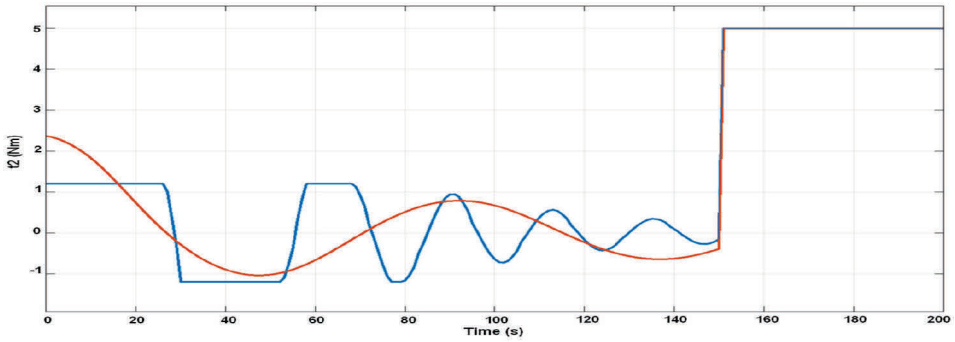


Figure 32 – Comparison of input control signals (yaw moment) of ASV in cases of simple proportional feedback control (red) and neural control (blue) for desired 135-degree heading angle.

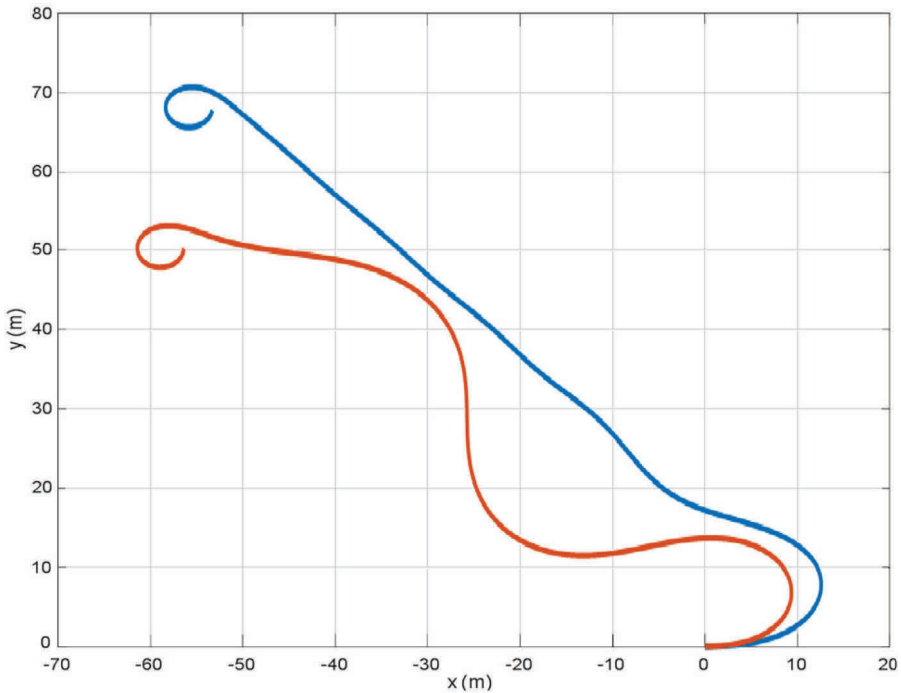


Figure 33 – Comparison of ASV trajectories for simple proportional feedback control (red) and neural control (blue) cases for desired 135-degree heading angle.

The simulation results clearly confirm the superiority of the predictive neural network control approach over the basic proportional feedback tracking method in order to assure the smoothness, fast response, and accuracy trajectory of control. Strictly speaking, demonstrated results even indicate that the traditional proportional feedback method cannot guarantee satisfactory quality of management at all, as it is constantly lagging behind in applying the necessary influences. Necessity of application of neural control approaches with predictive ability may be also formulated as a necessity of introduction of AI methods into control of AUV's. Although many details of this study are associated with the actual ASV model, the proposed model-based research approach may be extended to other types of automated surface vessels and AUV's.

3.8 Flight control of small size multirotor UAV

Contributing publication 6 [77] provides answer to the RQ6 of current thesis, how to develop flight control system for the disturbance sensitive small multi-rotor UAV?

The three-rotor UAV is composed of three rotors. It is clear that one of the advantages of trirotors with respect to quadrotors is that they require one motor less which can lead to a reduction in weight, volume and energy consumption and also design and manufacturing cost. The two main rotors in the forward part of the trirotor rotate in opposite directions and are fixed to the aircraft frame. The tail rotor can be tilted using a servomechanism.

The mechanical model of 3 rotor mini UAV with four control variables (3 rotor forces and tail rotor angle) is described by Figure 34.

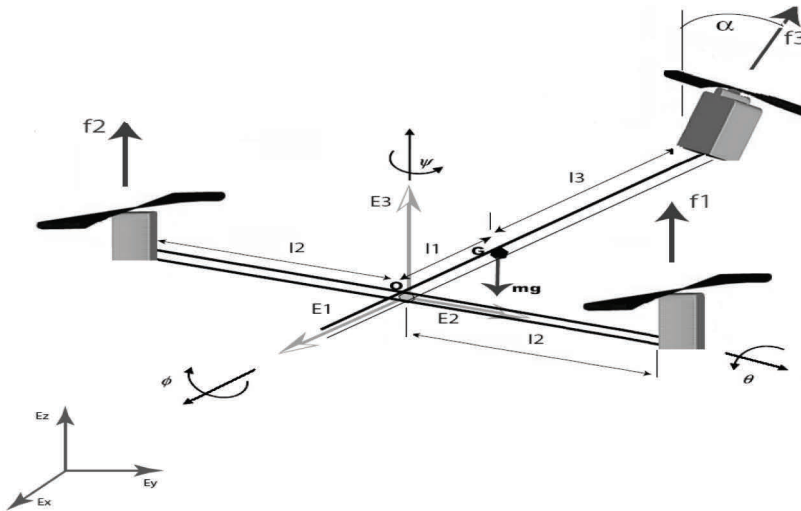


Figure 34 – Illustrative example for three-rotor UAV. The two main rotors in the forward part of the trirotor rotate in opposite directions. They are also fixed to the aircraft frame. Tail rotor can be tilted using a servomechanism.

The dynamics of the three-rotor UAV for the case of low speeds of motion can be represented by the following equations [91], [92]:

$$\ddot{x} = \frac{-\tau_4 \sin \theta}{m}, \quad (76)$$

$$\ddot{y} = \frac{\tau_4 \cos \theta \sin \phi}{m}, \quad (77)$$

$$\ddot{z} = \frac{\tau_4 \cos \theta \cos \phi}{m} - g, \quad (78)$$

$$JW\ddot{\eta} + J\dot{W}\dot{\eta} + W\dot{\eta} \times JW\dot{\eta} = \tau \quad (79)$$

where

$$\eta = \begin{bmatrix} \psi \\ \theta \\ \phi \end{bmatrix},$$

$$W = \begin{bmatrix} 0 & -\sin \psi & \cos \psi \cos \theta \\ 0 & \cos \psi & \sin \psi \cos \theta \\ 1 & 0 & -\sin \theta \end{bmatrix},$$

$$\dot{W} = \begin{bmatrix} 0 & -\cos \psi & -\cos \psi \sin \theta - \cos \theta \sin \psi \\ 0 & -\sin \psi & -\sin \psi \sin \theta + \cos \theta \cos \psi \\ 0 & 0 & -\cos \theta \end{bmatrix},$$

$$\tau = \begin{bmatrix} \tau_1 \\ \tau_2 \\ \tau_3 \end{bmatrix},$$

$$\tau_1 = l_2(f_1 - f_2),$$

$$\tau_2 = -l_1(f_1 + f_2) + l_3 f_3 \cos \alpha,$$

$$\tau_3 = -l_3 f_3 \sin \alpha,$$

$$\tau_4 = f_1 + f_2 + f_3 \cos \alpha, \quad (80)$$

with denotations:

x, y, z for coordinates of center of mass in the earth-frame;

ψ, θ, ϕ for yaw, pitch and roll angles;

α for the tilting angle of third rotor;

$f_i (i = 1, 2, 3)$ for the thrust generated by the i -th rotor;

l_1 for the distance from the centre of mass to the centre of line between the first and second rotors;

$2l_2$ for the distance between the first and second rotors;

l_3 for the distance from the centre of mass to the third rotor;

J for the inertia matrix;

g for the gravity constant;

m for the mass of the UAV.

Note that exists an orientation of body frame in which the inertia matrix in (79) simplifies to:

$$J = \text{diag}(I_x, I_y, I_z). \quad (81)$$

For simplicity we consider the matrix J in (81) as unit matrix, i.e.

$$J = \text{diag}(1, 1, 1),$$

$$\text{where } I_x = I_y = I_z = 1 \text{ kgm}^2 \quad (82)$$

Substituting (82) into (79), we obtain

$$W\ddot{\eta} + \dot{W}\dot{\eta} + W\dot{\eta} \times W\dot{\eta} = \tau. \quad (83)$$

If we apply the properties of vector product to (83), we obtain

$$W\ddot{\eta} + \dot{W}\dot{\eta} = \tau. \quad (84)$$

From (84), we have

$$\ddot{\eta} = W^{-1}\tau - W^{-1}\dot{W}\dot{\eta} \quad (85)$$

where

$$W^{-1} = \frac{1}{\cos\theta} \begin{bmatrix} \cos\psi \sin\theta & \sin\psi \sin\theta & \cos\theta \\ -\sin\psi \cos\theta & \cos\psi \cos\theta & 0 \\ \cos\psi & \sin\psi & 0 \end{bmatrix}. \quad (86)$$

We can regroup the three dynamics equations in (85) as

$$\ddot{\psi} = \dot{\theta}g\theta + \dot{\phi}\sec\theta + \tau_1tg\theta\cos\psi + \tau_2tg\theta\sin\psi + \tau_3, \quad (87)$$

$$\ddot{\theta} = -\dot{\phi}\cos\theta - \tau_1\sin\psi + \tau_2\cos\psi, \quad (88)$$

$$\ddot{\phi} = \dot{\theta}\sec\theta + \dot{\phi}g\theta + \tau_1\cos\psi\sec\theta + \tau_2\sin\psi\sec\theta. \quad (89)$$

From (76)–(78), (87)–(89) we can see that the attitude vector $(x, y, z)^T$ for given model of UAV can be computed.

The numerical values for three-rotor UAV's constant parameters of (76)–(80) for a case of small elevation above sea level are given by [91]:

$$m = 0.5 \text{ kg},$$

$$l_1 = 0.07 \text{ m}, l_2 = 0.24 \text{ m}, l_3 = 0.33 \text{ m},$$

$$g = 9.81 \text{ m/s}^2.$$

Control system with control of collective thrust can be formulated as show below. Note that the inputs in (80) then can be represented in matrix form as

$$\begin{bmatrix} \tau_1 \\ \tau_2 \\ \tau_3 \end{bmatrix} = \begin{bmatrix} l_2 & -l_2 & 0 \\ -l_1 & -l_1 & l_3 \cos \alpha \\ 0 & 0 & -l_3 \sin \alpha \end{bmatrix} \begin{bmatrix} f_1 \\ f_2 \\ f_3 \end{bmatrix}. \quad (90)$$

Then the individual forces in (90) will be

$$\begin{bmatrix} f_1 \\ f_2 \\ f_3 \end{bmatrix} = -\frac{1}{2} \begin{bmatrix} -\frac{1}{l_2} & \frac{1}{l_1} & \frac{ctg\alpha}{l_1} \\ \frac{1}{l_2} & \frac{1}{l_1} & \frac{ctg\alpha}{l_1} \\ 0 & 0 & \frac{2}{l_3 \sin \alpha} \end{bmatrix} \begin{bmatrix} \tau_1 \\ \tau_2 \\ \tau_3 \end{bmatrix}. \quad (91)$$

It is possible to consider the thrusts f_1 and f_2 in (80) as constant functions of time with one value. Hence, we have

$$f_1 = f_2 = \text{const}. \quad (92)$$

Hence

$$\tau_1 = 0. \quad (93)$$

Combining (89) and (92), we can write

$$\tau_2 = -2f_1(l_1 + l_3) + l_3\tau_4 . \quad (93)$$

Then, from (80) and (92), it follows that

$$\tau_3 = l_3 \operatorname{tg} \alpha (2f_1 - \tau_4) . \quad (94)$$

It is possible to consider the tilting angle α in (80) as a constant angle. Here, we take

$$\alpha = \operatorname{const} . \quad (95)$$

With selection of (92)-(95), a complex control problem is now turned into a control problem with using only one collective thrust τ_4 as control input for controlling the coordinate Z of altitude with respect to reference input z^0 .

The main equation defining the control system (see Figure 35 below) to regulate the input variable τ_4 can be specified in the following form (proposed by author in [32])

$$\dot{\tau}_4 = K(t_1(z^0 - z) - t_2\dot{z} - \ddot{z}) \quad (96)$$

where t_1, t_2 are constants to be determined.

It is possible to consider the variable τ_4 as a "fast" function of time. Hence, assuming that $\dot{\tau}_4 \approx 0$, from (96), we find

$$\ddot{z} + t_2\dot{z} + t_1z = t_1z^0 . \quad (97)$$

The following coefficients of (97) are obtained from [92], for overshooting with value of $\sigma \approx 5\%$

$$t_1 \approx \frac{9}{t_{d_z}^2}, t_2 \approx \frac{3\sqrt{2}}{t_{d_z}} \quad (98)$$

where t_{d_z} is desired transition time of coordinate Z .

For a hovering flight, angles of roll, pitch, and yaw must be zeros. Therefore, it follows from (78) that

$$\ddot{z}(t) = b\tau_4(t) - g \quad (99)$$

where

$$b \approx \frac{1}{m} . \quad (100)$$

Differentiating both sides of (99) with respect to time, we obtain

$$\ddot{z}(t) = b\dot{\tau}_4(t) . \quad (101)$$

Combining (96) and (101), we have

$$\ddot{z}(t) = bK (i_3(t) - \dot{z}(t)) \quad (102)$$

where

$$i_3(t) = t_1(z^0 - z(t)) - t_2\dot{z}(t). \quad (103)$$

Defining $\ddot{z}(t) = a(t)$ in (102), we obtain

$$\dot{a}(t) = bKi_3(t) - bKa(t) . \quad (104)$$

The variable $a(t)$ in (104) can be described in a common way through next expression

$$a(t) = (a_0 + \int_0^t e^{-A(\tau)} bKi_3(\tau) d\tau) e^{A(t)}, \quad (105)$$

where

$$A(t) = -\int_0^t bK d\tau . \quad (106)$$

Let us consider the behavior of the considered control system (see Figure 35) for the time t of time interval $t \geq t_{dz}$ during the hovering.

Hence, assuming that $a_0 = 0$, $z^0 - z(t) \approx \Delta z^0$, $\Delta = 0.05$, $\dot{z}(t) \approx 0$, from (105)–(106), we find

$$a(t) = i_3(1 - e^{-bKt}) \quad (107)$$

where

$$i_3(t) \approx t_1\Delta z^0 \approx const. \quad (108)$$

Assume now that for the desired transition time for control of acceleration $a(t)$ lies in the zone of overshooting with value of $\sigma \approx 5\%$, then, from (107)–(108), it follows that

$$t_{dz} \approx -\frac{\ln(\Delta)}{bK} . \quad (109)$$

Therefore, using (100) and (109), and the ratio of coordinate-to-acceleration transition times $N = \frac{t_{dz}}{t_{d\ddot{z}}}$ and that $\ln(\Delta) \approx -3$, we obtain

$$K \approx \frac{3Nm}{t_{dz}}. \quad (110)$$

Simulation results for control system with control of collective thrust. In this section, we present numerical example to evaluate the proposed technique in scenario involving control of the considered maneuver.

Consider the control of trirotor UAV model (76)–(78), (87)–(89) for the case of take-off and hovering maneuvers by hybrid constrained system of two control subsystems.

The goal of the following simulations is twofold. First, to verify that these control subsystems are able to control the take-off and hovering trajectories. Secondly to test achieving of such trajectory parameters as desired transition times, ratios of coordinate-to-acceleration transition times and heights of hovering of tri-rotor mini UAV.

Constant thrust forces of the first and second rotors, constant tilting angle of the third rotor, initial conditions, desired height positions, ratios of coordinate-to-acceleration transition times and desired transition times for control subsystems are chosen to be:

$$\begin{aligned} f_1 &= f_2 = 2.4 \text{ N}, \\ \alpha &= 89 \text{ deg}, \\ x(0) &= y(0) = z(0) = 0 \text{ m}, \\ z_1^0 &= 3 \text{ m}, \quad z_2^0 = 8 \text{ m}, \\ N_1 &= 40, \quad N_2 = 15, \\ t_{d1} &= 3 \text{ s}, \quad t_{d2} = 12 \text{ s}. \end{aligned}$$

Simulation results of the offered block scheme with two control subsystems (see Figure 35) are shown in Figures 36–40. Achieving of the desired height trajectory is shown on Figure 36.

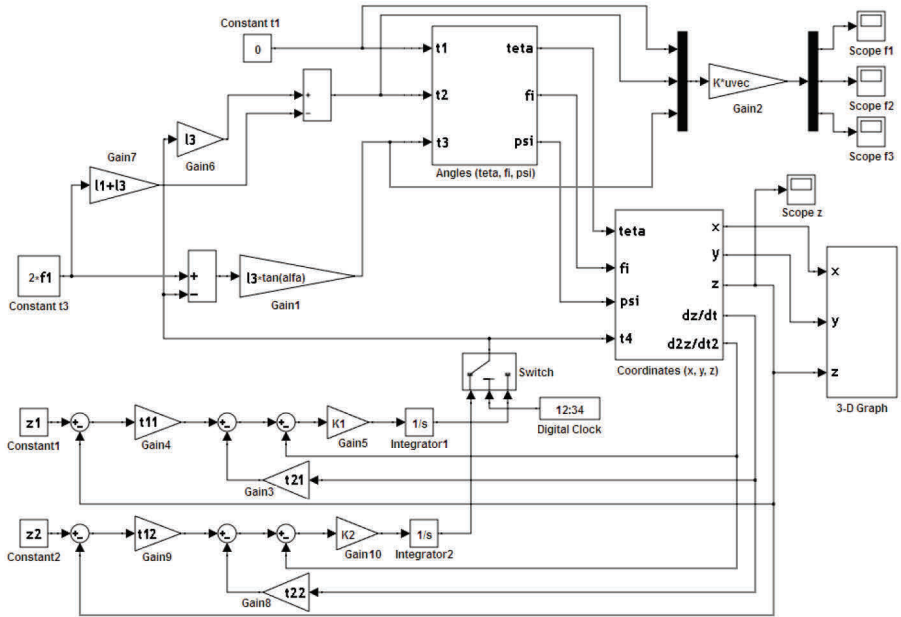


Figure 35 – Block diagram of hybrid control system with two control subsystems.

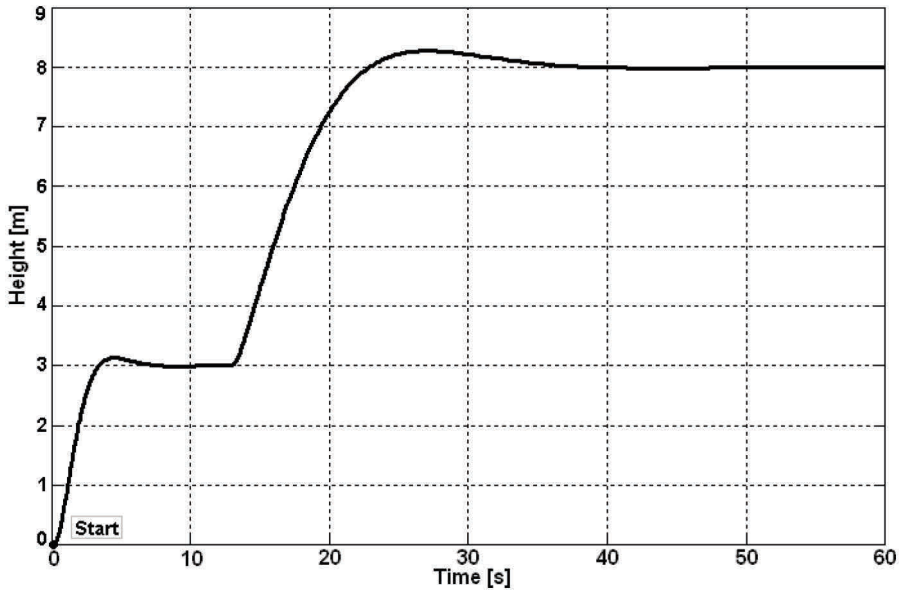


Figure 36 – Tri-rotor UAV height trajectory simulation results.

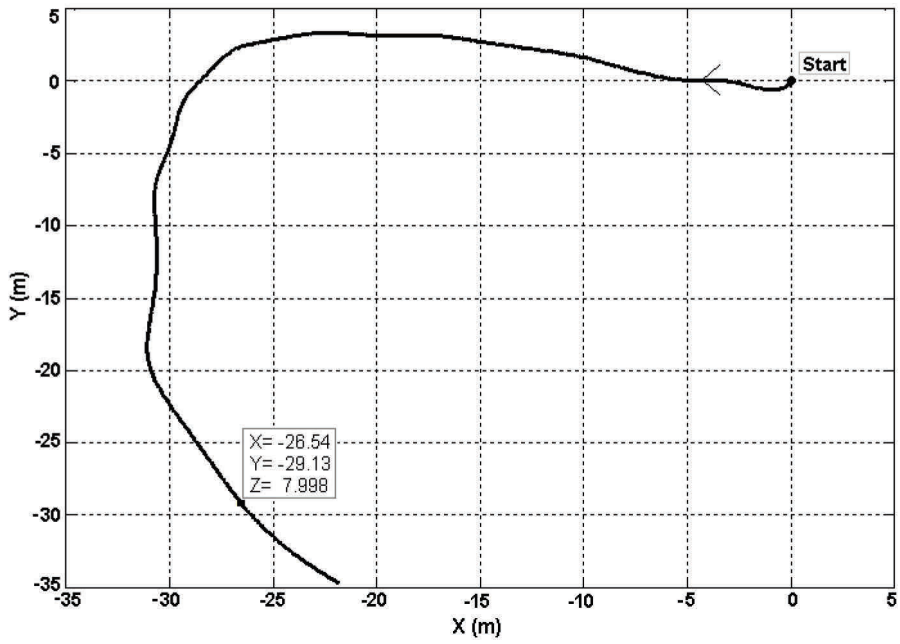


Figure 37 – X-Y view of tri-rotor UAV trajectory.

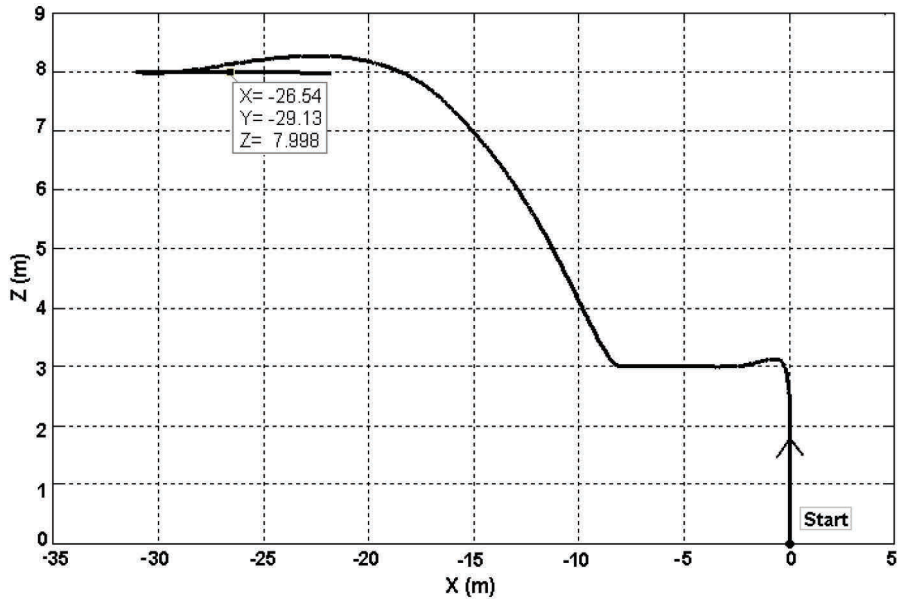


Figure 38 – X-Z view of tri-rotor UAV trajectory.

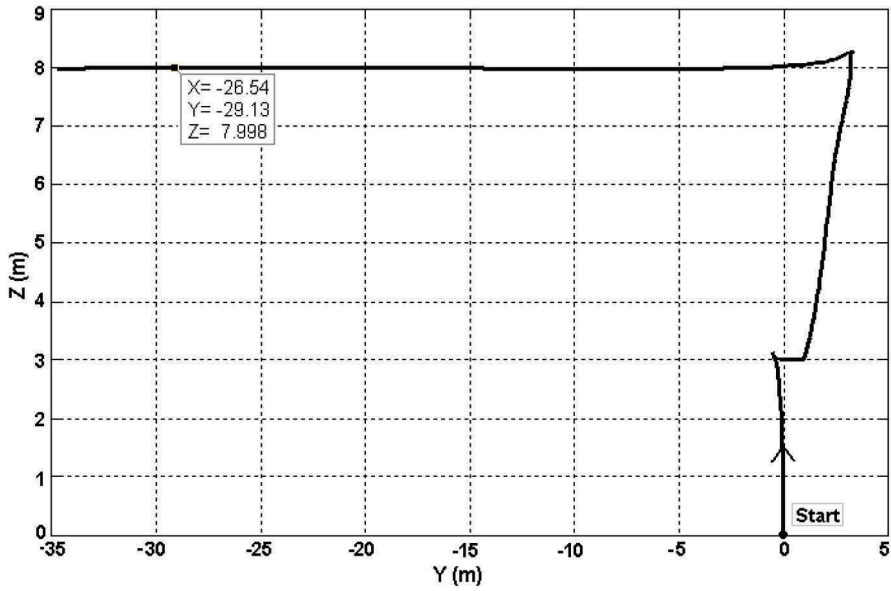


Figure 39 – Y-Z view of tri-rotor UAV trajectory.

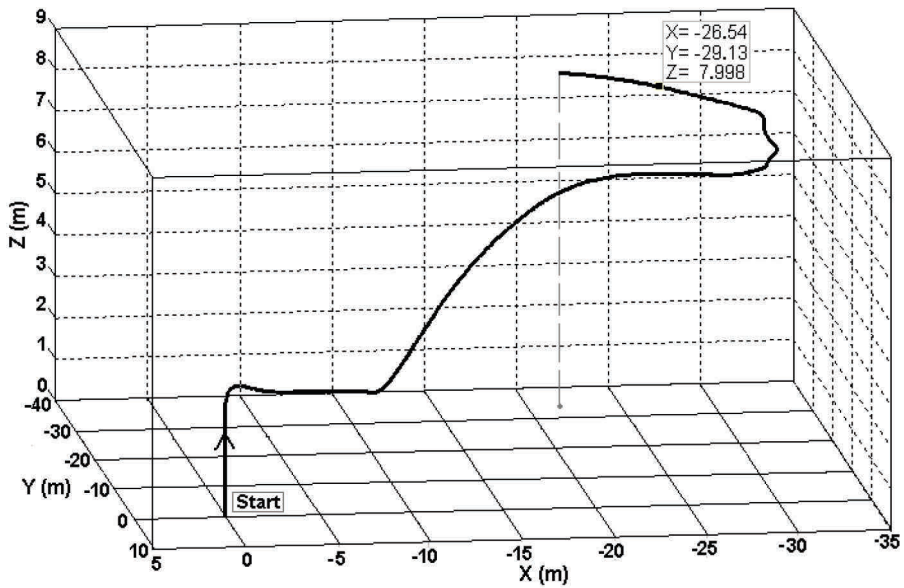


Figure 40 – 3-D motion trajectory of the tri-rotor UAV flight.

On the basis of mathematical model equations were constructed the block diagrams of subsystems as parts of hybrid control system (Figure 35). The full take-off and hovering trajectory was separated into two phases with time-dependent switching instant in the middle.

Numerical experiment demonstrated functioning of the proposed control mathematics and methodology:

- The desired transition times of 3 sec. and 12 sec. were achieved (see Figure 36);
- The overshoot values of height stabilization trajectory remained within desired 5% range;
- Combined use of two control subsystems forming the hybrid control system.

3.9 Summary of different objects and control systems studied

The generalized mechanical complexity (6 DOF) of different vehicles is described by Figure 41. Note that the control task may include more or less state variables than 6, depending on the level of detail of control task.

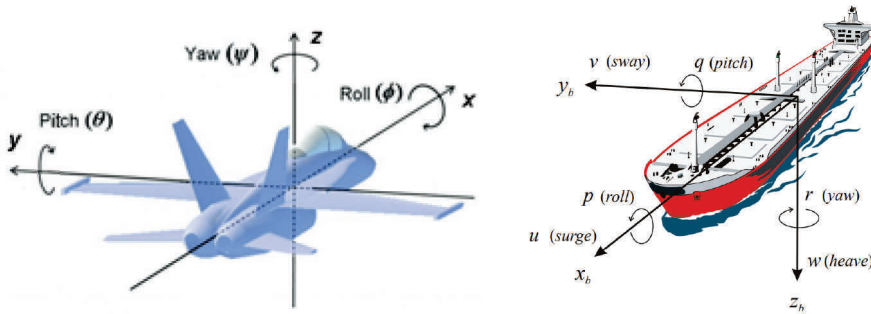


Figure 41 – Definition of 6 DOF (degrees of freedom) general mechanical task of movement of aircraft, drone or ship. In the case of restricted movement (e.g. surface vessel or autonomous car) the number of DOF may be reduced (data from [52]).

The summary of different types of autonomous vehicles considered in current thesis is consolidated in Table 6 below. The introduced and tested special features of different control systems are summarized in Table 7 below.

As a comment to Table 7 it should be mentioned that MATLAB/Simulink environment contains 3 main types of neural controllers [53]:

- NN Predictive controller;
- NARMA-L2 (Nonlinear Auto Regressive Moving Average) controller;
- Model-Reference neural controller.

In current thesis the two first mentioned types are used in different studies that were published after year 2012 (see Table 7). In addition to this, in earlier publications the ADALINE (ADAPtive Linear NEuron) principle based simple neural blocks were realized by authors without using standard neural controller blocks offered by MATLAB/Simulink. In some earlier publications between 2004 and 2008 also the Fuzzy Logic blocks of MATLAB/Simulink environment were applied (see Tables 6 and 7).

Table 6 – Summary of descriptive features and results of modelling and simulation of different studied autonomous vehicles.

No.	Object AV	Conferences and publications	Object model characterization	Control systems characterization	Goals	Main Results
1.	One rotor miniature (3.6 kg) helicopter	ICCAS 2008 [70], ICECE 2008 [71]	Nonlinear, 5 state variables, 2 input and 2 output var.	1 or 2 ADALINE (ADaptive 2-layer Linear NEural network style) controllers realized	Reliable control of destination height, testing usability of ADALINE idea	Two ADALINE controller models realized for 2 flight stages, exact (few cm) and fast (< 1 s) control of helicopter height demonstrated, necessity of separate controllers for take-off and hovering concluded, <u>work very well accepted (11 citations to [70])</u>
2.	One rotor intermediate (1962 kg) helicopter	ICIMA 2009 [80]	Nonlinear aerodynamics, 3 main state and output variables, 1 control variable (rotor pitch)	Specially designed nonlinear	Achieve desired transition times to another height	Methodology of to control nonlinear aerodynamics tested, achievability of wanted transition times (10s, 5s, 4s) with 5% overshoot limit demonstrated
3.	Two coaxial rotors (ducted fan) UAV (160 kg)	ICCAIS 2012 [82], SISY 2018 [81], SYSCON 2019 [67]	Linear system, full single rate task 9 variables in state vector and in output vector, 4 control variables. Noises (process and output) possibility included	Trainable neural networks based standard controllers NARMA-L2 of Simulink/MATLAB were used	Demonstrate multi-rate decomposition possibility, reduce the overshoot and settling time of transient processes	Correctness of matrices transformation methodology verified by simulation, possibility to reduce the settling times by factor of 2 and height establishing overshoots by factor of 3-5 due to multi-rate methodology were shown

4.	Three-rotor mini-UAV (0.5 kg)	ACMOS 2010 [62], ICAAE 2010 [77]	Nonlinear, 6 DOF task, 4 control variables (3 rotor forces + tilting angle of tail rotor)	Specially designed nonlinear for 2 flight stages	Test 3-rotor UAV control methodology, achieve desired transition times within given overshoot limits	Modelling methodology of 3-rotor drone control developed and tested by simulation, desired 2 height levels achieved with given transition times within given overshoot limits
5.	Four-rotor quadrotor mini-UAV (0.56 kg)	ACMOS 2011 [63], ICIA 2010 [60], CSCC 2010 [64]	Nonlinear, state and output 6 DOF (3 coordinates + 3 angles), 4 control variables (sums and differences of rotor forces)	Specially designed nonlinear for 2 flight stages, 2 parts (control of forces and angles)	Test 4-rotor control UAV methodology, achieve desired roll angle and transition times	Methodology of 4-rotor drone control developed and tested, desired roll angle and height values (6 m and 20 m) achieved with short (2 s) and long (28 s) transition times within specified overshoot limit 5% demonstrated
6.	X4-flyer mini-UAV (two swiveling rotors, 2.5 kg)	CSCC 2010 [83]	Nonlinear, 6 DOF task, full formulation with 6 control variables (4 forces + 2 swivelling angles)	Specially designed nonlinear for 2 flight stages	Test X4-flyer control methodology, achieve desired transition times within given overshoot limits	Modelling methodology of X4-flyer drone control developed and tested, transition to desired 2 height levels with short (3 s) and long (19 s) transition times within given overshoot limit 5% demonstrated
7.	Eight-rotor mini-UAV (1.2 kg)	CSCC 2011 [65], ICCESSE 2011 [66]	Nonlinear, 6 DOF, full formulation 12 control variables (4 vert. + 4 horizontal + 4 secondary forces due to air flow)	Specially designed nonlinear, control by rotor 3 and 4 forces	Test eight-rotor UAV control methodology, achieve desired transition times within given overshoot limits	Modelling methodology of eight-rotor drone control developed and tested, transition to desired 2 height levels with short (2 s) and long (30 s) transition times within given overshoot limit 5% demonstrated

8.	Underwater AUV (1630 kg)	ISCI 2011 [76], ICMA 2009 [78]	Linear, divided to 2 parts (4 + 4 state variables), 8 control variables (5 + 3), noises of process and output for both 2 parts included	Multi-rate division of matrix presentation to „slow“, „intermediate“ and „fast“ subsystems, in [73] Simulink/MATLAB NN Predictive control block used, in [78] ADALINE neural control (see above) used	Proving matrix mathematics correctness, assess control capability of diving, approaching and final circulation stages (fast, intermediate, slow)	Complex matrix transformations validated, desired motion of underwater AUV in simulation obtained, <u>work well recognized (4 citations to [76])</u>
9.	Surface ASV (200 kg)	CINTI-MACRo 2019 [79]	Nonlinear, 3 main state variables (3 DOF task with 2 speeds and heading angle), 2 control forces (surge and yaw)	NN Predictive control and simple proportional tracking control compared	Compare the difference between AI-based control and simple control	Unacceptable long delays of a simple tracking methodology clearly revealed, superiority and necessity of neural network-based control methods demonstrated

Table 7 – Summary of the introduced and tested features of different types of control systems.

No.	Control system feature	Conferences and publications	Control systems characterization	Goals and the main results
1.	Multi-rate decomposition of control task	SYSCON 2019 [67], ELEKTRO 2012 [69], ISAS 2004 [72], CCECE 2004 [73], SCI 2004 [74], WCICA 2004 [75], SYSCON 2019 [67], SISY 2018 [81], ICCAIS 2012 [82]	Linear matrix-based high order task replaced by 2 or 3 lower order tasks, in control system NARMA-L2 or NN Predictive controllers of Simulink/MATLAB environment trained and used	Offering matrix transformation methodology, achieving lowering of task order, demonstrate decrease of overshoot and settling times of transient processes
2.	Inclusion of neural network and fuzzy logic blocks in the control	ISAS 2004 [72], CCECE 2004 [73], SCI 2004 [74], WCICA 2004 [75]	Linear system of order 3 with 2 noise sources is decomposed to fast (order 1) and slow (order 2) subsystems, usage of LQG (Linear Quadratic Gaussian) controller of Simulink/MATLAB is realized and alternatively usage of ADALINE (linear 1-neuron) together with FL (fuzzy logic) blocks of Simulink/MATLAB are realized [75]	Applicability of combined neural fuzzy logic control in the case of two-rate decomposition is proven, <u>work well recognized (7 citations to [75])</u>
3.	Versatile testing of ADALINE neural control principle	ICCAS 2008 [70], ICECE 2008 [71]	1 or 2 ADALINE (ADaptive 2-layer Linear NEuron network style) controllers, realised from „scratch“	Demonstrate and test usability of simple 2-layer linear neural network style controllers
4.	Versatile testing of NARMA-L2 neural controllers of Simulink/MATLAB	ICCAIS 2012 [82], SISY 2018 [81], SYSCON 2019 [67]	Standard NARMA-L2 neural controller of Simulink/MATLAB, pretrained for hybrid multirate description of AV	Test usability together with complex matrix description of object for 3 stages of motion

5.	Testing of standard NN Predictive neural controller of Simulink/MATLAB	CINTI-MACRo 2019 [79]	NN Predictive controller of Simulink/MATLAB (recommended for strongly nonlinear tasks) compared with simple proportional tracking controller	Obtain quantitative proof of superiority of NN control with AI capability
6.	Specially designed height level transition controller	ICIMA 2009 [80], ACMOS 2011 [63], ICIA 2010 [60], CSCC 2010 [64]	Specially designed height level transition controller with possibility to achieve the desired transition times	Applicability confirmed, achieved desired transition times within given overshoot, <u>very well accepted work</u> (16 citations to [80])

4. Conclusions and further research

4.1 Conclusions

The main results described by the present thesis can be summarised in the following way:

1. Methodology for trajectory control of different types of AVs is developed. Methodology includes formulation of mathematical models, their integration to MATLAB/Simulink environment, specification of trajectory control targets, simulation experiment realizations, path output data analysis and processing.
2. Control systems for wide range of unmanned autonomous vehicle types are tested in modelling and simulation. The detailed description of main 9 types of studied AVs is presented in Table 6 above. From simple to more complex, the list of considered examples includes:
 - 1) One rotor miniature helicopter [70], [71]. ADALINE type controllers realized and applied, exact and fast control of helicopter height control obtained.
 - 2) One rotor intermediate helicopter [80]. Nonlinear aerodynamics modelled, specially designed non-linear controller applied, desired transition times to different heights with limited overshoot demonstrated.
 - 3) Two rotors coaxial rotor/ducted fan UAV. Matrix transformation methodology for single-rate [67], two-rate [81], three-rate [82] linear object modelling as well as methodology of MATLAB/Simulink NARMA-L2 neural controllers application developed, achieving of reduced settling times and overshoot values in the case of multi-rate control demonstrated.
 - 4) Three rotor mini-UAV [62], [77]. Nonlinear object modeling with 3 input forces and one rotor angle considered, specially designed height level transition controller functioning confirmed by simulation, desired short and long height transition times within given overshoot limit achieved.
 - 5) Four rotor quadrotor mini-UAV [60], [63], [64]. Special non-linear control for 2 flight stages and separate control for forces and angles designed, working methodology for 4 rotor drone demonstrated.
 - 6) X4-flyer mini-UAV (two swiveling rotors) [64]. Extended four rotor drone task with added control of angles of two rotors considered, specially designed height level transition controller functioning confirmed and achievement of desired short and long height transition times within given overshoot limits demonstrated.
 - 7) Eight rotors mini-UAV [65], [66]. Complex 8-rotor drone task with 8 primary and 4 secondary forces modelled, achievement of desired short and long height establishing times within given overshoot limit demonstrated.
 - 8) Underwater AUV [76], [78]. Linear control task divided to 2 parts, noises added, three-rate decomposition methodology implemented and tested, ADALINE [78] or NN Predictive control [76] applied, desired depth level changes of AUV obtained in simulations.
 - 9) Surface ASV [79]. Non-linear, 3 main state variables 3 DOF task, NN Predictive control compared with simple proportional control, superiority and necessity of NN based control demonstrated by direct comparison.

3. Advanced and novel approaches relevant to control systems were introduced and tested. The detailed description of introduced features and results is given in Table 7 above. Short summary of mentioned features includes:
 - 1) Multi-rate (two-rate and three-rate) parallel operation methodology based on state equations matrix A eigenvalues mathematics, discussed by Author since 2000 [52], [67], [69], [72], [73], [74], [75], [67], [81], [82]. Applicability of proposed system decomposition confirmed by MATLAB/Simulink simulations, improvements of control quality (reduced settling times, overshoots) demonstrated.
 - 2) Combination of simple 1-layer NN and standard MATLAB Fuzzy logic blocks in the control scheme, in order to enhance the control system with predictive AI capabilities and to minimize unwanted influence of stochastic noises: [72], [73], [74], [75]. Applicability of combined NN and Fuzzy Logic control methodology proven with specific control tasks.
 - 3) Adaptive linear neuron principle (ADALINE) testing [70]. Realization of 1 or 2 layer NN structures in control blocks, proof of applicability.
 - 4) Application of Nonlinear Auto Regressive Moving Average (NARMA-L2) controllers of MATLAB/Simulink environment [67], [81], [82]. Pretraining methodology tested, co-functioning together with multi-rate decomposition methodology confirmed, improved accounting of objects dynamics by NN based control approaches approved.
 - 5) Application of Predictive NN controllers of MATLAB/Simulink environment [79]. The same positive results hold than that of NARMA-L2. In addition, reliable applicability in the case of strongly non-linear control task of a surface vessel demonstrated.
 - 6) Specially designed non-linear controllers [60], [63], [64], [80]. The desired transition times within given overshoot limits achieved for different weight class UAV models.
4. Proposing the idea to extend the multi-rate control methodology to the field of demand and supply chain management in manufacturing environment [54]. More detailed description is presented below in section 4.2.

4.2 Extensions of methodology to other application fields

The control approaches described above can be extended to different applications fields. Improved control of the modern industry supply chain is considered by author in publication "Demand and Supply Chain Simulation in Telecommunication Industry by Multi-Rate Expert Systems" [54].

Intelligent unmanned autonomous systems are important applications of AI, they can be considered as complex systems created by fusion of various technologies related to mechanics, control, computer, communication and materials [55]. There are many definitions for the Complex System. In the recent years the scientific community has coined the rubric 'complex system' to describe phenomena, structure, aggregates, organisms, or problems that share some common theme [56]:

- They are inherently complicated or intricate;
- They are rarely completely deterministic;
- Mathematical models of the system are usually complex and involve non-linear, ill posed or chaotic behaviour;
- The systems are predisposed to unexpected outcomes.

During the research phase of thesis and many numerical experiments conducted with proposed object model decomposition and advanced controller realizations, the author has discussed the possibility to implement the proposed approaches also for different applications, not only related to unmanned vehicles.

Manufacturing operations are facing continuous challenge to stay competitive in global environment. Industrialists are continuously striving to increase productivity by introducing new technologies and production control systems [57]. Industry wide targets have been set up for monitoring and controlling the critical Key Performance Indicators (KPI's). In [54], the author of current thesis has proposed the use of Multi-Rate Expert Systems to improve the Demand and Supply Chain efficiency for the Telecommunications industry. This idea provides answer to the RQ6 of current thesis, to explore the alternative fields of implementation for the proposed advanced multi-rate control. The approach is in line with latest trends for manufacturing, including Industry 4.0 that is referring to new phase in the Industrial Revolution that focuses heavily on interconnectivity, automation, machine learning and real-time data.

In a modern telecommunications industry, demand and supply chain management (DSCM) needs reliable design and versatile tools to control the material flow. Industry 4.0 solutions provide operations with greater insight, control and data visibility across their entire operations. The objective for efficient DSCM is to reduce inventories, lead times and related costs in order to assure reliable and on-time deliveries from manufacturing units towards customers. Supply chain management (SCM) is the combination of art and science that goes into improving the way production company finds the raw components it needs to make a product or service and deliver it to customers [58]. Multi-rate expert system-based methodology is proposed to support developing simulation tools that enable optimal DSCM design for multi region, high volume, and high complexity manufacturing operations.

Modern telecommunication assembly production line is continuously working with 30 to 50 component suppliers and 300 to 400 different components. Component lead times could vary from few hours to several weeks. To minimize component buffers and tied-up capital in supply chain, planning and timing the components availability plays significant role. In a manufacturing supply chain, information about the end customer's demand is often distorted from one end of the supply chain to the other [84]. This phenomenon is called the Forrester effect (see Figure 42). Distortions in demand information often occur as we move further upstream in the supply chain, because each member makes decisions based on the information it receives from the subsequent member in the supply chain.

FORRESTER EFFECT: small changes in end user demand get amplified in each stage of the chain

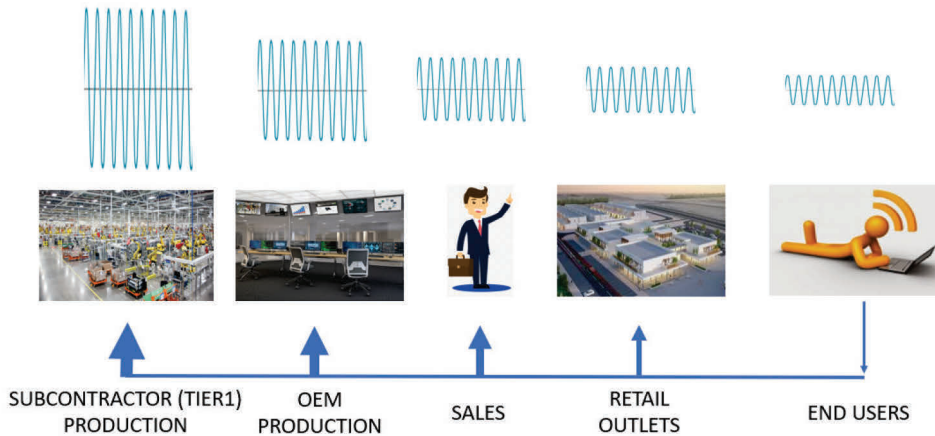


Figure 42 – Multi-rate expert systems are expected to reduce the Forrester effect throughout the whole supply chain. Demand fluctuations by different supply chain stakeholders can cause costly shortages or excess buffering.

Practical actions to improve efficiency in SCM are as follows.

- Set up continuous visibility to channel inventory demand information through the whole supply chain;
- Share the centralized demand information in the whole supply chain continuously;
- Plan and execute based on actual end user demand.

Difference between gross and net demand requirements are illustrated on Figure 43. To minimize the risk for components availability in case of demand fluctuations, supplier managed inventory (SMI) is often used. Through SMI the focus is shifted from monitoring single deliveries to monitoring stock levels. SMI component buffers will be kept near to manufacturing unit, providing necessary flexibility. Against forecasted demand, suppliers follow gross requirements and keep the component levels between agreed minimum and maximum levels. Traditional min & max levels are between 7 to 14 days. Keeping 14 days components in buffer ties-up lot of capital. Our intention was to prove that multi-rate expert systems could help manufacturing units release the capital from unnecessary component buffers by increased efficiency in demand-supply planning and demand-supply network management.

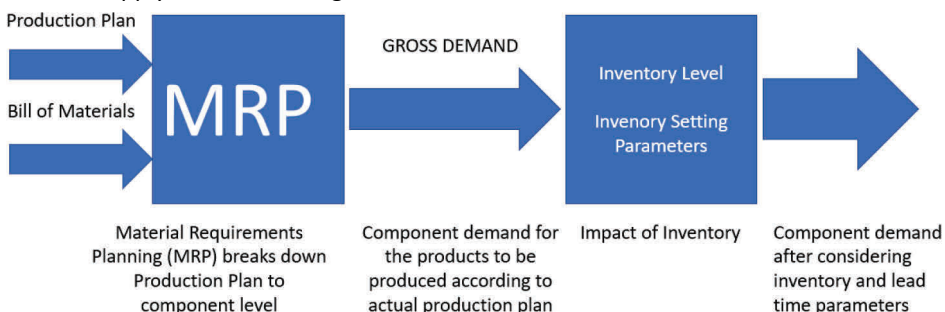


Figure 43 – Supplier managed inventory control is achievable by following gross requirements. Multi-rate expert systems may help manufacturing units to release the capital from unnecessary component buffers.

Applicable techniques and methods that could be useful for self-optimizing concepts and structures for supporting expert systems in DSCM can be divided into sub-symbolic and symbolic methods [85]:

- Sub-symbolic methods are based on neural net approaches. The capacity to learn makes NN a powerful tool for modelling cognitive abilities that develop and evolve over time [86]. The net can be trained by different training methods like supervised learning, unsupervised learning and reinforcement learning;
- Symbolic Methods are representing knowledge in a concrete form. They are influenced mainly by AI approaches [4]. The AI starts with symbols which represents parts of the world. There is problem with linking of real-world properties to symbols (the symbol grounding problem).

Author had focus to create self-optimizing structures by using fuzzy systems [87]–[88] and expert systems [89]. Proposed approach combines the above-mentioned methods in order to get the synergy effects. Optimizing methods similar to NN optimization and fuzzy logic was focused. The combination of NN and fuzzy logic has different goals. The ability to learn of NN and the white box behavior of fuzzy systems should be combined to get a learnable and symbolic interpretable overall system. Adding multi-rate control enables to define component level decision making priorities that are necessary for the tied-up capital and on-time deliveries management. The data has to be also readable also for a human operator.

User Controller Module (USM) was designed in [90]. In the DSCM modelling the USM will support the and structure the complex information processing. The USM consists of three parts: the multi-rate controller module, the reflective operator and the cognitive operator (Figure 44).

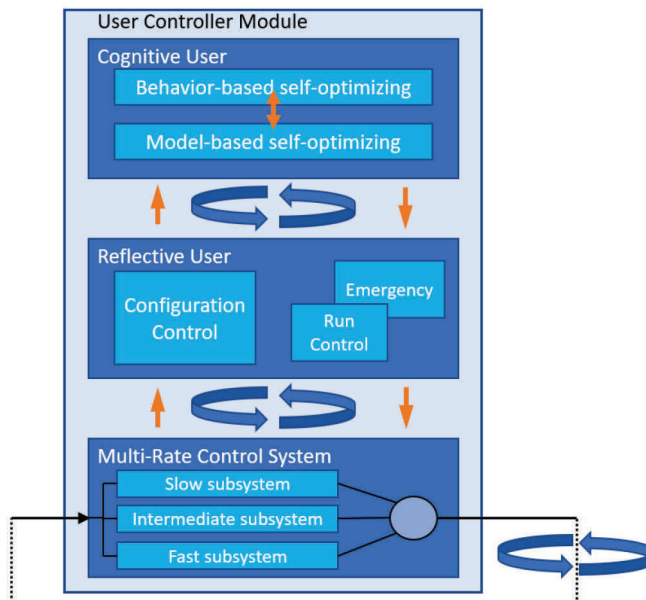


Figure 44 – Structure of information processing at the user-controller module. Localization of the neuro-fuzzy optimization takes place by the Cognitive User. Adoption of the optimization and controller switching is done by the Reflective User.

It is also possible to extend the proposed expert system with the capability to communicate with other UCMs and exchange the configuration information [91]. Resulting with collective set of UCM's that can communicate and exchange pre-stored fuzzy models.

The idea of supporting DSCM by multi-rate expert systems was proposed by author in [54]. Full supplier base could be categorized through different characteristics: actual component level lead times, agreed order quantities, current stock levels, latest forecasted demand, specific raw materials, geographical areas, etc. Component level attributes will form the continuously updated input data for the multi-rate UCM modelling tool. The different fuzzy configurations can be extracted and stored in an expert system. The expert system itself can restore configurations optimized before. Components with critical parameters will receive priority call-off recommendations from the fast subsystem, intermediate and slow subsystems will be defined accordingly to support the timely availability for non-critical component base.

4.3 Further research

As future work it may be proposed that the prototypes of considered AVs suitable for real world flight (movement) trials can be developed. It was confirmed by current thesis that proposed advanced neural control techniques can take into account real nonlinear behavior of AV's.

Presented results support the practical and theoretical predictions and demonstrate importance that proposed research techniques would help to design and implement model-based design for better autonomous devices and complex systems that work in harsh real-time conditions.

References

- [1] S. Hillemaier, S. Kriebel, E. Kusmenko, M. Lorang, B. Rumpe, A. Sema, G. Strobl, M. von Wenckstern. (2018). Model-Based Development of Self-Adaptive Autonomous Vehicles using the SMARTD Methodology. Proceedings of the 6th International Conference on Model-Driven Engineering and Software Development (MODELSWARD'18), SciTePress, pp. 163-178.
- [2] IHS Markit, 2020, The New Intelligence. Demand for Lidar systems to rise further with growing focus on self-driving vehicles. <https://ihsmarkit.com/index.html>. Accessed April 2020.
- [3] Roland Berger, (2020). Passenger drones ready for take-off. <https://www.rolandberger.com/en/Publications/Passenger-drones-ready-for-take-off.html>. Accessed April 2020.
- [4] A. Williams. (2015). Autonomous Systems. Issues for Defence Policymakers. NATO Capability Engineering and Innovation Division. https://www.act.nato.int/images/stories/media/capdev/capdev_02.pdf. Accessed April 2020.
- [5] Big Ideas 2020 by ARK Investment Management LLC. www.ark-invest.com. Accessed May 2020.
- [6] W. Schwarting, J. Mora, D. Rus. (2018). Planning and Decision-Making for Autonomous Vehicles. Annual Review of Control, Robotics, and Autonomous Systems. Annual Reviews 2018.
- [7] NATO Industrial Advisory Group, (2014). <https://www.ndia.org/divisions/systems-engineering>. Accessed April 2020.
- [8] B. Clough. (2000). Metric, Schmetrics! How the Heck Do You Determine UAV's Autonomy Anyway? Proceedings of AIAA 1st Technical Conference and Workshop on Unmanned Aerospace Vehicles. Air Force Research Lab., Wright-Patterson AFB, OH.
- [9] Society of Automotive Engineers. www.sae.org Accessed, April 2020.
- [10] A. Pedai and I. Astrov. (2014). Proactive approach to innovation management. International Journal of Social, Management, Economics and Business Engineering.
- [11] Report of the High-Level Group on Aviation Research. (2011). Flightpath 2050 Europe's Vision for Aviation. European Commission. Directorate-General for Research and Innovation. Directorate General for Mobility and Transport ISBN 978-92-79-19724-6.
- [12] G. Bernabei, C. Sassanelli, A. Corallo, M. Lazoi. A PLM-Based Approach for Un-manned Air System Design: A Proposal. May 26th, 2015. <http://www.researchgate.net/publication/277205402>. Accessed April 2020.
- [13] A.S.Vasilyev, A.V. Ushakov A.V. (2015). Modeling of dynamic systems with modulation by means of Kronecker vector-matrix representation. Scientific and Technical Journal of Information Technologies, Mechanics and Optics. 15 (5): State-space representation, pp. 839–848.
- [14] J. Zander, I. Schieferdecker, P. Mostermanl. (2017). Model-Based Testing for Embedded Systems. CRC Press.
- [15] A. Udal. (2020). Teaching slides for subject "ITB8816 Cyber Physical Systems", Tallinn University of Technology, Laboratory for Proactive Technologies, private communication.

- [16] R.L. Williams II, Douglas A. Lawrence. (2007). Linear State-Space Control Systems. John Wiley & Sons Inc.
- [17] T.E. Fortmann. (1977). An Introduction to Linear Control Systems. Marcel Dekker, Inc.
- [18] Y. Bavafa-Toosi. (2017). Introduction to Linear Control Systems. Elsevier Inc.
- [19] P.E. Caines. (2018). Linear Stochastic Systems. Society for Industrial and Applied Mathematics.
- [20] W.E. Xixon, A. Behal, M. Darren. (2003). Nonlinear Control of Engineering Systems: A Lyapunov-Based Approach. Birkhäuser Boston.
- [21] B. Lantos, L. Marton. (2011). Nonlinear Control of Vehicles and Robots. Springer-Verlag London Limited.
- [22] Z. Kovacic, S. Bogdan. (2005). Fuzzy Controller Design. Theory and Applications. CRC Press, Taylor and Francis Group, LLC.
- [23] Patan, K. (2019). Robust and Fault-Tolerant Control: Neural Network Based Solutions. Springer Nature Switzerland AG.
- [24] B. Widrow, Sterns S. (1985). Adaptive Signal Processing. Prentice-Hall.
- [25] K. Prasanna, K. Ramesha. (2017). Adaptive Filter Algorithms Based Noise Cancellation Using Neural Network in Mobile Applications. International Conference on Intelligent Computing and Applications. Advances in Intelligent Systems and Computing, vol 632. Springer, Singapore.
- [26] MathWorks help center.
<https://se.mathworks.com/help/deeplearning/ug/adaptive-neural-network-filters.html>. Accessed May 2020.
- [27] M. Singh, D. Parhi, J. Pothal. (2009). ANFIS Approach for Navigation of Mobile Robots. Proceedings IEEE International Conference on Advances in Recent Technologies in Communication and Computing.
- [28] Yamaguchi, T., Hirata, M. (2014). Advances in High-Performance Motion Control of Mechatronic Systems. Taylor & Francis Group.
- [29] S. Choi, D. Cha. (2019). Unmanned aerial vehicles using machine learning for autonomous flight; state-of-the-art. Advanced Robotics, DOI. ISSN: 0169-1864
- [30] J.K. Hendrik, A. Girard. (2005). Control of Nonlinear Dynamic Systems: Theory and Applications.
http://automatica.dei.unipd.it/public/Schenato/TESI/Tosin_2009/materiale/feedback%20linearization.PDF. Accessed April 2020.
- [31] Longo, S., Su, T., Hermann, G., Barber, P. (2013). Optimal and Robust Scheduling for Networked Control Systems. Taylor & Francis Group.
- [32] A. Pedai (supervisors E. Rüstern; I. Astrov), (1999). Modelling of three-rate stochastic multivariable control systems. Graduation Thesis, Tallinn University of Technology.
- [33] Vepa, R. (2016). Nonlinear Control of Robots and Unmanned Aerial Vehicles: An Integrated Approach. CRC Press.
- [34] IGI Global. (2019). Unmanned Aerial Vehicles: Breakthroughs in Research and Practice. Information Resources Management Association.
- [35] Wu, Wei. (2017). Model-Based Design for Effective Control System Development. Information Science Reference (an imprint of IGI Global).
- [36] Phillip H. Schmidt, Sanjay Grag, Brian R. Holowecky. (1993). A parameter optimisation approach to controller partitioning for integrated flight/propulsion control application. IEEE Transactions on Control Systems Technology, vol 1.

- [37] Igor Astrov, Juri Em, Ennu Rüstern. (1998). Design of three-rate stochastic multivariable continuous – time control system. Proc. 6th Biennial Conference on Electronics and Microsystems Technology (BEC '98, Tallinn, Estonia, October 7-9), pp. 325-328.
- [38] ICAO Annex 7. The Convention of International Civil Aviation. Annexes 1 to 18. https://www.icao.int/safety/airnavigation/NationalityMarks/annexes_booklet_en.pdf. Accessed May 2020.
- [39] K.M. Zemalache, L. Beji, and H. Maaref. (2008). Control of a drone: study and analysis of robustness. Journal of Automation, Mobile Robotics and Intelligent Systems, vol. 2, pp. 33-42.
- [40] K. Benzemrane, G.L. Santosuosso, and G. Damm. (2007). Unmanned aerial vehicle speed estimation via nonlinear adaptive observers. Proc. 2007 American Control Conference, New York, USA.
- [41] I. Astrov, A. Pedai, and E. Rüstern (2004). Simulation of three-rate neural and neuro-fuzzy hybrid control for the multidimensional stochastic model of a fighter aircraft. Proc. 8th World Multi-Conf. Systemics, Cybernetics and Informatics, Orlando, USA, 2004, pp. 351-356.
- [42] S. Shouzhao, A.A. Mian, Z. Chao, and J. Bin. (2010). Autonomous takeoff and landing control for a prototype unmanned helicopter. Control Engineering Practice, vol. 18, pp. 1053-1059.
- [43] I. Astrov, A. Pedai, and E. Rüstern. (2004). Simulation of three-rate neural and neuro-fuzzy hybrid control for the multidimensional stochastic model of a fighter aircraft. Proc. 8th World Multi-Conf. Systemics, Cybernetics and Informatics, Orlando, USA, 2004, pp. 351-356.
- [44] EU Drone regulations. <https://www.easa.europa.eu/domains/civil-drones-rpas>. Accessed June 2020.
- [45] K.S. Narendra and S. Mukhopadhyay. (1997). Adaptive control using neural networks and approximate models. IEEE Trans. Neural Networks, vol. 8, pp. 475-485.
- [46] A. Jadbabaie, J. Yu, and J. Hauser. (1999). Receding horizon control of the Caltech ducted fan: a control Lyapunov function approach. Proc. IEEE Conf. Control Applications, Kohala Coast, USA, pp. 51-56.
- [47] I. Astrov. (2016). Two-rate motion control of VTAV by NARMA-L2 controller for enhanced situational awareness. Proc. 39th International Convention on Information and Communication Technology, Electronics and Microelectronics/ International Conf. Computers in Technical Systems, Opatija, Croatia, pp. 1333-1338.
- [48] I. Astrov. (2016). Model-Based Design of Multirate Control Systems: Modeling and Simulation. Saarbrücken: Lambert Academic Publishing.
- [49] C.-Z. Pan, X.-Z. Lai, S. X. Yang, and M. Wu. (2013). An efficient neural network approach to tracking control of an autonomous surface vehicle with unknown dynamics. Expert Systems with Applications, vol. 40, April 2013, pp. 1629-1635.
- [50] Z. Peng, J. Wang, and D. Wang. (2018). "Distributed maneuvering of autonomous surface vehicles based on neurodynamic optimization and fuzzy approximation," vol. 26, pp. 1083-1090.
- [51] R. Polvara, S. Sharma, J. Wan, A. Manning, and R. Sutton. (2018). Obstacle avoidance approaches for autonomous navigation of unmanned surface vehicles. Journal of Navigation, vol. 71, pp. 241-256.

- [52] T. I. Fossen. (2011) Handbook of Marine Craft Hydrodynamics and Motion Control. John Wiley & Sons.
- [53] Mathworks. Deep Learning Toolbox. Time Series and Dynamic Systems. Neural Network Control Systems.
<https://www.mathworks.com/help/deeplearning/neural-network-control-systems.html>. Accessed August 2020.
- [54] A. Pedai, I. Astrov. (2008). Multi-Rate Expert Systems in Supply Chain Simulation for Telecommunication Industry. 2008, 4th International Conference on Wireless Communications, Networking and Mobile Computing. Dalian, China. IEEE WICOM 2008.
- [55] T. Zhang, Q. Li, C. Zhang, H. Liang, P. Li, T. Wang, S. Li, Y. Zhu, C. Wu. (2017). Current trends in the development of intelligent unmanned autonomous systems. *Frontiers of Information Technology & Electronic Engineering*, vol. 18, pp. 69-85.
- [56] R. Foote. (2007). *Mathematics and complex systems*. Science, pp. 318: 410-412.
- [57] R. Usubamatov. (2018). *Productivity Theory for Industrial Engineering*. Taylor Francis Group.
- [58] S. Kulkarni, A. Sharma. (2008). *Supply Chain Management, Creating Linkages for Faster Business Turnaround*. Tata McGraw-Hill Publishing Company Limited.
- [59] I. Astrov, A. Pedai. (2010). Multirate depth control of an AUV by neurocontroller for enhanced situational awareness. *International Conference on Computational Intelligence, Man-Machine Systems and Cybernetics. CIMMACS'10, Merida, Venezuela, December 14-16, 2010*.
- [60] I. Astrov, A. Pedai, and E. Rüstern. (2010). Desired trajectory generation of a quadrotor helicopter using hybrid control for enhanced situational awareness. *Proc. 2010 IEEE International Conference on Information and Automation (IEEE ICIA 2010, Harbin, China, June 20-23, 2010)*, pp. 1003-1007.
- [61] T.-H. Kim, T. Basar, and I.-J. Ha. (2002). Asymptotic stabilization of an underactuated surface vessel via logic-based control. *Proc. 2002 American Control Conf., Anchorage, USA*, pp. 4678-4683.
- [62] I. Astrov, A. Pedai. (2010). Situational awareness-based flight control of a three-rotor mini-aircraft. *Proc. of Int. Conf. on Automatic Control, Modelling and Simulation. ACMOS'10, Catania, Island of Sicily, Italy*, pp. 71-76.
- [63] I. Astrov, A. Pedai. (2011). Situational awareness-based flight control of a four-rotor type UAV, *Proc. of Int. Conf. on Automatic Control, Modelling and Simulation. ACMOS'11, Playa Blanca, Lanzarote, Canary Islands, Spain*, pp. 63-68.
- [64] I. Astrov, A. Pedai. (2010). Motion control of X4-flyer for enhanced situational awareness. *Proc. of Int. Multiconf. on Circuits, Systems, Communications and Computers. CSCC'10, Kanoni, Corfu Island, Greece*, pp. 123-128.
- [65] I. Astrov, A. Pedai. (2011). Flight trajectory control of an eight-rotor UAV for enhanced situational awareness. *Proc. of Int. Multiconf. on Circuits, Systems, Communications & Computers. CSCC'11, Kanoni, Corfu Island, Greece*. pp. 77-82.
- [66] I. Astrov, A. Pedai. (2011). Motion control of TUAV having eight rotors for enhanced situational awareness. *International Conference on Computer, Electrical, and Systems Sciences, and Engineering, ICCESSE 2011, Patong, Phuket Island, Thailand*.
- [67] A. Pedai, I. Astrov, A. Udai, R. Sell. (2019). Single-rate versus three-rate neural assisted control approaches for coaxial rotor ducted fan TUAV for situation awareness applications. *13th Annual IEEE International Systems Conference, April 8-11, 2019, Orlando, Florida, USA. SYSCON 2019*.

- [68] I. Astrov, A. Pedai, B. Gordon. (2012). Flight control of TUAV with coaxial rotor and ducted fan configuration by NARMA-L2 controllers for enhanced situational awareness. International Conference on Computer Engineering and Applications. ICCEA 2012, Copenhagen, Denmark.
- [69] I. Astrov, A. Pedai, B. Gordon. (2012). Two-rate neural control of TUAV with coaxial rotor and ducted fan configuration for enhanced situational awareness. 9th International Conference. ELEKTRO 2012, Rajecské Teplice, Slovakia.
- [70] I. Astrov, A. Pedai. (2008). Enhancing situational awareness by means of hybrid adaptive neural control of vertical flight in unmanned helicopter. International Conference on Control, Automation and Systems 2008. Seoul, Korea. ICCAS 2008.
- [71] I. Astrov, A. Pedai. (2008). Situational awareness based on neural control of an autonomous helicopter during hovering manoeuvres. 5th International Conference on Electrical and Computer Engineering. ICECE 2008, Dhaka, Bangladesh.
- [72] I. Astrov, A. Pedai, E. Rüstern. (2004). Simulation of two-rate adaptive hybrid control with neural and neuro-fuzzy networks for stochastic model of an experimental aircraft. 10th International Conference on Information Systems Analysis and Synthesis ISAS 2004. Orlando, Florida, USA.
- [73] I. Astrov, A. Pedai, E. Rüstern. (2004). Simulation of two-rate adaptive neural network and fuzzy logic hybrid control for stochastic model of an experimental aircraft. 2004 IEEE Canadian Conference on Electrical and Computer Engineering. CCECE 2004, Niagara Falls, Ontario, Canada.
- [74] I. Astrov, A. Pedai, E. Rüstern. (2004). Simulation of three-rate neural and neuro-fuzzy hybrid control for the multidimensional stochastic model of a fighter aircraft. 8th World Multi-Conference on Systemics, Cybernetics and Informatics. SCI 2004, Orlando, Florida, USA.
- [75] I. Astrov, A. Pedai, E. Rüstern. (2004). Simulation of two-rate adaptive hybrid control with neural and neuro-fuzzy networks for stochastic model of missile autopilot. 5th World Congress on Intelligent Control and Automation. WCICA 2004, Hangzhou, China.
- [76] I. Astrov, A. Pedai. (2011). Multirate depth control of an AUV by neural networks. Symposium on Computational Intelligence and Intelligent Informatics. ISCIII 2011, Floriana, Malta.
- [77] I. Astrov, A. Pedai. (2010). Flight control of a trirotor mini-UAV for enhanced situational awareness. Volume [2010-376X] of Proceedings of World Acad. Science, Engineering and Technology (Extended papers of Int. Conf. on Aeronautical and Astronautical Engineering ICAAE 2010, Amsterdam, Netherlands), volume 70, pp. 271-277 (referenced in Scopus, www.etis.ee classification 1.1 paper).
- [78] I. Astrov, A. Pedai, E. Rüstern. (2009). Enhancing situational awareness through multirate control of an autonomous underwater vehicle. 2009 IEEE International Conference on Mechatronics and Automation. IEEE ICMA 2009, Changchun, China.
- [79] I. Astrov, A. Udal, A. Pedai, R. Sell. (2019). Simulink/MATLAB based comparison of neural and basic tracking control for an autonomous surface vessel for situation awareness applications. IEEE Joint 19th International Symposium on Computational Intelligence and Informatics and 7th IEEE International Conference on Recent Achievements in Mechatronics, Automation, Computer Sciences and Robotics. CINTI-MACRO 2019, Szeged, Hungary.

- [80] I. Astrov, A. Pedai. (2009). Control of hovering manoeuvres in unmanned helicopter for enhanced situational awareness. International Conference on Industrial Mechatronics and Automation. ICIMA 2009, Chengdu, China.
- [81] A. Pedai, I. Astrov, A. Udal. (2018). Comparison of single-rate and two-rate neural control approaches for coaxial rotor/ducted-fan TUAV for situational awareness applications. SISY 2018: IEEE 16th International Symposium on Intelligent Systems and Informatics. Subotica, Serbia, September 13-15, 2018.
- [82] I. Astrov, A. Pedai. (2012). Three-rate neural control of TUAV with coaxial rotor and ducted fan configuration for enhanced situational awareness. International Conference on Control, Automation and Information Sciences. IEEE ICCAIS 2012, Ho Chi Minh City, Vietnam.
- [83] W. Johnson (2013). Rotorcraft Aeromechanics. Cambridge University Press, New York.
- [84] T. Skjott-Larsen, P. Schary, H. Kotzab, J. Mikkola. (2007). Managing the Global Supply Chain. Copenhagen Business School Press DK.
- [85] M. Koch, B. Kleinjohann, A. Schmidt, P. Scheideler, A. Saskevic, E. Münch, A. Gambuzza, O. Oberschelp, and T. Hestermeyer. (2004). Neurofuzzy approaches for self-optimizing concepts and structures of mechatronic systems. Proc. International Conf. Computing, Communications and Control Technologies, Austin, TX, USA, pp. 263-268.
- [86] J.L. Bermudez. (2014). Cognitive Science. An Introduction to the Science in the Mind. Cambridge University Press, New York.
- [87] D. Dubois, H. Prade. (2000). Fundamentals of Fuzzy Sets. Springer Science + Business Media, New York.
- [88] F. Klawonn, E.P. Klement. (1997). Mathematical analysis of fuzzy classifiers. Advances in Intelligent Data Analysis, Reasoning about Data. Berlin: Springer, 1997, pp. 359-370.
- [89] M. Negnevitsky. (2005). Artificial Intelligence. A Guide to the Intelligent Systems. Pearson Education Limited.
- [90] M. Koch, B. Kleinjohann, A. Schmidt, P. Scheideler, A. Saskevic, E. Münch, A. Gambuzza, O. Oberschelp, T. Hestermeyer. (2004). Neurofuzzy approaches for self-optimizing concepts and structures of mechatronic systems. Proc. International Conf. Computing, Communications and Control Technologies, Austin, TX, USA, pp. 263-268.
- [91] S. Salazar-Cruz, F. Kendoul, R. Lozano, and I. Fantoni. (2006). Real-time control of a small-scale helicopter having three rotors. Proc. IEEE/RSJ International Conference on Intelligent Robots and Systems (IROS 2006, Beijing, China, October 9-15, 2006), pp. 2924-2929.
- [92] S. Salazar-Cruz, F. Kendoul, R. Lozano, and I. Fantoni. (2008). Real-time stabilization of a small three-rotor aircraft. IEEE Transactions on Aerospace and Electronic Systems, vol. 44, pp. 783-794.
- [93] I. Astrov and A. Pedai. (2011). Situational awareness based flight control of a drone. Proc. 2011 IEEE International Systems Conference (SysCon 2011, Montreal, Quebec, Canada, April 4-7, 2011), IEEE, pp. 574-578.

Acknowledgements

This research was supported by following programs:

1. EstSF (Estonian Science Foundation) research grant No ETF3423, “Methods for Control and Modelling of Dynamic Systems”, (01.01.1998-31.12.2001), personnel of research staff.
2. TFP (Targeted Financing Project of Ministry of Education and Research of Estonia) No 0140237s98, “Analysis, Modelling and Control of Systems”, (01.01.1998-31.12.2002), personnel of research staff.
3. EstSF research grant No ETF5170, “Development of Robust Methods and Algorithms for Control Systems”, (01.01.2002-31.12.2005), personnel of research staff.
4. TFP No SF0142509s03, “Intelligent Components and their Integration Problems”, (01.01.2003-31.12.2007), personnel of research staff.
5. EstSF research grant No ETF6837, “Robust Methods for Complex Systems Control: an Integrated Approach”, (01.01.2006-31.12.2009), personnel of research staff.
6. TFP No SF0140113As08, “Proactivity and Situation-Awareness”, (01.01.2008-31.12.2013), personnel of research staff.

During the extended time for my PhD study at TalTech, I worked with many amazing people who I am very thankful and grateful. First of all, I am deeply indebted by my PhD advisors Prof. Raivo Sell, Dr. Andres Udal and Dr. Igor Astrov. Their continued advice, guidance and support helped me to navigate the most complex challenges during my PhD journey. I greatly appreciate Dr. Igor Astrov’s support in the early phases of my research, to let me explore different research topics and being very patient to let me figure out what my strength and potentials are. Igor also supported me to attend several conferences and workshops, which greatly enriched my research and cultural experience. Current thesis would have not been finalized without focused and professional guidance by Dr. Andres Udal and Prof. Raivo Sell. Close co-operation with Andres and Raivo enabled me to systematically consolidate the vast research data to the appropriate format for doctoral thesis. Andres and Raivo have been true advocates for their student and superb mentors.

Finally, I have to admit that this thesis would not exist without my great love Greete and our wonderful daughters Nora and Laura. I admire Greete’s patience for being so supportive and her ability to constantly be involved in my (sometimes fuzzy) creation process. My family gave me the energy to finalize this work.

Abstract

Modelling and simulation of autonomous vehicles and systems and their advanced control methods

This publications-based thesis concentrates to the summary of the selected 5 main research publications by the Author published during the years 2011–2019 in the field of modelling and simulation of unmanned vehicles control systems.

Author has strong manufacturing environment background, both from electronics and automotive industries. In parallel to working with specific industrialization projects, Author has maintained close co-operation with Tallinn University of Technology and continued his research in the field of control methods for autonomous vehicles and systems. Out of the wide research scope, advanced methodology for multi-rate control systems has been developed and applied by author in number of technical papers and having specific modelling and simulation examples described in the thesis.

The main results of the described work may be summarized as following:

1. Development of methodology for modelling and simulation of control of autonomous airborne and waterborne vehicles via construction of mathematical models and their testing in MATLAB/Simulink environment.
2. Testing of the developed modelling and simulation approaches for 8 types of autonomous airborne and 2 autonomous waterborne vehicles, starting from a miniature one rotor helicopter and ending with the eight-rotor drone and mini-submarine.
3. Demonstration of applicability of several advanced approaches like multi-rate object model decomposition and employment of different types of neural network based controllers in control of autonomous vehicles.

Applied multi-rate (two-rate and three-rate) parallel operation methodology is based on state equations matrix eigenvalues mathematics, developed by the Author in several publications since early 2000's. On the system block diagram level this means decomposition of the original control system to the parallel slow, intermediate and fast subsystems in order to achieve better transition processes results together with maintaining necessary stability.

The neural network types, considered in thesis achieve proactive predictive control and to suppress the stochastic disturbances, include the adaptive linear neural networks (ADALINE), nonlinear autoregressive moving average (NARMA-L2) controllers, and neural network predictive controllers.

High level of the presented work and the universality of the offered approaches has been earlier confirmed by the best paper award in 2010 for the autonomous underwater vehicle modelling.

Lühikokkuvõte

Autonoomsete sõidukite ja süsteemide ning nende täiustatud juhtimismetoodikate modelleerimine ja simuleerimine

Käesolev publikatsioonidel põhinev dissertatsioon koondab autori poolt alates 2011. aastast avaldatud 5 põhipublikatsiooni tulemused mehitamata sõidukite juhtimissüsteemide modelleerimise ja simuleerimise alal.

Autori põhitöö on olnud seotud elektroonika- ja autotööstusega, mitmes rahvusvahelises ettevõttes. Paralleelselt oma põhitööga tööstuses hoidis Autor tihedat kontakti Tallinna Tehnikaülikooliga ja jätkas arendustööd mehitamata seadmete juhtimissüsteemide valdkonnas. Antud töö käigus fookuses olnud uudne mitmekiiruseline meetodika juhtimissüsteemide ülesehitusele on leidnud läbivalt arendamist ja rakendamist paljudes publikatsioonides ja enamuses käesoleva dissertatsiooni mehitamata seadmete näidisülesannetes.

Kirjeldatud teadustöö põhitulemused võib kokku võtta järgmiselt:

1. Autonoomsete õhu- ja veesõidukite juhtimise modelleerimise ja simuleerimise meetodikate läbitöötamine kasutades matemaatiliste mudelite konstrueerimist ja testimist MATLAB/Simulink arenduskeskkonnas;
2. On läbi viidud modelleerimise ja simuleerimise meetodikate testimine 8 erineva autonoomse õhusõiduki ja 2 veesõiduki tüüpi jaoks alustades lihtsamast üherootorisest minihelikopterist ja lõpetades kaheksarootoriselise drooniga ning minialveelaevaga;
3. Mitmete täiustatud meetodikate nagu erinevat tüüpi närvivõrkudel baseeruvate kontrollerite rakendamine ja objekti mudeli mitmekiiruseline dekompositsioon kasutusvõimaluste demonstreerimine autonoomsete sõidukite juhtimisülesannetes.

Käesolevas väitekirjas kirjeldatud mitmekiiruselise (2- või 3-kiiruselise) paralleeljuhtimise meetodika baseerub olekuvõrrandite maatriksite omaväärtuste matemaatil, mida autor on arendanud alates 2000-ndast aastast. Süsteemi plokk skeemil tähendab see dekompositsiooni aeglasemaks, keskmiseks ja kiiremaks alamsüsteemiks, et saavutada parema kvaliteediga siirdeprotsesse ilma juhitava süsteemi stabiilsust kaotamata. Käsitatud närvivõrkude tüübid, mida on esitatud töös rakendatud proaktiivsuse sissetoomiseks ja juhuslike häirete paremaks mahasurumiseks, on näiteks adaptiivsed lineaarnärvivõrgud (ADALINE), mittelineaarsed autoregressiivsed nihkuga keskmisega (NARMA-L2) neurokontrollerid, ennustamisvõimega neurokontrollerid.

Esitatud väitekirja tase ja soovitatud meetodikate universaalsus on leidnud kinnitust prima konverentsiartikli auhinnaga autonoomse allveesõiduki juhtimisele pühendatud uuringu eest aastal 2010.

Appendices I-VI

Publication I

Astrov and A. Pedai (2011). Situational awareness based flight control of a drone. IEEE International Systems Conference. SysCon 2011, Montreal, Canada.

Situational Awareness based Flight Control of a Drone

Igor Astrov and Andrus Pedai
Department of Computer Control
Tallinn University of Technology
Tallinn, Estonia
igor.astrov@dcc.ttu.ee

Abstract—This paper focuses on a critical component of the situational awareness (SA), the control of autonomous vertical flight for an unmanned aerial vehicle (UAV). With the SA strategy, we proposed a two stage flight control procedure to address the dynamics variation and performance requirement difference in initial and final stages of flight trajectory for a nontrivial nonlinear model of four-rotor helicopter robot called drone. This control strategy for chosen drone model has been verified by simulation of hovering maneuvers using software package Simulink and demonstrated good performance for fast stabilization of engines in hovering, consequently, fast SA with economy in energy of batteries can be asserted during the flight.

Keywords—*flight control; four-rotor helicopter; simulation; situational awareness; unmanned aerial vehicle.*

I. INTRODUCTION

Situation awareness has been formally defined as “the perception of elements in the environment within a volume of time and space, the comprehension of their meaning, and the projection of their status in the near future” [1]. As the term implies, situation awareness refers to awareness of the situation. Grammatically, situational awareness (SA) refers to awareness that only happens sometimes in certain situations.

SA has been recognized as a critical, yet often elusive, foundation for successful decision-making across a broad range of complex and dynamic systems, including emergency response and military command and control operations [2].

The term SA have become commonplace for the doctrine and tactics, and techniques in the U.S. Army [3]. SA is defined as “the ability to maintain a constant, clear mental picture of relevant information and the tactical situation including friendly and threat situations as well as terrain”.

The tactical unmanned aerial vehicle (TUAV) is one of the key tools to gather the information to build SA for all leaders. The TUAV provides the commander with a number of capabilities including:

- Enhanced SA.
- Target acquisition.

Some conditions for conducting aerial reconnaissance with TUAVs are as follows.

- Time is limited or information is required quickly.
- Detailed reconnaissance is not required.
- Verification of a target is needed.
- Terrain restricts approach by ground units.

The current state of TUAVs throughout the world is outlined [4]. A novel design of a multiple rotary wing platform which provide for greater SA in the urban terrain is then presented.

A mini-TUAV offers many advantages, including low cost, the ability to fly within a narrow space and the unique hovering and vertical take-off and landing (VTOL) flying characteristics.

Autonomous vertical flight is a challenging but important task for TUAVs to achieve high level of autonomy under adverse conditions. The fundamental requirement for vertical flight is the knowledge of the height above the ground, and a properly designed controller to govern the process.

In [5], a three stage flight control procedure for a nontrivial nonlinear model on the basis of equations of vertical motion for the center of mass of unmanned helicopter was proposed. This strategy has been verified by simulation of hovering maneuvers using software package Simulink and demonstrated good performance for fast SA.

This paper concentrates on issues related to the area of [5], but demonstrates another field for application of these ideas, i.e., research technique using control system modeling and simulation on the basis of equations of motion for the center of mass of TUAV drone for fast SA.

The contribution of the paper is twofold: to develop new schemes appropriate for SA enhancement using hybrid flight control of a TUAV drone in real-time search-and-rescue operations, and to present the results of hovering maneuvers for chosen model of a TUAV drone for fast SA in simulation form using the MATLAB/Simulink environment.

II. DRONE MODEL

The drone is equipped with four rotors where two are directionals. Compared to quadrotors, the drone has some advantages: given that two rotors 3 and 4 rotate counterclockwise while the other two (1 and 2) rotate

clockwise, gyroscopic effects and aerodynamic torques tend, in trimmed flight, to cancel. The main feature of the presented drone in comparison with the existing quadrotors, is the swiveling of the actuators supports rotors 1 and 3 around the pitching axis. This permits a more stabilized horizontal flight and a suitable cornering.

The dynamics of the drone for the case of low speeds of motion can be represented by the following equations [6]

$$\ddot{x} = \frac{u_2 \sin \psi \cos \theta}{m} - \frac{u_3 \sin \theta}{m} \quad (1)$$

$$\ddot{y} = \frac{u_2 (\sin \theta \sin \psi \sin \phi + \cos \psi \cos \phi)}{m} + \frac{u_3 \cos \theta \sin \phi}{m} \quad (2)$$

$$\ddot{z} = \frac{u_2 (\sin \theta \sin \psi \cos \phi - \cos \psi \cos \phi)}{m} + \frac{u_3 \cos \theta \cos \phi}{m} - g \quad (3)$$

$$\ddot{\theta} = \frac{u_4 + I_x \dot{\theta} \dot{\phi} \sin \phi}{I_x \cos \phi} \quad (4)$$

$$\ddot{\phi} = \frac{u_5 + I_y \dot{\phi} (\dot{\phi} \sin \phi \cos \theta + \dot{\theta} \sin \theta \cos \phi)}{I_y \cos \theta \cos \phi} \quad (5)$$

$$\ddot{\psi} = \frac{u_6}{I_z} \quad (6)$$

where

$$u_2 = f_1 \sin \xi_1 + f_3 \sin \xi_3, \quad (7)$$

$$u_3 = f_1 \cos \xi_1 + f_3 \cos \xi_3 + f_2 + f_4, \quad (8)$$

$$u_4 = l(f_2 - f_4), \quad (9)$$

$$u_5 = l(f_1 \cos \xi_1 - f_3 \cos \xi_3), \quad (10)$$

$$u_6 = l(f_1 \sin \xi_1 - f_3 \sin \xi_3) + \frac{K_M}{K_T} (f_1 \cos \xi_1 - f_3 \cos \xi_3 + f_4 - f_2), \quad (11)$$

$$f_i = K_T \omega_i^2, \quad (12)$$

x, y, z are coordinates of center of mass in the earth-frame; ψ, θ, ϕ are yaw, pitch and roll angles; ξ_1, ξ_3 are swivel angles of the actuators supports rotors 1 and 3 around the axis of pitching; $f_i (i=1,2,3,4)$ is the thrust generated by the i -th rotor; ω_i is the angular speed of rotor i ; K_M, K_T are given constants; l is the distance from the centre of mass to the rotors; I_x, I_y, I_z are the moments of inertia along x, y, z directions of the inertia matrix $J = \text{diag}(I_x, I_y, I_z)$; g is the gravity constant; m is the total mass of the drone.

The inputs in (7)-(11) then can be represented in matrix form as

$$\begin{bmatrix} u_2 \\ u_3 \\ u_4 \\ u_5 \end{bmatrix} = \begin{bmatrix} \sin \xi_1 & 0 & \sin \xi_3 & 0 \\ \cos \xi_1 & 1 & \cos \xi_3 & 1 \\ 0 & l & 0 & -l \\ l \cos \xi_1 & 0 & -l \cos \xi_3 & 0 \end{bmatrix} \begin{bmatrix} f_1 \\ f_2 \\ f_3 \\ f_4 \end{bmatrix} \quad (13)$$

Then the individual forces in (13) will be

$$\begin{bmatrix} f_1 \\ f_2 \\ f_3 \\ f_4 \end{bmatrix} = \begin{bmatrix} \sin \xi_1 & 0 & \sin \xi_3 & 0 \\ \cos \xi_1 & 1 & \cos \xi_3 & 1 \\ 0 & l & 0 & -l \\ l \cos \xi_1 & 0 & -l \cos \xi_3 & 0 \end{bmatrix}^{-1} \begin{bmatrix} u_2 \\ u_3 \\ u_4 \\ u_5 \end{bmatrix} \quad (14)$$

It is now seen that the angular speed ω_i of rotor i simplifies to:

$$\omega_i = 2\pi \frac{n_{m_i}}{60} \approx \frac{n_{m_i}}{10} \quad (15)$$

where n_{m_i} (rpm) is the number of revolutions per minute of rotor i .

Combining (12) and (15), we have

$$n_{m_i} \approx 10 \sqrt{\frac{f_i}{K_T}} \quad (16)$$

From (1)-(11), we can see that the attitude vector $(x, y, z)^T$ for given model of the drone can be computed.

The numerical values for drone parameters of (1)-(12) for a case of small elevation above sea level are given by [7]:

$$m = 2.5 \text{ kg}, l = 0.23 \text{ m}, I_x = 0.022493 \text{ kgm}^2,$$

$$I_y = 0.022261 \text{ kgm}^2, I_z = 0.0325130 \text{ kgm}^2,$$

$$K_T = 10^{-5} \text{ N s}^2, K_M = 9 \times 10^{-6} \text{ N m s}^2, g = 9.81 \text{ m/s}^2.$$

III. CONTROL SYSTEM

It is possible to consider the thrusts f_1 and f_3 as fixed constants, and to consider the swivel angles ξ_1 and ξ_3 as fixed constants in (7)-(11).

Hence, we have

$$f_1 = f_3 = \text{const} \quad (17)$$

$$\xi_1 = \xi_3 = \text{const} \quad (18)$$

Combining (7)-(11) and (17)-(18), we have

$$u_2 = 2f_1 \sin \xi_1 \quad (19)$$

$$u_4 = -u_6 \frac{K_T}{K_M} \quad (20)$$

$$u_5 = 0 \quad (21)$$

With selection of (19)-(21), the complex control problem is now turned into a hybrid control problem with using u_3 as control input for controlling the coordinate z of altitude with respect to reference input z^0 and with using u_6 for controlling the yaw angle ψ with respect to reference input ψ^0 .

The control system configuration to regulate the input variable u_3 is thus designed, to have the next structure (see Fig. 1)

$$\dot{u}_3 = K(t_1(z^0 - z) - t_2\dot{z} - \ddot{z}) \quad (22)$$

where t_1, t_2 are constants to be determined.

It is possible to consider the variable u_3 as a "fast" function of time. Hence, assuming that $\dot{u}_3 = 0$, from (22), we find

$$\ddot{z} + t_2\dot{z} + t_1z = t_1z^0 \quad (23)$$

The following coefficients of (23) are obtained from [8], for overshooting with value of $\sigma \approx 5\%$

$$t_1 \approx \frac{9}{t_{dz}^2}, t_2 \approx \frac{3\sqrt{2}}{t_{dz}} \quad (24)$$

where t_{dz} is desired transition time of coordinate z .

For a hovering flight, angles of roll, pitch, and yaw must be zeros. Therefore, the equation (3) becomes

$$\ddot{z} = -\frac{u_2}{m} + \frac{u_3}{m} - g \quad (25)$$

Differentiating both sides of (25) with respect to time, we obtain

$$\ddot{\ddot{z}}(t) = b\dot{u}_3(t) \quad (26)$$

where

$$b \approx \frac{1}{m}. \quad (27)$$

Combining (22) and (26), we have

$$\ddot{\ddot{z}}(t) = bK(i_3(t) - \ddot{z}(t)), \quad (28)$$

where

$$i_3(t) = t_1(z^0 - z(t)) - t_2\dot{z}(t). \quad (29)$$

Defining $\ddot{z}(t) = a(t)$ in (28), we obtain

$$\dot{a}(t) = bKi_3(t) - bKa(t) \quad (30)$$

The variable $a(t)$ in (30) can be described in a common way through next expression as indicated in [9]

$$a(t) = (a_0 + \int_0^t e^{-A(\tau)} bKi_3(\tau) d\tau) e^{A(t)}, \quad (31)$$

where

$$A(t) = -\int_0^t bKd\tau. \quad (32)$$

Let us consider the behavior of the considered control system (see Fig. 1) for time t of time interval $t \geq t_{dz}$ during the hovering.

Hence, assuming that $a_0 = 0$, $z^0 - z(t) \approx \Delta z^0$, $\Delta = 0.05$, $\dot{z}(t) \approx 0$, from (31)-(32), we find

$$a(t) = i_3(1 - e^{-bKt}) \quad (33)$$

where

$$i_3(t) \approx t_1\Delta z^0 = \text{const}. \quad (34)$$

Using (33) and (34), and the ratio of coordinate-to-acceleration transition times $N = \frac{t_{dz}}{t_{d\ddot{z}}}$, we obtain

$$K \approx \frac{3Nm}{t_{dz}} \quad (35)$$

Note that the structure of control system using control input u_6 for controlling the yaw angle ψ is similar to the control structure for controlling the coordinate z which was described above.

IV. SIMULATION RESULTS

Consider the control of drone model (1)-(6) for the case of take-off and hovering maneuvers by hybrid constrained system of three control subsystems.

The goal of the following simulations is twofold. First, we verify that this hybrid control system is able to control the flight trajectories. Second, we observed the effect of enhancing SA because the variety of chosen trajectory parameters easily can be changed the desired flight trajectories of a drone.

These trajectory parameters are chosen to be:

$$n_{m_1} = n_{m_3} = 8945rpm,$$

$$\xi_1 = \xi_3 = 1 \text{ deg},$$

$$z_1^0 = 3m, z_2^0 = 40m, \psi^0 = 0.1 \text{ deg},$$

$$N_1 = 15, N_2 = 30, N_3 = 5, t_{d1} = 3s, t_{d2} = 25s, t_{d3} = 5s.$$

Simulation results of the offered block scheme (see Fig. 1) are shown in Figs. 2-4.

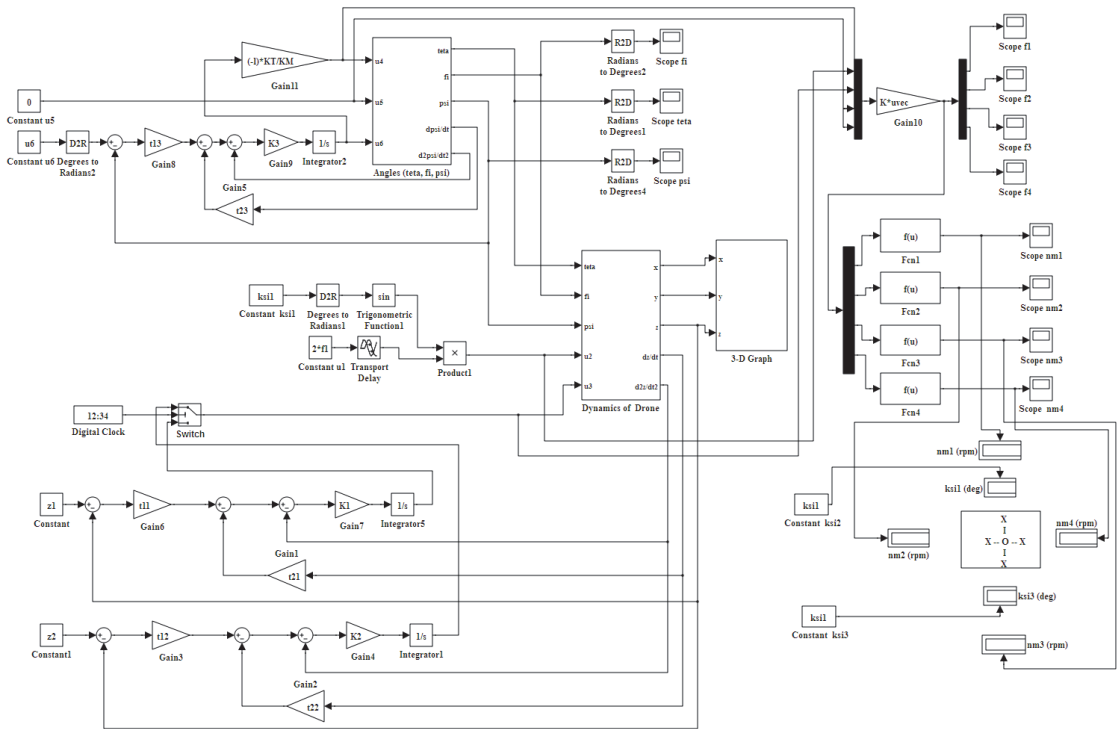


Figure 1. Block diagram of hybrid control system.

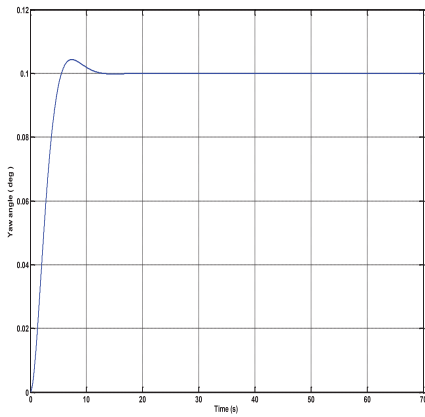


Figure 2. Transient behavior of yaw angle.

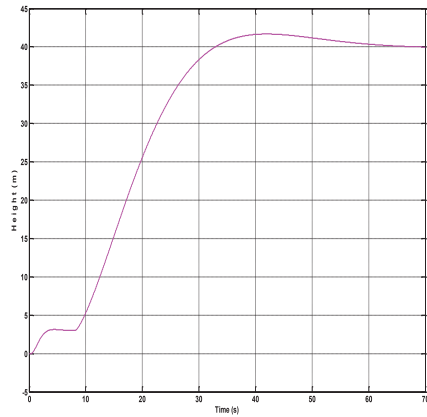


Figure 3. Height trajectory of flight control.

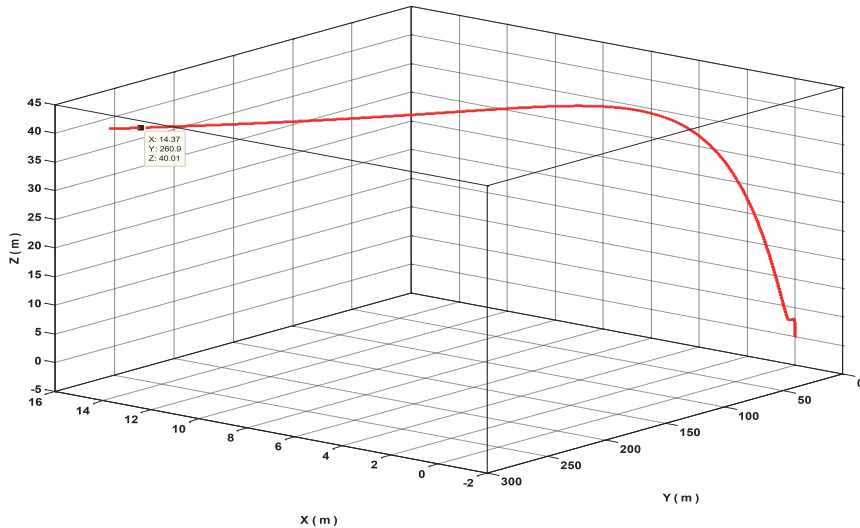


Figure 4. 3-D motion of the drone.

V. CONCLUSION

A new research technique is presented in this paper for enhanced SA in applications to VTOL class TUAVs.

The need for highly reliable and stable hovering for VTOL class autonomous vehicles has increased morbidly for critical situations in real-time search-and-rescue operations for fast SA.

For fast, stable and smooth hovering maneuvers, we proposed a two stage flight strategy, which separates the flight process into initial and final phases. The effectiveness of this flight strategy has been verified in field of flight simulation tests for chosen model of the TUAV using software package Simulink.

Although many of the details inevitably relate with chosen drone model, there is sufficient generality for this research technique to be applied to others models of TUAVs during hovering maneuvers.

From the applications viewpoint, we believe that this flight strategy using flexible and effective hybrid control furnish a powerful approach for enhancing SA in applications to VTOL class TUAVs.

Future work will involve further validation of the performance of the proposed research technique and exploring other relevant and interesting missions of a drone.

REFERENCES

- [1] M.R. Endsley, "Toward a theory of situation awareness in dynamic systems," *Human Factors*, vol. 37, pp. 32-64, March 1995.
- [2] J. Gorman, N. Cooke, and J. Winner, "Measuring team situation awareness in decentralized command and control environments," *Ergonomics*, vol. 49, pp. 1312-1325, October 2006.
- [3] Interim Brigade Combat Team Newsletter. [Online]. Available: http://www.globalsecurity.org/military/library/report/call/call_01-18_toc.htm
- [4] S.D. Prior, S.-T. Shen, A.S. White, S. Odedra, M. Karamanoglu, M.A. Erbil, and T. Foran, "Development of a novel platform for greater situational awareness in the urban military terrain," Proc. 8th International Conference on Engineering Psychology and Cognitive Ergonomics, San Diego, USA, 2009, pp. 120-125.
- [5] I. Astrov and A. Pedai, "Control of hovering manoeuvres in unmanned helicopter for enhanced situational awareness," Proc. International Conference on Industrial Mechatronics and Automation, Chengdu, China, 2009, pp. 143-146.
- [6] K.M. Zemalache, L. Beji, and H. Maaref, "Control of a drone: study and analysis of robustness," *Journal of Automation, Mobile Robotics and Intelligent Systems*, vol. 2, pp. 33-42, January 2008.
- [7] K. Benzemrane, G.L. Santosuosso, and G. Damm, "Unmanned aerial vehicle speed estimation via nonlinear adaptive observers," Proc. 2007 American Control Conference, New York, USA, 2007, pp. 985-990.
- [8] P.D. Krutko, *Inverse Problems of Control System Dynamics: Nonlinear Models*. Moscow: Nauka, 1989.
- [9] L.S. Pontryagin, *Ordinary Differential Equations*. Moscow: Nauka, 1974.

Publication II

Astrov and A. Pedai (2012). Three-rate neural control of TUAV with coaxial rotor and ducted fan configuration for enhanced situational awareness. Proc. 2012 International Conference on Control, Automation and Information Sciences (ICCAIS 2012, Ho Chi Minh City, Vietnam, November 26-29, 2012), IEEE, pp. 78-83.

Three-Rate Neural Control of TUAV with Coaxial Rotor and Ducted Fan Configuration for Enhanced Situational Awareness

Igor Astrov, *Senior Member, IEEE*, and Andrus Pedai

Abstract—This paper describes a critical component of the situational awareness (SA), the control of tactical unmanned aerial vehicle (TUAV) during autonomous flight operations. With the SA strategy, we proposed a three-rate flight control procedure using three autonomous decomposed control subsystems with single NARMA-L2 controller for an unmanned helicopter model with coaxial rotor and ducted fan configuration. This strategy for chosen model of TUAV has been verified by simulation of flight tests using Simulink environment and demonstrated valuable qualities for fast stabilization of TUAV's engines during flight, consequently, fast SA with economy in energy can be asserted during possible missions.

I. INTRODUCTION

SITUATION awareness has been formally defined as “the perception of elements in the environment within a volume of time and space, the comprehension of their meaning, and the projection of their status in the near future” [1]. The term “situational awareness” refers to awareness of the situation. Grammatically, the term “situational awareness” (SA) refers to awareness that only happens sometimes in certain situations.

SA has been recognized as a critical, yet often elusive, foundation for successful decision-making across a broad range of complex and dynamic systems, including emergency response and military command and control operations [2].

The term SA has become trivial for the doctrine, tactics, techniques, and procedures in the U.S. Army [3]. SA is defined as “the ability to maintain a constant, clear mental picture of relevant information and the tactical situation including friendly and threat situations as well as terrain”. SA allows leaders to avoid unpleasant surprises, make rapid decisions and minimize risk, and to decide when and where to conduct the effective and successful engagements, and achieve these desired outcomes.

The tactical unmanned aerial vehicle (TUAV) is designed as a ground maneuver commander's primary day/night reconnaissance, surveillance, target acquisition, and battle damage assessment system.

Manuscript received April 18, 2012; revised August 9, 2012. This work was supported in part by the Ministry of Education and Research of Estonia under Targeted Financing Project SF0140113As08.

I. Astrov is with the Department of Computer Control, Tallinn University of Technology, Tallinn 19086, Estonia (phone: 372-620-2113; fax: 372-620-2101; e-mail: igor.astrov@dcc.ttu.ee).

A. Pedai is with the Department of Computer Control, Tallinn University of Technology, Tallinn 19086, Estonia (e-mail: andrus.pedai@dcc.ttu.ee).

The TUAV provides the commander with a number of capabilities including:

- Enhanced SA.
- Target acquisition.
- Battle damage assessment.
- Enhanced battle management capabilities (friendly situation and battlefield visualization).

The combination of these benefits promotes to the commander's dominant SA allowing him to protect forces on the battlefield and to maneuver to gain a positional advantage over an enemy.

The main conditions for conducted aerial reconnaissance flights with TUAVs are as follows.

- Time is limited or information is required quickly.
- Detailed reconnaissance is not required.
- Extended duration surveillance is not required.
- Target is at extended range.
- Threat conditions are known; also the risk to ground assets is high.
- Verification of a target is needed.
- Terrain restricts approach by ground units.

Among mini-TUAVs, promising advantages are the low cost, the ability to fly in confined space and the unique hovering and vertical take-off and landing (VTOL) flying characteristics.

In [4], a novel design of a multi-rotor wing platform which has great potential for both military and civilian application areas is presented. These platforms can provide the greater SA in the urban terrain.

The knowledge of the height above the ground is important task for TUAVs to achieve high level of autonomy, especially under adverse conditions. Emphasis must be given to design of controller to govern the process of autonomous flight.

In [5], a three stage flight control strategy for a nonlinear helicopter model on the basis of equations of vertical motion for the center of mass of helicopter was presented. The proposed control strategy has been verified by simulation of hovering maneuvers using software package Simulink and demonstrated efficiency for fast SA.

This paper concentrates on issues related to the area of [5], but demonstrates another field for application of these ideas, i.e., research technique using control system modeling and simulation on the basis of equations of motion of coaxial unmanned helicopter with ducted fan configuration for fast SA.

In this paper our research results in the study of vertical flight (take-off, approach and hovering cases) by three-rate control of unmanned helicopter with coaxial rotor and ducted fan configuration which make such SA task scenario as "go-search-find-return" possible are presented.

The contribution of the paper is twofold: to develop new schemes appropriate for SA enhancement by three-rate control of vertical flight of UAVs, and to present the results of flight maneuvers for chosen three-rate model of UAV for fast SA in simulation form using the MATLAB/Simulink environment.

II. UAV MODEL

In [6], a model of prototype coaxial unmanned helicopter with ducted fan configuration was proposed.

The prototype unmanned helicopter, with a net weight 160kg and height of $l=1.9m$, is a VTOL aircraft that includes a fuselage with toroidal part and coaxial rotors. A duct extends from the top to the bottom of the fuselage. The propeller assembly is mounted to the top portion of the fuselage with a main rotor of diameter 4.4m. A ducted rotor assembly is installed in fuselage compensating the propeller antitorque besides providing some fraction of lift. The coaxial rotors, main and ducted, rotate at 800rpm in opposite directions. The main rotor provides about 80% of lift, drag, pitch and roll movements of unmanned helicopter and the ducted rotor provides about 20% of lift and yaw movements.

In comparison with conventional main and tail rotor configuration, the coaxial rotors with ducted fan configuration provide more lift and move easily in any direction, during take-off and landing. These design features not only increase the maneuver ability of unmanned helicopter but also increase its stability making it easier to fly especially in narrow and bumpy take-off and landing site.

The dynamic model for control yields the general form of state equations for the prototype unmanned helicopter [6]

$$\dot{x}(\tau) = Ax(\tau) + Bu(\tau) + v(\tau) \quad (1)$$

$$y(\tau) = Cx(\tau) + w(\tau) \quad (2)$$

where $x(\tau)$, $u(\tau)$, $y(\tau)$, $v(\tau)$, $w(\tau)$ are the state, control input, output, process noise and measurement noise vectors, respectively.

The variables of this model are:

$$x = (V_x \ V_y \ V_z \ \omega_x \ \omega_y \ \omega_z \ \phi \ \theta \ \psi)^T, \quad (3)$$

$$u = (\delta_{mr} \ \delta_{lat} \ \delta_{lon} \ \delta_{fan})^T$$

where V_x, V_y, V_z are forward, lateral and vertical velocities; $\omega_x, \omega_y, \omega_z$ are roll, pitch and yaw rates; ϕ, θ, ψ are roll, pitch and yaw angles; $\delta_{mr}, \delta_{lat}, \delta_{lon}, \delta_{fan}$ are main rotor collective, lateral cyclic, longitudinal cyclic and fan collective pitches.

We notice that the velocities from (3) can be expressed in the form

$$V_x = \dot{x}_c, V_y = \dot{y}_c, V_z = \dot{z}_c \quad (4)$$

where x_c, y_c, z_c are coordinates of center of mass of UAV in the earth-frame.

Combining (3) and (4), we have

$$x = (\dot{x}_c \ \dot{y}_c \ \dot{z}_c \ \omega_x \ \omega_y \ \omega_z \ \phi \ \theta \ \psi)^T,$$

$$u = (\delta_{mr} \ \delta_{lat} \ \delta_{lon} \ \delta_{fan})^T \quad (5)$$

The matrix structure of A, B, C for the state-space model of system (1)-(2) is given by

$$A = \begin{bmatrix} a_1 & a_2 & 0 & a_3 & a_4 & 0 & 0 & a_5 & 0 \\ a_6 & a_7 & 0 & a_8 & a_9 & 0 & a_{10} & 0 & 0 \\ 0 & 0 & a_{11} & 0 & 0 & a_{12} & 0 & 0 & 0 \\ a_{13} & a_{14} & 0 & a_{15} & a_{16} & 0 & 0 & 0 & 0 \\ a_{17} & a_{18} & 0 & a_{19} & a_{20} & 0 & 0 & 0 & 0 \\ 0 & 0 & a_{21} & 0 & 0 & a_{22} & 0 & 0 & 0 \\ 0 & 0 & 0 & 1 & 0 & 0 & 0 & 0 & 0 \\ 0 & 0 & 0 & 0 & 1 & 0 & 0 & 0 & 0 \\ 0 & 0 & 0 & 0 & 0 & 1 & 0 & 0 & 0 \end{bmatrix},$$

$$B = \begin{bmatrix} 0 & b_1 & b_2 & 0 \\ 0 & b_3 & b_4 & 0 \\ b_5 & 0 & 0 & b_6 \\ 0 & b_7 & b_8 & 0 \\ 0 & b_9 & b_{10} & 0 \\ b_{11} & 0 & 0 & b_{12} \\ 0 & 0 & 0 & 0 \\ 0 & 0 & 0 & 0 \\ 0 & 0 & 0 & 0 \end{bmatrix}, C = I_9 \quad (6)$$

The parameters a_1 through a_{22} and parameters b_1 through b_{12} in (6) are given by:

$$a_1 = 0.0058, \quad a_2 = 0.0017, \quad a_3 = 0.0081, \quad a_4 = 0.0329,$$

$$a_5 = -9.8000, \quad a_6 = -0.0015, \quad a_7 = -0.0058, \quad a_8 = -0.0329,$$

$$a_9 = 0.0081, \quad a_{10} = 9.8000, \quad a_{11} = -0.9816, \quad a_{12} = 0.0794,$$

$$a_{13} = -0.0072, \quad a_{14} = -0.0154, \quad a_{15} = -0.0867, \quad a_{16} = 0.0153,$$

$$a_{17} = 0.0106, \quad a_{18} = -0.0049, \quad a_{19} = -0.0106, \quad a_{20} = -0.0697,$$

$$a_{21} = -0.0416, \quad a_{22} = -0.1691;$$

$$b_1 = -0.1294, \quad b_2 = -2.8845, \quad b_3 = 2.8845, \quad b_4 = -0.1294,$$

$$b_5 = 122.0518, \quad b_6 = 11.8688, \quad b_7 = 7.5964, \quad b_8 = -0.9077,$$

$$b_9 = 0.8578, \quad b_{10} = 7.2260, \quad b_{11} = -26.0034, \quad b_{12} = 10.7727.$$

Then, we have

$$x_c(\tau) = \int_0^\tau \dot{x}_c(t) dt, y_c(\tau) = \int_0^\tau \dot{y}_c(t) dt, z_c(\tau) = \int_0^\tau \dot{z}_c(t) dt, \quad (7)$$

where

$$x_c(0) = 0, y_c(0) = 0, z_c(0) = 0.$$

From (1)-(2), (5)-(7) we can see that the attitude vector $(x_c, y_c, z_c)^T$ for given model of UAV can be computed.

III. THREE-RATE SUBSYSTEMS

In [7], it is offered the three-rate state space decomposition technique for stochastic linear systems.

Setting $q(\tau) = T x(\tau)$, where T is a nonsingular $n \times n$ matrix, we see that (1)-(2) are transformed into the equations

$$\dot{q}(\tau) = J_c q(\tau) + \tilde{B} u(\tau) + T v(\tau) \quad (8)$$

$$y(\tau) = \tilde{C} q(\tau) + w(\tau) \quad (9)$$

where

$$J_c = T A T^{-1}, \tilde{B} = T B, \tilde{C} = C T^{-1}.$$

The equations (8)-(9) may be written in terms of submatrices as

$$\dot{z}_1(\tau) = A_1 z_1(\tau) + B_1 u(\tau) + T_1 v(\tau) \quad (10)$$

$$\dot{z}_2(\tau) = A_2 z_2(\tau) + B_2 u(\tau) + T_2 v(\tau) \quad (11)$$

$$\dot{z}_3(\tau) = A_3 z_3(\tau) + B_3 u(\tau) + T_3 v(\tau) \quad (12)$$

$$y(\tau) = C_1 z_1(\tau) + C_2 z_2(\tau) + C_3 z_3(\tau) + w(\tau) \quad (13)$$

where

small eigenvalues of a matrix $A_1 : |\lambda(A_1)| < \gamma_{s_{\max}}$,
intermediate eigenvalues of a matrix $A_2 : \gamma_{i_{\min}} < |\lambda(A_2)| < \gamma_{i_{\max}}$,
large eigenvalues of a matrix $A_3 : |\lambda(A_3)| > \gamma_{f_{\min}}$,

$$J_c = \begin{bmatrix} A_1 & 0 & 0 \\ 0 & A_2 & 0 \\ 0 & 0 & A_3 \end{bmatrix}, \tilde{B} = \begin{bmatrix} B_1 \\ B_2 \\ B_3 \end{bmatrix}, \tilde{C} = [C_1 \ C_2 \ C_3],$$

$$T = \begin{bmatrix} T_1 \\ T_2 \\ T_3 \end{bmatrix}, q(\tau) = \begin{bmatrix} z_1(\tau) \\ z_2(\tau) \\ z_3(\tau) \end{bmatrix}.$$

Definition 1: A function with a large derivative which is fastly decreasing is said to be the “fast” function; a function with a small derivative which is slowly decreasing is said to be the “slow” function. A function is said to be the “intermediate” function if its derivative is intermediate between small and large values.

Consider the first time interval $0 < \tau_f \leq \tau_{fi}$. Applying a method of the Euler to (10), (11) and assuming that $z_1(0) = 0$ and $z_2(0) = 0$, we find

$$z_1(\tau_f) \approx \tau_f B_1 u(\tau_f) + \tau_f T_1 v(\tau_f),$$

$$z_2(\tau_f) \approx \tau_f B_2 u(\tau_f) + \tau_f T_2 v(\tau_f). \quad (14)$$

Using (12)-(14), we obtain the state equations for a “fast” subsystem

$$\dot{z}_f(\tau_f) = A_f z_f(\tau_f) + B_f u_f(\tau_f) + T_f v_f(\tau_f) \quad (15)$$

$$y_f(\tau_f) = C_f z_f(\tau_f) + D_f u_f(\tau_f) + w_f(\tau_f) \quad (16)$$

where

$$A_f = A_3, B_f = B_3, T_f = T_3, C_f = C_3,$$

$$D_f = \tau_f (C_1 B_1 + C_2 B_2), V_f = \tau_f (C_1 T_1 + C_2 T_2),$$

$$z_f(\tau_f) = z_3(\tau_f), u_f(\tau_f) = u(\tau_f), v_f(\tau_f) = v(\tau_f),$$

$$y_f(\tau_f) = y(\tau_f), w_f(\tau_f) = w(\tau_f) + V_f v(\tau_f).$$

Consider the second time interval $\tau_{fi} < \tau_i \leq \tau_{is}$. According to the Definition 1, a variable z_3 can be considered as a “fast” function, achieving on this interval a steady meaning. Inserting $\dot{z}_3(\tau_i) \approx 0$ in (12) gives

$$z_3(\tau_i) \approx -A_3^{-1} B_3 u(\tau_i) - A_3^{-1} T_3 v(\tau_i) \quad (17)$$

Using the implicit formula of the Euler for (10) and assuming that $z_1(0) = 0$ leads to

$$z_1(\tau_i) \approx \tau_i (I - \tau_i A_1)^{-1} B_1 u(\tau_i) + \tau_i (I - \tau_i A_1)^{-1} T_1 v(\tau_i) \quad (18)$$

Combining (11), (13), (17) and (18), we find that an “intermediate” subsystem is given by

$$\dot{z}_i(\tau_i) = A_i z_i(\tau_i) + B_i u_i(\tau_i) + T_i v_i(\tau_i) \quad (19)$$

$$y_i(\tau_i) = C_i z_i(\tau_i) + D_i u_i(\tau_i) + w_i(\tau_i) \quad (20)$$

where

$$A_i = A_2, B_i = B_2, T_i = T_2, C_i = C_2,$$

$$D_i = \tau_i C_1 (I - \tau_i A_1)^{-1} B_1 - C_3 A_3^{-1} B_3,$$

$$V_i = \tau_i C_1 (I - \tau_i A_1)^{-1} T_1 - C_3 A_3^{-1} T_3,$$

$$z_i(\tau_i) = z_2(\tau_i), u_i(\tau_i) = u(\tau_i), v_i(\tau_i) = v(\tau_i),$$

$$y_i(\tau_i) = y(\tau_i), w_i(\tau_i) = w(\tau_i) + V_i v(\tau_i).$$

Consider the last time interval $\tau_s > \tau_{is}$. According to the Definition 1 it is possible to consider variables z_2 and z_3

as the “intermediate” functions achieving on this interval the steady meanings. Then, from (12) and (13), we have

$$z_2(\tau_s) \approx -A_2^{-1}B_2u(\tau_s) - A_2^{-1}T_2v(\tau_s),$$

$$z_3(\tau_s) \approx -A_3^{-1}B_3u(\tau_s) - A_3^{-1}T_3v(\tau_s) \quad (21)$$

Further, from (11), (14) and (22), we find that the state equations for a “slow” subsystem may be written as

$$\dot{z}_s(\tau_s) = A_s z_s(\tau_s) + B_s u_s(\tau_s) + T_s v_s(\tau_s) \quad (22)$$

$$y_s(\tau_s) = C_s z_s(\tau_s) + D_s u_s(\tau_s) + w_s(\tau_s) \quad (23)$$

where

$$A_s = A_1, B_s = B_1, T_s = T_1, C_s = C_1,$$

$$D_s = -C_2 A_2^{-1} B_2 - C_3 A_3^{-1} B_3, V_s = -C_2 A_2^{-1} T_2 - C_3 A_3^{-1} T_3,$$

$$z_s(\tau_s) = z_1(\tau_s), u_s(\tau_s) = u(\tau_s), v_s(\tau_s) = v(\tau_s).$$

IV. SIMULATION RESULTS

Consider the control of given three-rate TUAV model with coaxial rotor and ducted fan configuration for the case of take-off, approach and hovering maneuvers by hybrid constrained system of three control subsystems.

Initial conditions and desired height are chosen to be:

$$x(0) = y(0) = z(0) = 0m, z_1^0 = 30m.$$

Simulation results of the offered block scheme with three control subsystems (see Fig. 1) are shown in Figs. 4-7.

In [8], the two approximations to the nonlinear autoregressive moving average (NARMA) model are introduced. They are widely known as NARMA-L1 and the NARMA-L2 models. It is found that the NARMA-L2 model to be simpler to realize than the NARMA-L1 model.

In this section, we used only the NARMA-L2 approximate model [8]. Block diagram for the NARMA-L2 Controller from Fig. 1 is given in Fig. 2. The structure of the NARMA-L2 approximate model was detailed in Fig. 3. The NARMA-L2 Controller tuning can be accomplished quickly and accurately using internal windows for this block.

Some advantages of this example are as follows.

- Opportunity of smooth switching of regulation from one control subsystem to another.
- Ability for take-off, approach and hovering maneuvers by single neurocontroller.
- Possibility of hovering in different selected height positions.

The trajectory tracking display forms give a researcher an immediate view of given TUAV motion with a range of such parameter as main rotor collective pitch. This allows us to investigate the sensitivity of the three-rate control system, providing a medium for such development and evaluation and enhancing the researcher’s understanding of flight maneuvers.

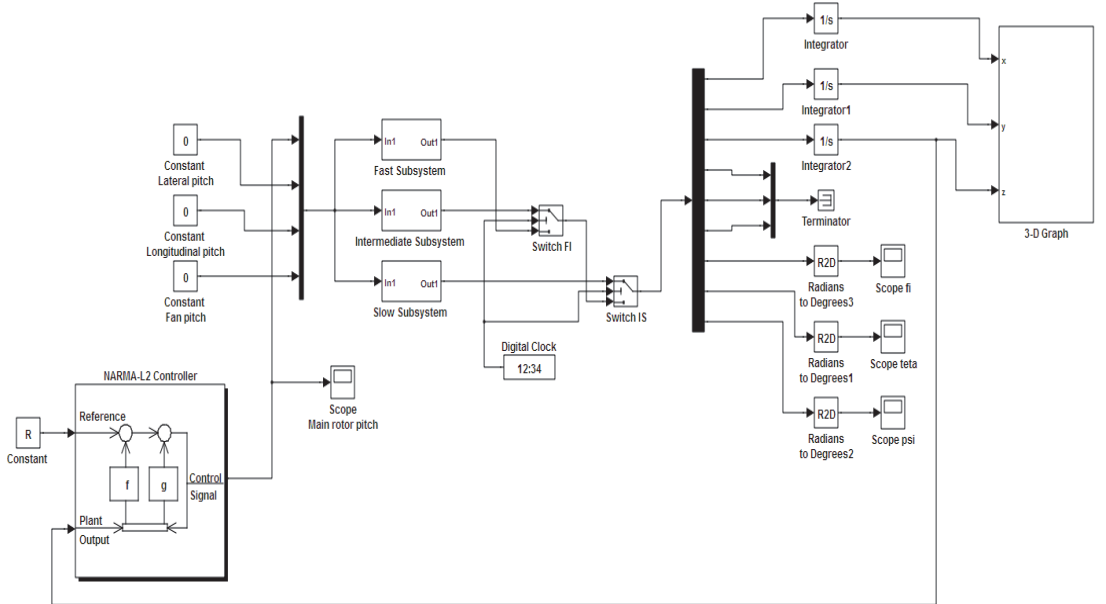


Fig. 1. Block diagram of three-rate control system.

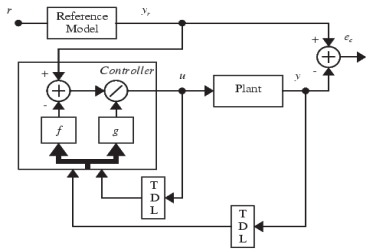


Fig. 2. Block diagram of the NARMA-L2 Controller.

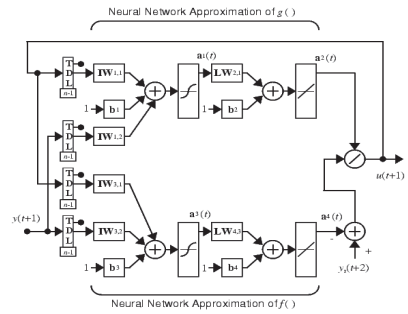


Fig. 3. Structure of the NARMA-L2 approximate model.

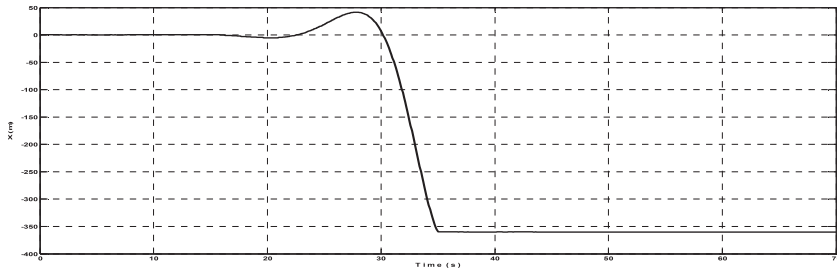


Fig. 4. View of x-coordinate of the center of mass of UAV.

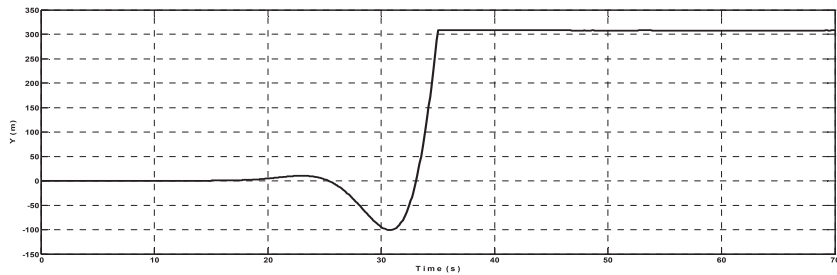


Fig. 5. View of y-coordinate of the center of mass of UAV.

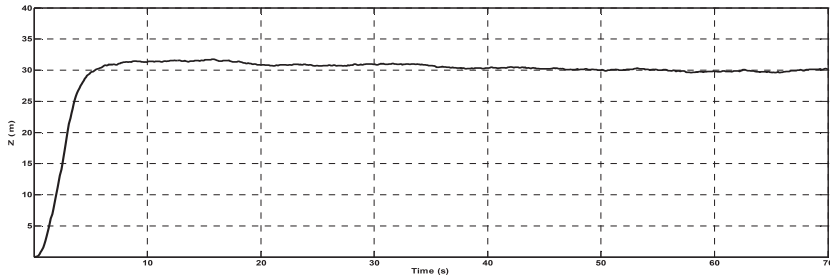


Fig. 6. View of z-coordinate of the center of mass of UAV.

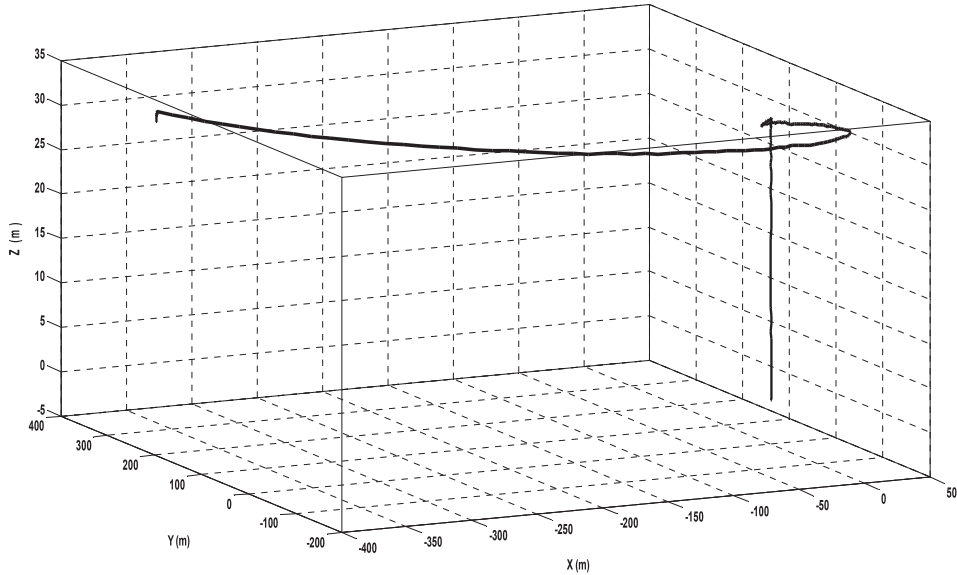


Fig. 7. 3-D motion of TUAV.

V. CONCLUSIONS

A new research technique is presented in this paper for enhanced SA in possible missions of TUAV with coaxial rotor and ducted fan configuration.

For fast, stable and smooth flight maneuvers, we proposed a three-rate flight strategy. From the applications viewpoint, we believe that the three-rate flight strategy furnishes a powerful approach for enhancing SA in applications to VTOL class autonomous vehicles.

By following the proposed methodology, the TUAV model (1)-(2) of 9th order is decomposed into three subsystems: the "fast" subsystem of 3th order used in the initial phase of trajectory (take-off), the "intermediate" subsystem of 4th order used in the middle phase of trajectory (approach), and the "slow" subsystem of 2th order used in the final phase of trajectory (hovering). It can be seen (see Figs. 4-6) that it is possible to accept the time intervals between "fast" and "intermediate" subsystems and between "intermediate" and "slow" subsystems as 15 and 35 seconds, respectively.

Future work will involve further validation and exploring of proposed research technique for other missions of TUAVs having coaxial rotor and ducted fan configuration.

REFERENCES

- [1] M. R. Endsley, "Toward a theory of situation awareness in dynamic systems," *Human Factors*, vol. 37, pp. 32–64, March 1995.
- [2] J. Gorman, N. Cooke, and J. Winner, "Measuring team situation awareness in decentralized command and control environments," *Ergonomics*, vol. 49, pp. 1312–1325, October 2006.
- [3] Interim Brigade Combat Team Newsletter. [Online]. Available: http://www.globalsecurity.org/military/library/report/call/call_01-18_toc.htm
- [4] S. D. Prior, S. T. Shen, A. S. White, S. Odedra, M. Karamanoglu, M. A. Erbil, and T. Foran, "Development of a novel platform for greater situational awareness in the urban military terrain," in *Proc. 8th International Conf. Engineering Psychology and Cognitive Ergonomics*, San Diego, USA, 2009, pp. 120–125.
- [5] I. Astrov and A. Pedai, "Control of hovering manoeuvres in unmanned helicopter for enhanced situational awareness," in *Proc. International Conf. Industrial Mechatronics and Automation*, Chengdu, China, 2009, pp. 143–146.
- [6] S. Shouzhao, A. A. Mian, Z. Chao, and J. Bin, "Autonomous takeoff and landing control for a prototype unmanned helicopter," *Control Engineering Practice*, vol. 18, pp. 1053–1059, September 2010.
- [7] I. Astrov, A. Pedai, and E. Rüstern, "Simulation of three-rate neural and neuro-fuzzy hybrid control for the multidimensional stochastic model of a fighter aircraft," in *Proc. 8th World Multi-Conf. Systemics, Cybernetics and Informatics*, Orlando, USA, 2004, pp. 351–356.
- [8] K. S. Narendra and S. Mukhopadhyay, "Adaptive control using neural networks and approximate models," *IEEE Trans. Neural Networks*, vol. 8, pp. 475–485, May 1997.

Publication III

Pedai, Andrus; Astrov, Igor; Udal, Andres (2018). Comparison of single-rate and two-rate neural control approaches for coaxial rotor/ducted-fan TUAV for situational awareness applications. SISY 2018: IEEE 16th International Symposium on Intelligent Systems and Informatics, Proceedings, Subotica, Serbia, September 13-15, 2018.

Comparison of Single-Rate and Two-Rate Neural Control Approaches for Coaxial Rotor/Ducted-Fan TUAV for Situational Awareness Applications

Andrus Pedai, Igor Astrov, and Andres Udal

School of Information Technologies

Tallinn University of Technology

Tallinn, Estonia

andrus.pedai@gmail.com, igor.astrov@gmail.com, andres.udal@ttu.ee

Abstract—Paper discusses the modeling and control methodologies of a tactical unmanned aerial vehicle (TUAV) of coaxial rotor type with ducted fan via introduction of two-rate control and neural network methods in order to achieve more stabilized flight control. The effectiveness of the proposed single-rate and two-rate control strategies was illustrated and confirmed by numerical simulations of flight maneuvers using programming environment Simulink for chosen model of TUAV. At that earlier developed decomposition methodologies have been applied and adjusted for the actual unmanned aerial vehicle. As the TUAVs are becoming one of the most important information collection devices for the modern situation awareness (SA) systems, the achieved improvements in stabilization of flight trajectories and relevant energy economy enhancements will help to design better SA systems for search, rescue and situation reconnaissance operations.

Keywords—coaxial rotors, ducted fan, multi-rate control, neural network controller, situation awareness, tactical unmanned aerial vehicle.

I. INTRODUCTION

There has occurred exponential burst of world research intensity under the topic of “Unmanned Aerial Vehicle” (UAV) during the recent years – see Fig. 1 below.

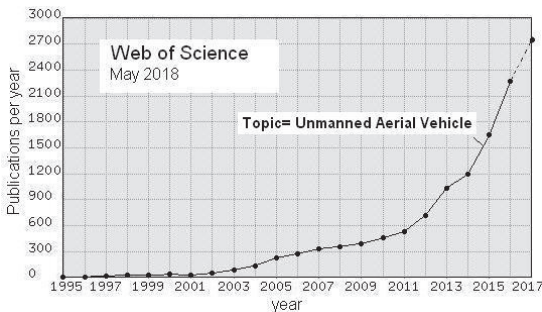


Fig. 1. Explosive growth of the annual world publications number under the topic of “UAV”. The previous doubling by 3-4 years has been accelerated to doubling in every 2 years. Data from Clarivate Analytics Web of Science database.

Thus the development of UAV R&D has grown even faster than expected in 2010 [1]. It may be estimated that most of the recent burst has been caused by versatile applications opportunities where the conventional helicopters can be replaced by UAVs. Recent supporting step forward was made in 2016 by US Federal Aviation Administrator making it easier for news organizations to use UAVs as news gathering tool. All fast growing UAVs application fields [1] demand also efforts from scientists to tackle the flight control, stability and economy issues.

Situation awareness (SA) has been mostly a military term defined as “the perception of elements in the environment within a volume of time and space, the comprehension of their meaning, and the projection of their status in the near future” [2]. SA has been recognized as a critical, yet often elusive, foundation for successful decision-making across a broad range of complex and dynamic systems, including emergency response and military command and control operations [3]. The tactical unmanned aerial vehicles (TUAVs) are expected to become an important information gathering tool to build SA systems for all military leaders [4]. At that helicopter type TUAVs offer at low cost same noticeable additional advantages like the ability to fly within a narrow space due to vertical take-off and landing (VTOL) flying capabilities. In the present work we study the VTOL characteristics of one certain TUAV prototype with net weight of 160 kg [5].

Well controlled vertical flight is a challenging important subtask for helicopter type TUAVs to assure reliable performance under possible disadvantageous conditions. The main requirement for vertical flight and also horizontal hovering is a properly designed controller to govern the height control above the ground. In [6], a three stage flight control methodology using three autonomous control subsystems on the basis of nonlinear equations of vertical motion for the center of mass of helicopter was developed. The developed control strategy was verified by simulation of flight maneuvers using the software package Simulink.

The present paper extends the earlier approach [6] on the basis of modeling and simulation of state-space equations in Simulink/MATLAB environment. Here additionally the two-rate control system technique is compared with the basic

single-rate realization for a realistic coaxial rotor/ducted-fan TUAV mechanical model defined by 9-component state vector [5]. Observed changes in take-off and hovering (“go-search-and-find” scenario) flight characteristics due to replacement of initial single-rate control system with a more sophisticated two-rate control system will be compared. Paper presents below in detail the matrix formulations of the initial mechanical model and the matrix formulations of the “fast” and “slow” subsystems of the decomposed two-rate mechanical model.

II. SINGLE-RATE TUAV MODEL

The aerodynamic parameters of VTOL type UAVs are often difficult and expensive to define precisely. In [7], the dynamics of a VTOL aircraft, such as a Harrier around hover, were described. It is shown that a simple choice of control Lyapunov function, i.e., the one obtained from Jacobian linearization of the dynamics at hover, will achieve a good performance. In [5], a reliable model of coaxial rotor/ducted-fan TUAV with parameters measured in wind tunnel was described.

This TUAV [5], with the height of $l=1.9$ m and a net weight of 160 kg is a VTOL aircraft containing two coaxial rotors, main and ducted, rotating at 800rpm in opposite directions. The main propeller with a diameter of 4.4 m is mounted on the top of the fuselage and it provides about 80% of lift together with drag, pitch and roll movements. A duct is formed through the fuselage from the top to the bottom and it contains the auxiliary rotor compensating the main propeller antitorque and yielding also some fraction (20%) of lift together with yaw movements. It is estimated that this coaxial two-rotor ducted fan configuration can provide more lift and easier movement control in any direction during take-off and landing in comparison with conventional helicopter having main and tail rotors. Mentioned features increase the stability and maneuverability of TUAV making it easier to fly in difficult and narrow space conditions met in SA missions.

This TUAV is used mainly for low-speed flight missions. The nonlinear system as a coaxial rotor/ducted-fan TUAV can be linearized near the hover flight condition and the linearized model can be received.

The dynamic model for this TUAV may be constructed on the basis of traditional state equations formalism [5] completed here with presence of stochastic disturbances available in Simulink/MATLAB environment:

$$\dot{x}(\tau) = Ax(\tau) + Bu(\tau) + v(\tau), \quad (1)$$

$$y(\tau) = Cx(\tau) + w(\tau) \quad (2)$$

where $x(\tau), u(\tau), y(\tau), v(\tau), w(\tau)$ denote the state vector, control input vector, output vector, process noise and measurement noise vectors, respectively.

Following [5], the state vector incorporates 6 degree-of-freedom parameters and 3 mechanical parameters while the

input control vector is defined by 4 parameters for the present task:

$$x = (V_x \ V_y \ V_z \ \omega_x \ \omega_y \ \omega_z \ \phi \ \theta \ \psi)^T, \\ u = \begin{bmatrix} \delta_{mr} \\ \delta_{lat} \\ \delta_{lon} \\ \delta_{fan} \end{bmatrix} \quad (3)$$

where V_x, V_y, V_z are forward, lateral and vertical velocities; $\omega_x, \omega_y, \omega_z$ denote the roll, pitch and yaw rates; ϕ, θ, ψ are roll, pitch and yaw angles; and $\delta_{mr}, \delta_{lat}, \delta_{lon}, \delta_{fan}$ are main rotor collective, lateral cyclic, longitudinal cyclic and fan collective pitches.

The velocities in (3) are actually time derivatives

$$V_x = \dot{x}_c, V_y = \dot{y}_c, V_z = \dot{z}_c \quad (4)$$

where x_c, y_c, z_c represent the coordinates of TUAVs center of mass in the earth-frame.

After combining (3) and (4), we have

$$x = (\dot{x}_c \ \dot{y}_c \ \dot{z}_c \ \omega_x \ \omega_y \ \omega_z \ \phi \ \theta \ \psi)^T, \\ u = \begin{bmatrix} \delta_{mr} \\ \delta_{lat} \\ \delta_{lon} \\ \delta_{fan} \end{bmatrix}. \quad (5)$$

The general structure of matrices A, B, C of the state-space model system (1) -(2) may be written as

$$A = \begin{bmatrix} a_1 & a_2 & 0 & a_3 & a_4 & 0 & 0 & a_5 & 0 \\ a_6 & a_7 & 0 & a_8 & a_9 & 0 & a_{10} & 0 & 0 \\ 0 & 0 & a_{11} & 0 & 0 & a_{12} & 0 & 0 & 0 \\ a_{13} & a_{14} & 0 & a_{15} & a_{16} & 0 & 0 & 0 & 0 \\ a_{17} & a_{18} & 0 & a_{19} & a_{20} & 0 & 0 & 0 & 0 \\ 0 & 0 & a_{21} & 0 & 0 & a_{22} & 0 & 0 & 0 \\ 0 & 0 & 0 & 1 & 0 & 0 & 0 & 0 & 0 \\ 0 & 0 & 0 & 0 & 1 & 0 & 0 & 0 & 0 \\ 0 & 0 & 0 & 0 & 0 & 1 & 0 & 0 & 0 \end{bmatrix}, \\ B = \begin{bmatrix} 0 & b_1 & b_2 & 0 \\ 0 & b_3 & b_4 & 0 \\ b_5 & 0 & 0 & b_6 \\ 0 & b_7 & b_8 & 0 \\ 0 & b_9 & b_{10} & 0 \\ b_{11} & 0 & 0 & b_{12} \\ 0 & 0 & 0 & 0 \\ 0 & 0 & 0 & 0 \\ 0 & 0 & 0 & 0 \end{bmatrix},$$

$$C = \begin{bmatrix} 1 & 0 & 0 & 0 & 0 & 0 & 0 & 0 & 0 \\ 0 & 1 & 0 & 0 & 0 & 0 & 0 & 0 & 0 \\ 0 & 0 & 1 & 0 & 0 & 0 & 0 & 0 & 0 \\ 0 & 0 & 0 & 1 & 0 & 0 & 0 & 0 & 0 \\ 0 & 0 & 0 & 0 & 1 & 0 & 0 & 0 & 0 \\ 0 & 0 & 0 & 0 & 0 & 1 & 0 & 0 & 0 \\ 0 & 0 & 0 & 0 & 0 & 0 & 1 & 0 & 0 \\ 0 & 0 & 0 & 0 & 0 & 0 & 0 & 1 & 0 \\ 0 & 0 & 0 & 0 & 0 & 0 & 0 & 0 & 1 \end{bmatrix}. \quad (6)$$

The parameters a_1 through a_{22} and b_1 through b_{12} have been adjusted from wind tunnel experiments [5] and have the following numerical values in SI-system:

$$\begin{aligned} a_1 &= 0.0058, & a_2 &= 0.0017, & a_3 &= 0.0081, \\ a_4 &= 0.0329, & a_5 &= -9.8000, & a_6 &= -0.0015, \\ a_7 &= -0.0058, & a_8 &= -0.0329, & a_9 &= 0.0081, \\ a_{10} &= 9.8000, & a_{11} &= -0.9816, & a_{12} &= 0.0794, \\ a_{13} &= -0.0072, & a_{14} &= -0.0154, & a_{15} &= -0.0867, \\ a_{16} &= 0.0153, & a_{17} &= 0.0106, & a_{18} &= -0.0049, \\ a_{19} &= -0.0106, & a_{20} &= -0.0697, & a_{21} &= -0.0416, \\ & & a_{22} &= -0.1691; \\ b_1 &= -0.1294, & b_2 &= -2.8845, & b_3 &= 2.8845, \\ b_4 &= -0.1294, & b_5 &= 122.0518, & b_6 &= 11.8688, \\ b_7 &= 7.5964, & b_8 &= -0.9077, & b_9 &= 0.8578, \\ b_{10} &= 7.2260, & b_{11} &= -26.0034, & b_{12} &= 10.7727. \end{aligned}$$

Then, we have

$$x_c(\tau) = \int_0^\tau \dot{x}_c(t) dt, \quad y_c(\tau) = \int_0^\tau \dot{y}_c(t) dt, \quad z_c(\tau) = \int_0^\tau \dot{z}_c(t) dt \quad (7)$$

with initial conditions

$$x_c(0) = 0, \quad y_c(0) = 0, \quad z_c(0) = 0.$$

One can see that from model (1)-(2), (5)-(7) the location vector $(x_c, y_c, z_c)^T$ of the studied TUAV can be computed.

III. TWO-RATE TUAV MODEL

The methodology of multi-rate decomposition is discussed lately in [8] and more systematically in [9]. Following this methodology, in the present TUAV case the below described “fast” and “slow” subsystem models were constructed.

In [9], such basic heuristic reception in the theory of dynamic systems as frequency-response separation of motions, that is, the separation of motions on “fast” and “slow” motions in a given case, was developed.

The offered block scheme (see Fig. 2) allows us to compare the following outputs: the original system’s outputs and the “fast” system’s outputs, the original system’s outputs and the “slow” system’s outputs. It was obtained that it is possible to accept 15 s as a border of the temporary division of the “fast” and “slow” control subsystems.

The state equations for a “fast” subsystem may be written via 5 matrices as [8,9]:

$$\dot{z}_f(\tau_f) = A_f z_f(\tau_f) + B_f u_f(\tau_f) + T_f v_f(\tau_f), \quad (8)$$

$$y_f(\tau_f) = C_f z_f(\tau_f) + D_f u_f(\tau_f) + w_f(\tau_f) \quad (9)$$

where

$$A_f = \begin{bmatrix} 0.2896 & 0.4114 & 0 & 0 & 0 & 0 & 0 \\ -0.4114 & 0.2896 & 0 & 0 & 0 & 0 & 0 \\ 0 & 0 & 0.1723 & 0.4734 & 0 & 0 & 0 \\ 0 & 0 & -0.4734 & 0.1723 & 0 & 0 & 0 \\ 0 & 0 & 0 & 0 & -0.5401 & 0.0714 & 0 \\ 0 & 0 & 0 & 0 & -0.0714 & 0.5401 & 0 \\ 0 & 0 & 0 & 0 & 0 & 0 & -0.9775 \end{bmatrix},$$

$$B_f = \begin{bmatrix} 0 & -6.0354 & 0.3019 & 0 \\ 0 & 2.0201 & -8.3919 & 0 \\ 0 & 3.4868 & -8.4436 & 0 \\ 0 & -6.1029 & -1.4434 & 0 \\ 0 & 5.1137 & 5.7297 & 0 \\ 0 & -7.2234 & 9.5826 & 0 \\ -8.0021 & 0 & 0 & -0.6943 \end{bmatrix},$$

$$T_f = \begin{bmatrix} 0.0300 & 0.0152 & 0 & -0.7946 & -0.0458 & 0 & -0.1411 & -0.4645 & 0 \\ -0.0080 & 0.0195 & 0 & 0.3844 & -1.1159 & 0 & 0.4604 & -0.3879 & 0 \\ -0.0148 & -0.0273 & 0 & 0.5934 & -1.1004 & 0 & -0.2233 & -0.4203 & 0 \\ -0.0284 & 0.0023 & 0 & -0.7700 & -0.3078 & 0 & -0.4833 & 0.4591 & 0 \\ -0.0138 & 0.0212 & 0 & 0.5679 & 0.8592 & 0 & -0.3244 & -0.3285 & 0 \\ -0.0353 & -0.0229 & 0 & -1.0756 & 1.1765 & 0 & 0.4591 & -0.5970 & 0 \\ 0 & 0 & -0.0642 & 0 & 0 & 0.0063 & 0 & 0 & 0 \end{bmatrix},$$

$$C_f = \begin{bmatrix} 9.6047 & -7.8929 & -1.2775 & -11.1129 & -6.7949 & -6.2523 & 0 \\ 4.0458 & 13.8678 & -12.2900 & 6.7570 & 10.5179 & -4.0968 & 0 \\ 0 & 0 & 0 & 0 & 0 & 0 & -15.6507 \\ -0.3746 & -0.0192 & 0.1296 & -0.3416 & 0.2725 & -0.2000 & 0 \\ -0.1053 & -0.3009 & -0.2079 & -0.2020 & 0.2489 & 0.1315 & 0 \\ 0 & 0 & 0 & 0 & 0 & 0 & -0.8054 \\ -0.4599 & 0.5869 & -0.5493 & -0.4736 & -0.5439 & 0.2983 & 0 \\ -0.6094 & -0.1732 & -0.5178 & 0.2507 & -0.4212 & -0.2992 & 0 \\ 0 & 0 & 0 & 0 & 0 & 0 & 0.8239 \end{bmatrix},$$

$$D_f = 10^{12} \times \begin{bmatrix} 0 & 0 & 0 & 0 \\ 0 & 0 & 0 & 0 \\ 0 & 0 & 0 & 0 \\ 0 & 0 & 0 & 0 \\ 0 & 0 & 0 & 0 \\ 0 & 0 & 0 & 0 \\ 0 & 0 & 0 & 0 \\ -1.8077 & 0 & 0 & 0.5955 \end{bmatrix}$$

The state equations for a “slow” subsystem may be written as via 5 matrices as [8,9]:

$$\dot{z}_s(\tau_s) = A_s z_s(\tau_s) + B_s u_s(\tau_s) + T_s v_s(\tau_s), \quad (10)$$

$$y_s(\tau_s) = C_s z_s(\tau_s) + D_s u_s(\tau_s) + w_s(\tau_s) \quad (11)$$

where

$$A_s = \begin{bmatrix} 0 & 0 \\ 0 & -0.1732 \end{bmatrix},$$

$$B_s = \begin{bmatrix} -11.2979 & 0 & 0 & 3.7217 \\ -14.2467 & 0 & 0 & 4.4844 \end{bmatrix},$$

$$T_s = \begin{bmatrix} 0 & 0 & -0.0154 & 0 & 0 & 0.3624 & 0 & 0 & 0.0625 \\ 0 & 0 & -0.0227 & 0 & 0 & 0.4413 & 0 & 0 & 0 \end{bmatrix},$$

$$C_s = \begin{bmatrix} 0 & 0 \\ 0 & 0.2237 \\ 0 & 0 \\ 0 & 0 \\ 0 & 2.2776 \\ 0 & 0 \\ 0 & 0 \\ 16.0000 & -13.1511 \end{bmatrix},$$

$$D_s = \begin{bmatrix} 0 & 120.9563 & -582.9545 & 0 \\ 0 & 436.7217 & 213.6086 & 0 \\ 128.1196 & 0 & 0 & 11.1156 \\ 0 & 0 & 0 & 0 \\ 0 & 0 & 0 & 0 \\ 6.5929 & 0 & 0 & 0.5720 \\ 0 & -0.0174 & 0.0504 & 0 \\ 0 & 0.1341 & -0.6023 & 0 \\ -6.7445 & 0 & 0 & -0.5852 \end{bmatrix}.$$

IV. SIMULATION RESULTS

Below we consider simulation of take-off, approach and hovering flight maneuvers using the above described single-rate and two-rate control system variants.

Initial and desired final height for simulation example were specified as:

$$x(0) = y(0) = z(0) = 0 \text{ m}, \quad z_1^0 = 20 \text{ m}.$$

Simulink runs under MATLAB. Before running the models, we need to assign numerical values to each of the variables used in the models through MATLAB. Simulink was used to simulate the complete control system.

In [10], the two approximations to the nonlinear autoregressive moving average (NARMA) model called the NARMA-L1 and the NARMA-L2 are proposed. From a practical stand-point, the NARMA-L2 model is found to be simpler to realize than the NARMA-L1 model. The neurocontrollers used in this section are based only on the NARMA-L2 model [10]. Simulink tuning tools let us tune control systems containing NARMA-L2 Controller Simulink block.

In [11], the model predictive control method is proposed. This controller uses a neural network (NN) model to predict future plant responses to potential control signals. An optimization algorithm then computes the control signals that optimize future plant performance. The NN Predictive Controller tuning can be accomplished quickly and accurately using internal windows for this block.

The problem of noise reducing without additional filtering can be decided using appropriate design strategies with these NN controllers.

The block schemes of single-rate and two-rate TUAV control systems realization are presented in Fig. 2.

Main simulation results of the offered block schemes with one control system or two control subsystems are shown in Figs. 3-5.

Fig. 3 presents straightforward comparison of two-rate system takeoff and hovering ability with original single-rate system. The main observations are:

- Rise Time (t_r) for single-rate system is 2.12 s, but for two-rate system is 4.79 s.
- Time to First Peak (t_p) for single-rate system is 5 s, but for two-rate system is 10 s.
- Settling Time (t_s) for single-rate system is 20 s, but for two-rate system is 10 s.
- Overshoot (O) for single-rate system is 5.5 %, but for two-rate system only 1.05 %
- Small height oscillations on the hovering part of flight are missing in the case of two-rate control

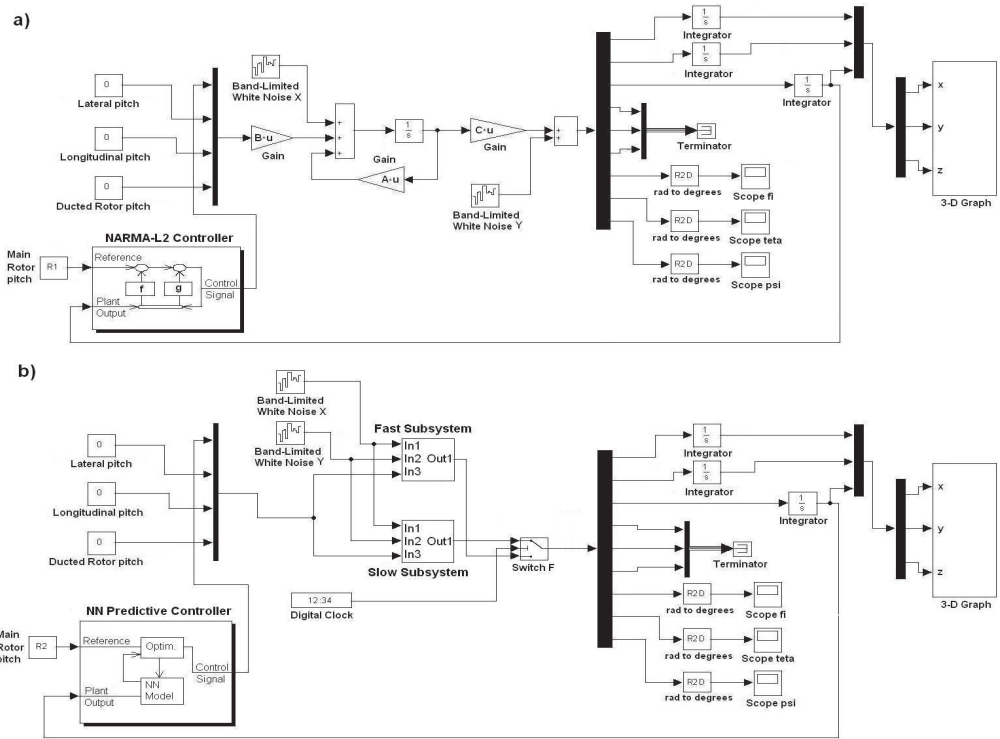


Fig. 2. Simulink style block diagrams of single-rate (a) and two-rate control systems (b).

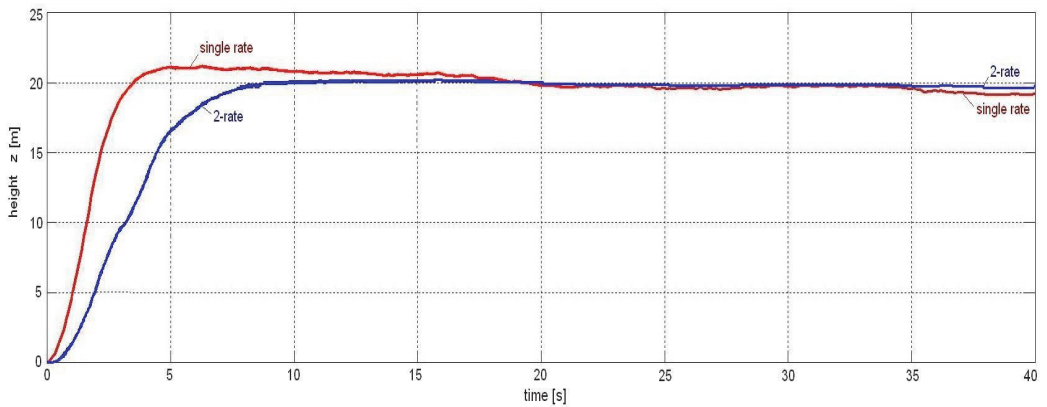


Fig. 3. Comparison of TUAV takeoff and hovering trajectories at height 20 m in the case of single- rate and two-rate control systems (TUAV center of mass plotted).

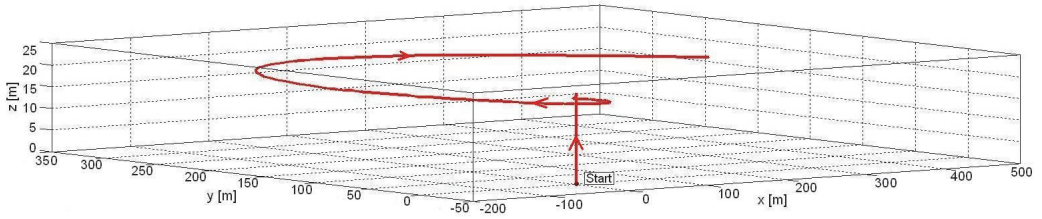


Fig. 4. 3D presentation of takeoff and hovering trajectory at height 20 m in the case of single-rate TUAV control.

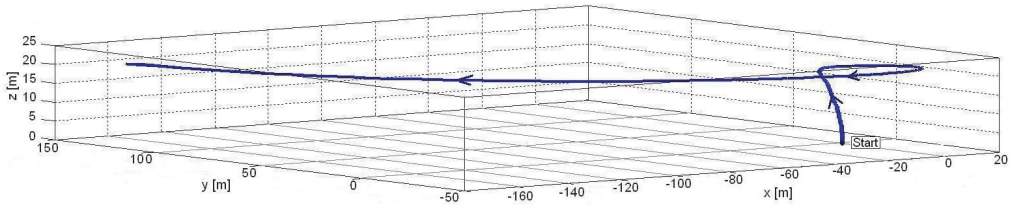


Fig. 5. 3D presentation of takeoff and hovering trajectory at height 20 m in the case of two-rate TUAV control.

V. CONCLUSIONS

A new modeling and simulation technique is presented in this paper for a TUAV with coaxial rotor and ducted fan. The proposed methodology may be used for improvement of model-based design on UAVs dedicated for different application fields including the different SA systems.

For stable and smooth flight maneuvers, we proposed a two-rate decomposition of the initial control task. By following the proposed methodology, the original TUAV model of 9th order was decomposed into two parts: the “fast” subsystem of 7th order for the initial phase of trajectory (take-off and approach motions) and the “slow” subsystem of 2nd order for the final phase of trajectory (hovering motion).

From the applications viewpoint, we believe that the modeled and simulated flight control strategy may offer a reasonable possibility to improve VTOL class UAVs flight characteristics needed for information collection in sophisticated SA systems.

Future work will involve the generalization, automation and testing of the proposed methodology with further validation of time domain control system performance parameters for other relevant missions of TUAVs.

REFERENCES

- [1] K. Nonami, F. Kendoul, S. Suzuki, W. Wang, and D. Nakazawa, *Autonomous Flying Robots: Unmanned Aerial Vehicles and Micro Aerial Vehicles*. New York: Springer, 2010.
- [2] M. R. Endsley, “Toward a theory of situation awareness in dynamic systems,” *Human Factors*, vol. 37, pp. 32–64, March 1995.
- [3] J. Gorman, N. Cooke, and J. Winner, “Measuring team situation awareness in decentralized command and control environments,” *Ergonomics*, vol. 49, pp. 1312–1325, October 2006.
- [4] S. D. Prior, S. T. Shen, A. S. White, S. Odedra, M. Karamanoglu, M. A. Erbil, and T. Foran, “Development of a novel platform for greater situational awareness in the urban military terrain,” *Proc. 8th International Conf. Engineering Psychology and Cognitive Ergonomics*, San Diego, USA, pp. 120–125, 2009.
- [5] S. Shouzhao, A. A. Mian, Z. Chao, and J. Bin, “Autonomous takeoff and landing control for a prototype unmanned helicopter,” *Control Engineering Practice*, vol. 18, pp. 1053–1059, September 2010.
- [6] I. Astrov and A. Pedai, “Control of hovering manoeuvres in unmanned helicopter for enhanced situational awareness,” *Proc. International Conf. Industrial Mechatronics and Automation*, Chengdu, China, pp. 143–146, 2009.
- [7] A. Jadbabaie, J. Yu, and J. Hauser, “Receding horizon control of the Caltech ducted fan: a control Lyapunov function approach,” *Proc. IEEE Conf. Control Applications*, Kohala Coast, USA, pp. 51–56, 1999.
- [8] I. Astrov, “Two-rate motion control of VTAV by NARMA-L2 controller for enhanced situational awareness,” *Proc. 39th International Convention on Information and Communication Technology, Electronics and Microelectronics/ International Conf. Computers in Technical Systems*, Opatija, Croatia, pp. 1333–1338, 2016.
- [9] I. Astrov, *Model-Based Design of Multirate Control Systems: Modeling and Simulation*. Saarbrücken: Lambert Academic Publishing, 2016.
- [10] K. S. Narendra and S. Mukhopadhyay, “Adaptive control using neural networks and approximate models,” *IEEE Trans. Neural Networks*, vol. 8, pp. 475–485, May 1997.
- [11] J. M. Maciejowski, *Predictive Control with Constraints*. London: Prentice Hall, 2002.

Publication IV

Pedai, Andrus; Astrov, Igor; Udal, Andres; Sell, Raivo (2019). Single-rate versus three-rate neural assisted control approaches for coaxial rotor ducted fan TUAV for situation awareness applications. SysCon 2019 : The 13th Annual IEEE International Systems Conference, April 8-11, 2019, Orlando, Florida, USA.

Single-Rate versus Three-Rate Neural Assisted Control Approaches for Coaxial Rotor Ducted Fan TUAV for Situation Awareness Applications

Andrus Pedai, Igor Astrov, Andres Udal, and Raivo Sell
Department of Mechanical and Industrial Engineering
Tallinn University of Technology
Tallinn, Estonia

andrus.pedai@gmail.com, igor.astrov@ieec.org, andres.udal@taltech.ee, raivo.sell@taltech.ee

Abstract—Paper studies the modeling and control approaches of a tactical unmanned aerial vehicle (TUAV) as a coaxial unmanned helicopter with ducted fan configuration via implementation of three-rate control and neural network techniques to achieve more stabilized flight height control. The single-rate and three-rate control strategies for selected type of TUAV are verified and compared by simulation of flight maneuvers using MATLAB products. At that previously developed decomposition methodologies are applied and adjusted for the actual TUAV. As this kind of unmanned flight drones are becoming more important information collection tools for the modern situation awareness (SA) systems, the achieved advancements in stabilization of flight trajectories together with improved energy economy will help to design better SA systems for search, rescue and surveillance applications.

Keywords—coaxial rotors, ducted fan, multi-rate control, neural network controller, situation awareness, tactical unmanned aerial vehicle.

I. INTRODUCTION

During the recent years an exponentially accelerating growth of world research intensity under the topic of “Unmanned Aerial Vehicle” (UAV) has occurred – see Fig. 1 below.

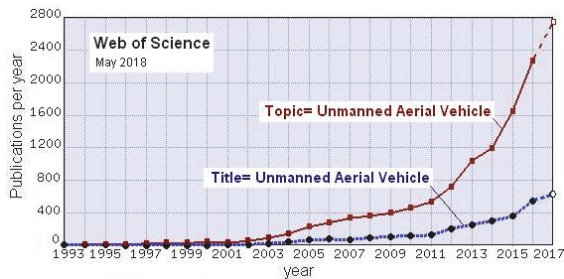


Fig. 1. Continuing and accelerating growth of the annual world publications number under the topic of “Unmanned Aerial Vehicle”. The previous doubling by 3–4 years has been accelerated to doubling in every 2 years. Data from Clarivate Analytics Web of Science database.

Thus R&D in this field has grown even more faster than expected recently in 2010 [1]. It may be surmised that reason for this still accelerating burst may be caused by versatile

possibilities to replace the conventional helicopters. It should be noted that recently in 2016 US Federal Aviation Administrator simplified to use UAVs as news gathering tool for news organizations. Fast expanding application fields [1] of UAVs demand also efforts from researchers to handle better the flight control, stability and energy economy issues.

Situation awareness (SA) is “the perception of elements in the environment within a volume of time and space, the comprehension of their meaning, and the projection of their status in the near future” [2]. SA has been recognized as a critical, yet often elusive, foundation for successful decision-making across a broad range of complex and dynamic systems, including emergency response in military command and control operations [3]. The tactical unmanned aerial vehicles (TUAVs) may become the key tools to gather the information to build SA systems for all military leaders [4]. At that vertical takeoff and landing (VTOL) type TUAVs offer multiple additional advantages, including low cost, the ability to fly within a narrow space and the unique hovering and vertical takeoff and landing. In the present paper we study the VTOL characteristics of one certain TUAV with net weight of 160 kg [5].

Exactly controlled vertical flight is a challenging subtask for helicopter type TUAVs to achieve high level of autonomy under disadvantageous conditions. The main requirement for vertical and also horizontal flight is the knowledge of the height above the ground and properly designed controller to govern the process. In [6], a three stage flight control procedure using three autonomous control subsystems for a nonlinear helicopter model defined by the equations of vertical motion for the center of mass of helicopter was proposed. The respective control methodology was verified by flight maneuvers simulation using the software package Simulink.

Here we extend and test the earlier approach [6] on the basis of modeling and simulation of state-space equations in Simulink/MATLAB environment. As a special feature, here the three-rate control system technique is compared with the basic single-rate realization for a realistic TUAV mechanical model defined by 9-component state vector [5]. Below are compared changes in takeoff and hovering (“go-search-and-find” scenario) flight characteristics due to replacement of initial single-rate control system with a more sophisticated

three-rate control system. The matrix formulations of the initial mechanical model and of the “fast”, “intermediate” and “slow” subsystems of the decomposed three-rate mechanical model will be given.

II. SINGLE-RATE TUAV MODEL

In [5], a model of coaxial rotor/ducted-fan TUAV with parameters adjusted in wind tunnel was described. This prototype TUAV, with a net weight 160 kg and height of $l=1.9\text{ m}$, is a VTOL aircraft that includes a fuselage with toroidal portion and two coaxial rotors, main and ducted, rotating at 800rpm in opposite directions. A duct is formed through the fuselage and extends from the top to the bottom of the fuselage. The main propeller with a diameter 4.4 m is mounted to the top section of the fuselage. A ducted rotor is installed in fuselage compensating the propeller antitorque and also yielding some fraction of lift. The main rotor provides about 80% of lift, drag, pitch and roll movements of TUAV and the ducted rotor provides about 20% of lift and yaw movements. In comparison with conventional helicopter main and tail rotor configuration, the coaxial rotors with ducted fan configuration can provide more lift and move easily in any direction during takeoff and landing. These design features increase the stability and maneuverability of TUAV making it easier to fly in difficult and narrow space conditions met in SA missions.

The dynamic model for this TUAV may be constructed on the basis of so-called state-space description [5] completed here with noise terms available in MATLAB/Simulink environment:

$$\dot{x}(\tau) = Ax(\tau) + Bu(\tau) + v(\tau), \quad (1)$$

$$y(\tau) = Cx(\tau) + w(\tau), \quad (2)$$

where $x(\tau)$, $u(\tau)$, $y(\tau)$, $v(\tau)$, $w(\tau)$ are the state, input, output, process noise and measurement noise vectors, respectively.

Following [5], the state vector incorporates 6 degree-of-freedom parameters and 3 mechanical parameters while the input control vector is defined by 4 parameters for the present task:

$$x = [V_x \ V_y \ V_z \ \omega_x \ \omega_y \ \omega_z \ \phi \ \theta \ \psi]^T, \quad (3)$$

$$u = \begin{bmatrix} \delta_{mr} \\ \delta_{lat} \\ \delta_{lon} \\ \delta_{fan} \end{bmatrix}$$

where V_x, V_y, V_z are forward, lateral and vertical velocities; $\omega_x, \omega_y, \omega_z$ are roll, pitch and yaw rates; ϕ, θ, ψ are roll, pitch and yaw angles; and $\delta_{mr}, \delta_{lat}, \delta_{lon}, \delta_{fan}$ are main rotor collective, lateral cyclic, longitudinal cyclic and fan collective

pitchs.

The velocities from (3) can be expressed in the form

$$V_x = \dot{x}_c, V_y = \dot{y}_c, V_z = \dot{z}_c \quad (4)$$

where x_c, y_c, z_c are coordinates of center of mass of TUAV in the earth-frame.

Combining (3) and (4), we have

$$x = [\dot{x}_c \ \dot{y}_c \ \dot{z}_c \ \omega_x \ \omega_y \ \omega_z \ \phi \ \theta \ \psi]^T,$$

$$u = \begin{bmatrix} \delta_{mr} \\ \delta_{lat} \\ \delta_{lon} \\ \delta_{fan} \end{bmatrix}. \quad (5)$$

The state-space system (1)-(2) representation may be given by

$$A = \begin{bmatrix} a_1 & a_2 & 0 & a_3 & a_4 & 0 & 0 & a_5 & 0 \\ a_6 & a_7 & 0 & a_8 & a_9 & 0 & a_{10} & 0 & 0 \\ 0 & 0 & a_{11} & 0 & 0 & a_{12} & 0 & 0 & 0 \\ a_{13} & a_{14} & 0 & a_{15} & a_{16} & 0 & 0 & 0 & 0 \\ a_{17} & a_{18} & 0 & a_{19} & a_{20} & 0 & 0 & 0 & 0 \\ 0 & 0 & a_{21} & 0 & 0 & a_{22} & 0 & 0 & 0 \\ 0 & 0 & 0 & 1 & 0 & 0 & 0 & 0 & 0 \\ 0 & 0 & 0 & 0 & 1 & 0 & 0 & 0 & 0 \\ 0 & 0 & 0 & 0 & 0 & 1 & 0 & 0 & 0 \end{bmatrix},$$

$$B = \begin{bmatrix} 0 & b_1 & b_2 & 0 \\ 0 & b_3 & b_4 & 0 \\ b_5 & 0 & 0 & b_6 \\ 0 & b_7 & b_8 & 0 \\ 0 & b_9 & b_{10} & 0 \\ b_{11} & 0 & 0 & b_{12} \\ 0 & 0 & 0 & 0 \\ 0 & 0 & 0 & 0 \\ 0 & 0 & 0 & 0 \end{bmatrix},$$

$$C = \begin{bmatrix} 1 & 0 & 0 & 0 & 0 & 0 & 0 & 0 & 0 \\ 0 & 1 & 0 & 0 & 0 & 0 & 0 & 0 & 0 \\ 0 & 0 & 1 & 0 & 0 & 0 & 0 & 0 & 0 \\ 0 & 0 & 0 & 1 & 0 & 0 & 0 & 0 & 0 \\ 0 & 0 & 0 & 0 & 1 & 0 & 0 & 0 & 0 \\ 0 & 0 & 0 & 0 & 0 & 1 & 0 & 0 & 0 \\ 0 & 0 & 0 & 0 & 0 & 0 & 1 & 0 & 0 \\ 0 & 0 & 0 & 0 & 0 & 0 & 0 & 1 & 0 \\ 0 & 0 & 0 & 0 & 0 & 0 & 0 & 0 & 1 \end{bmatrix}. \quad (6)$$

The parameters a_1 through a_{22} and b_1 through b_{12} have been adjusted from wind tunnel experiments [5] and have the following numerical values in SI-system:

$$\begin{aligned}
a_1 &= 0.0058, a_2 = 0.0017, a_3 = 0.0081, \\
a_4 &= 0.0329, a_5 = -9.8000, a_6 = -0.0015, \\
a_7 &= -0.0058, a_8 = -0.0329, a_9 = 0.0081, \\
a_{10} &= 9.8000, a_{11} = -0.9816, a_{12} = 0.0794, \\
a_{13} &= -0.0072, a_{14} = -0.0154, a_{15} = -0.0867, \\
a_{16} &= 0.0153, a_{17} = 0.0106, a_{18} = -0.0049, \\
a_{19} &= -0.0106, a_{20} = -0.0697, a_{21} = -0.0416, \\
a_{22} &= -0.1691; \\
b_1 &= -0.1294, b_2 = -2.8845, b_3 = 2.8845, \\
b_4 &= -0.1294, b_5 = 122.0518, b_6 = 11.8688, \\
b_7 &= 7.5964, b_8 = -0.9077, b_9 = 0.8578, \\
b_{10} &= 7.2260, b_{11} = -26.0034, b_{12} = 10.7727.
\end{aligned}$$

Then, we have

$$x_c(\tau) = \int_0^\tau \dot{x}_c(t) dt, \quad y_c(\tau) = \int_0^\tau \dot{y}_c(t) dt, \quad z_c(\tau) = \int_0^\tau \dot{z}_c(t) dt \quad (7)$$

where

$$x_c(0) = 0, \quad y_c(0) = 0, \quad z_c(0) = 0.$$

Note that the attitude vector $[x_c, y_c, z_c]^T$ for TUAV is calculated using (1)-(2), (5)-(7).

III. THREE-RATE TUAV MODEL

The methodology of multi-rate decomposition is discussed lately in [7] and more systematically in [8]. Following this methodology, in the present TUAV case the below described “fast” and “slow” subsystem models were constructed.

In [8], such basic heuristic reception in the theory of dynamic systems as frequency-response separation of motions, that is, the separation of motions on “fast” and “slow” motions in a given case, was developed.

The offered block scheme (see Fig. 2) allows us to compare the following outputs: the original system’s outputs and the “fast” system’s outputs, the original system’s outputs and the “intermediate” system’s outputs, the original system’s outputs and the “slow” system’s outputs. Via the system properties analysis [8], the borders of temporary division of the “fast”, “intermediate” and “slow” control subsystems were defined. It was obtained that it is possible to accept 15 and 35 seconds, respectively, as a border of temporary division of the “fast” and “intermediate” control subsystems and as a border of temporary division of the “intermediate” and “slow” control subsystems.

The “fast” subsystem state-space model may be written as

$$\dot{x}_f(\tau_f) = A_f x_f(\tau_f) + B_f u_f(\tau_f) + T_f v(\tau_f), \quad (8)$$

$$y_f(\tau_f) = C_f x_f(\tau_f) + D_f u_f(\tau_f) + V_f v(\tau_f) + w(\tau_f), \quad (9)$$

where

$$\begin{aligned}
A_f &= \begin{bmatrix} -0.5401 & 0.0714 & 0 \\ -0.0714 & -0.5401 & 0 \\ 0 & 0 & -0.9775 \end{bmatrix}, \\
B_f &= \begin{bmatrix} 0 & 5.1137 & 5.7297 & 0 \\ 0 & -7.2234 & 9.5826 & 0 \\ -8.0021 & 0 & 0 & -0.6943 \end{bmatrix}, \\
T_f &= \begin{bmatrix} -0.0138 & 0.0212 & 0 & 0.5679 & 0.8592 & 0 & -0.3244 & -0.3285 & 0 \\ -0.0353 & -0.0229 & 0 & -1.0756 & 1.1765 & 0 & 0.4591 & -0.5970 & 0 \\ 0 & 0 & -0.0642 & 0 & 0 & 0.0063 & 0 & 0 & 0 \end{bmatrix}, \\
C_f &= \begin{bmatrix} -6.7949 & -6.2523 & 0 \\ 10.5179 & -4.0968 & 0 \\ 0 & 0 & -15.6507 \\ 0.2725 & -0.2000 & 0 \\ 0.2489 & 0.1315 & 0 \\ 0 & 0 & -0.8054 \\ -0.5439 & 0.2983 & 0 \\ -0.4212 & -0.2992 & 0 \\ 0 & 0 & 0.8239 \end{bmatrix}, \\
D_f &= \begin{bmatrix} 0 & -52.7260 & 479.8096 & 0 \\ 0 & -402.4680 & -105.6834 & 0 \\ -15.9347 & 0 & 0 & 5.0157 \\ 0 & 23.7941 & -2.7636 & 0 \\ 0 & 2.6756 & 22.7002 & 0 \\ -162.2402 & 0 & 0 & 51.0678 \\ 0 & 24.6799 & 1.2906 & 0 \\ 0 & -0.0364 & 26.4012 & 0 \\ 32.9644 & 0 & 0 & 2.8600 \end{bmatrix}, \\
V_f &= \begin{bmatrix} 3.4293 & 0.0040 & 0 & -14.3333 & 65.9690 & 0 & 3.3322 & -29.8238 & 0 \\ 0.0003 & 3.4140 & 0 & -51.8970 & -21.0833 & 0 & 26.4639 & 5.0476 & 0 \\ 0 & 0 & -0.0254 & 0 & 0 & 0.4936 & 0 & 0 & 0 \\ -0.0166 & -0.0518 & 0 & 3.1510 & 0.0058 & 0 & 0.9009 & -0.1493 & 0 \\ 0.0403 & -0.0113 & 0 & 0.0007 & 3.1574 & 0 & 0.1017 & 0.8013 & 0 \\ 0 & 0 & -0.2586 & 0 & 0 & 5.0254 & 0 & 0 & 0 \\ 0.0152 & 0.0919 & 0 & 3.1485 & 0.5818 & 0 & 3.4331 & -0.0030 & 0 \\ -0.0818 & 0.0104 & 0 & -0.4132 & 3.5693 & 0 & 0.0037 & 3.4151 & 0 \\ 0 & 0 & 0.2645 & 0 & 0 & -0.0260 & 0 & 0 & 5.0000 \end{bmatrix}.
\end{aligned}$$

The state-space description of an “intermediate” subsystem may be given as

$$\dot{x}_i(\tau_i) = A_i x_i(\tau_i) + B_i u_i(\tau_i) + T_i v(\tau_i), \quad (10)$$

$$y_i(\tau_i) = C_i x_i(\tau_i) + D_i u_i(\tau_i) + V_i v(\tau_i) + w(\tau_i), \quad (11)$$

where

$$A_i = \begin{bmatrix} 0.2896 & 0.4114 & 0 & 0 \\ -0.4114 & 0.2896 & 0 & 0 \\ 0 & 0 & 0.1723 & 0.4734 \\ 0 & 0 & -0.4734 & 0.1723 \end{bmatrix},$$

$$B_s = \begin{bmatrix} 0 & -6.0354 & 0.3019 & 0 \\ 0 & 2.0201 & -8.3919 & 0 \\ 0 & 3.4868 & -8.4436 & 0 \\ 0 & -6.1029 & -1.4434 & 0 \end{bmatrix},$$

$$T_s = \begin{bmatrix} 0.0300 & 0.0152 & 0 & -0.7946 & -0.0458 & 0 & -0.1411 & -0.4645 & 0 \\ -0.0080 & 0.0195 & 0 & 0.3844 & -1.1159 & 0 & 0.4604 & -0.3879 & 0 \\ -0.0148 & -0.0273 & 0 & 0.5934 & -1.1004 & 0 & -0.2233 & -0.4203 & 0 \\ -0.0284 & 0.0023 & 0 & -0.7700 & -0.3078 & 0 & -0.4833 & 0.4591 & 0 \end{bmatrix},$$

$$C_s = \begin{bmatrix} 9.6047 & -7.8929 & -1.2775 & -11.1129 \\ 4.0458 & 13.8678 & -12.2900 & 6.7570 \\ 0 & 0 & 0 & 0 \\ -0.3746 & -0.0192 & 0.1296 & -0.3416 \\ -0.1053 & -0.3009 & -0.2079 & -0.2020 \\ 0 & 0 & 0 & 0 \\ -0.4599 & 0.5869 & -0.5493 & -0.4736 \\ -0.6094 & -0.1732 & -0.5178 & 0.2507 \\ 0 & 0 & 0 & 0 \end{bmatrix},$$

$$D_s = 1000 \times \begin{bmatrix} 0 & 0.0385 & -0.1869 & 0 \\ 0 & 0.1385 & 0.0681 & 0 \\ 0.1243 & 0 & 0 & 0.0121 \\ 0 & 0.0049 & 0.0003 & 0 \\ 0 & 0 & 0.0053 & 0 \\ -0.0322 & 0 & 0 & 0.0106 \\ 0 & -0.0084 & -0.0021 & 0 \\ 0 & 0.0011 & -0.0102 & 0 \\ -3.1258 & 0 & 0 & 1.0620 \end{bmatrix},$$

$$V_s = \begin{bmatrix} 0.6086 & 0.0680 & 0 & 7.8300 & -24.6399 & 0 & -2.4517 & 11.3360 & 0 \\ -0.1030 & 0.5401 & 0 & 16.7245 & 11.4983 & 0 & -8.7889 & -3.6721 & 0 \\ 0 & 0 & 1.0187 & 0 & 0 & 0.0009 & 0 & 0 & -0.0807 \\ 0.0030 & 0.0184 & 0 & 0.6297 & 0.1164 & 0 & -0.3134 & -0.0006 & 0 \\ -0.0164 & 0.0021 & 0 & -0.0826 & 0.7139 & 0 & 0.0007 & -0.3170 & 0 \\ 0 & 0 & -0.0437 & 0 & 0 & 1.0323 & 0 & 0 & -0.8219 \\ 0.0001 & -0.0320 & 0 & -1.0458 & -0.4274 & 0 & 0.5335 & 0.1028 & 0 \\ 0.0323 & 0.0001 & 0 & 0.3003 & -1.3564 & 0 & -0.0712 & 0.6137 & 0 \\ 0 & 0 & -3.7316 & 0 & 0 & 102.6914 & 0 & 0 & 30.5193 \end{bmatrix}$$

The state-space equations for a "slow" subsystem may be written as

$$\dot{x}_s(\tau_s) = A_s x_s(\tau_s) + B_s u_s(\tau_s) + T_s v(\tau_s), \quad (12)$$

$$y_s(\tau_s) = C_s x_s(\tau_s) + D_s u_s(\tau_s) + V_s v(\tau_s) + w(\tau_s), \quad (13)$$

where

$$A_s = \begin{bmatrix} 0 & 0 \\ 0 & -0.1732 \end{bmatrix},$$

$$B_s = \begin{bmatrix} -11.2979 & 0 & 0 & 3.7217 \\ -14.2467 & 0 & 0 & 4.4844 \end{bmatrix},$$

$$T_s = \begin{bmatrix} 0 & 0 & -0.0154 & 0 & 0 & 0.3624 & 0 & 0 & 0.0625 \\ 0 & 0 & -0.0227 & 0 & 0 & 0.4413 & 0 & 0 & 0 \end{bmatrix},$$

$$C_s = \begin{bmatrix} 0 & 0 \\ 0 & 0 \\ 0 & 0.2237 \\ 0 & 0 \\ 0 & 0 \\ 0 & 2.2776 \\ 0 & 0 \\ 0 & 0 \\ 16.0000 & -13.151 \end{bmatrix},$$

$$D_s = \begin{bmatrix} 0 & 120.9563 & -582.9545 & 0 \\ 0 & 436.7217 & 213.6086 & 0 \\ 128.1196 & 0 & 0 & 11.1156 \\ 0 & 0 & 0 & 0 \\ 0 & 0 & 0 & 0 \\ 6.5929 & 0 & 0 & 0.5720 \\ 0 & -0.0174 & 0.0504 & 0 \\ 0 & 0.1341 & -0.6023 & 0 \\ -6.7445 & 0 & 0 & -0.5852 \end{bmatrix},$$

$$V_s = \begin{bmatrix} 0 & 0 & 0 & 24.6827 & -77.5740 & 0 & 1.3177 & -5.78460 \\ 0 & 0 & 0 & 53.3951 & 136.2684 & 0 & 5.0138 & 1.7110 \\ 0 & 0 & 1.0282 & 0 & 0 & -0.1010 & 0 & 0 \\ 0 & 0 & 0 & 0 & 0 & 0 & -1.000 & 0 \\ 0 & 0 & 0 & 0 & 0 & 0 & 0 & -1.00000 \\ 0 & 0 & 0.0529 & 0 & 0 & -0.0052 & 0 & 0 \\ 0 & -0.1020 & 0 & 0.0354 & 0.0096 & 0 & -0.0002 & 0.0010 \\ 0.1020 & 0 & 0 & 0.0239 & -0.0396 & 0 & 0.0008 & -0.00650 \\ 0 & 0 & -0.0541 & 0 & 0 & 0.0053 & 0 & 0 \end{bmatrix}$$

IV. SIMULATION RESULTS

Consider the control of given three-rate UAV model for the case of takeoff, approach and hovering maneuvers by hybrid constrained system of three control subsystems.

Initial and desired heights for control subsystems are chosen to be:

$$x(0) = y(0) = z(0) = 0 \text{ m}, z_1^0 = 25 \text{ m}.$$

Simulink runs under MATLAB. Before running the models, we need to assign numerical values to each of the variables used in the models through MATLAB. Simulink was used to simulate the complete control system.

The neurocontrollers used in this paper are based on the NARMA-L2 approximate model [9]. Simulink tuning tools let us tune control systems containing NARMA-L2 controller Simulink block.

The block schemes of single-rate and three-rate UAV control systems realization are presented in Fig. 2.

Main trajectories simulation results following the offered block schemes with one control system or three control subsystems are shown below in Figs. 3-6.

Fig. 3 presents straightforward comparison of three-rate system takeoff and hovering ability with original single-rate system. The main observations are summarized in Table I.

TABLE I. COMPARISON OF CONTROL SYSTEM PERFORMANCE PARAMETERS FOR SINGLE-RATE AND THREE-RATE SYSTEMS.

Systems	Control System Performance Parameters			
	Rise Time (t_r)	Time to First Peak (t_p)	Settling Time (t_s)	Overshoot (O)
Single-Rate System	2.25s	6.20s	47.0s	11.6%

Systems	Control System Performance Parameters			
	Rise Time (t_r)	Time to First Peak (t_p)	Settling Time (t_s)	Overshoot (O)
Three-Rate System	2.73s	8.85s	21.2s	4.0%

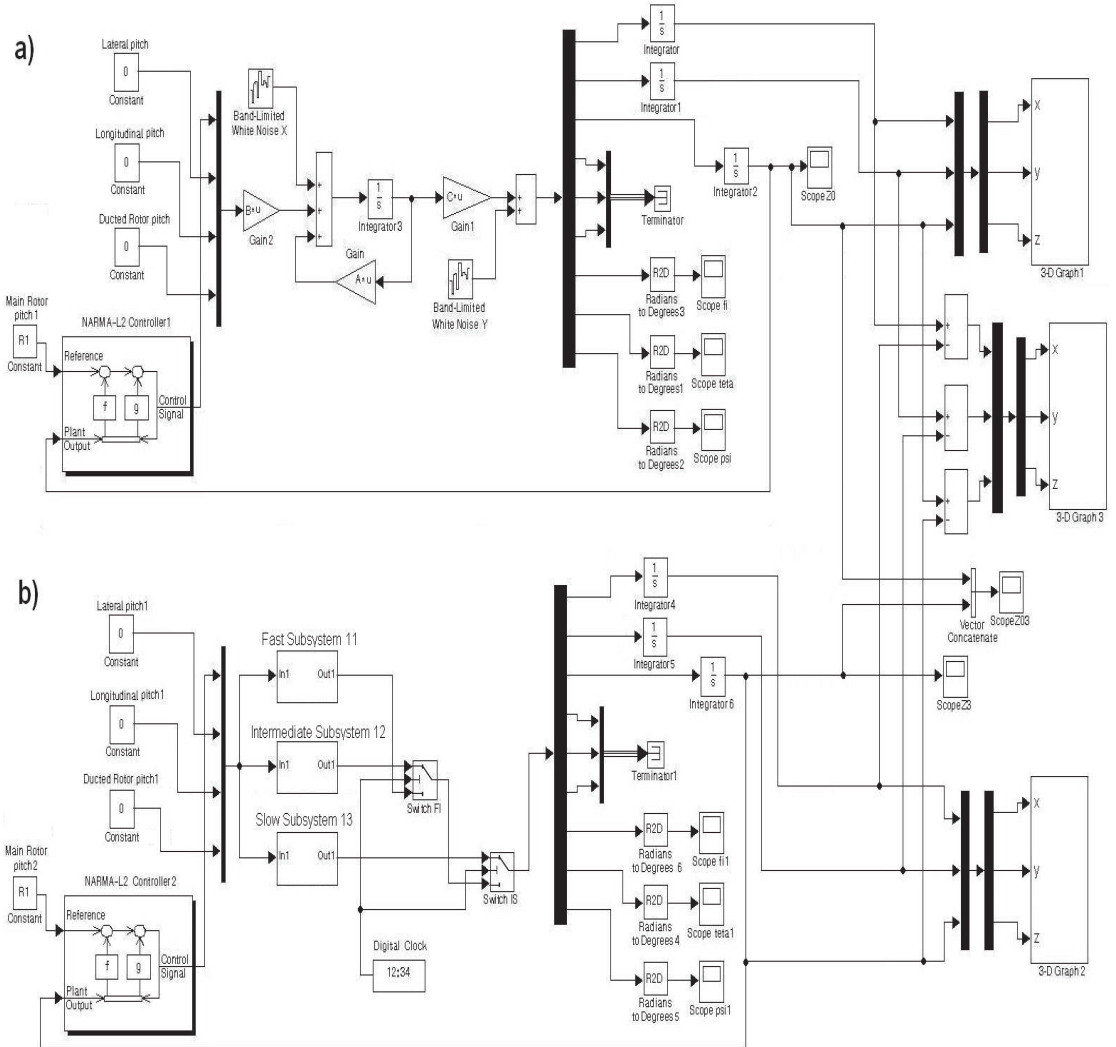


Fig. 2. Block diagrams of single-rate (part a) and three-rate (part b) control systems.

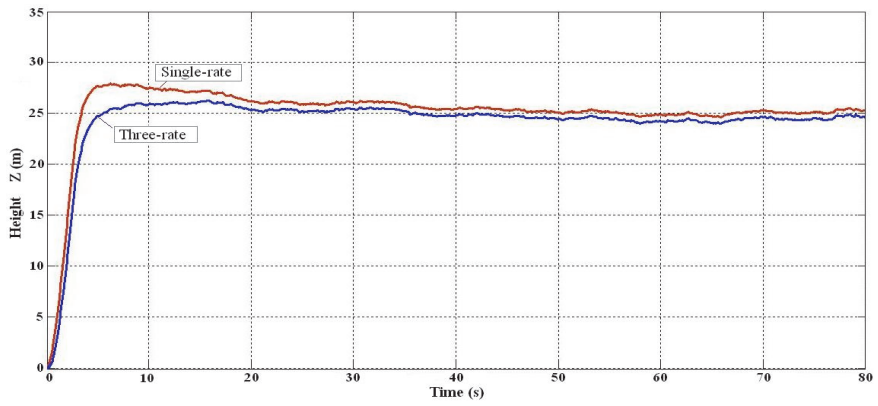


Fig. 3. Comparison of UAV takeoff and hovering trajectories at height 25 m in the case of single-rate (red) and three-rate (blue) control systems (UAV center of mass z-coordinate plotted).

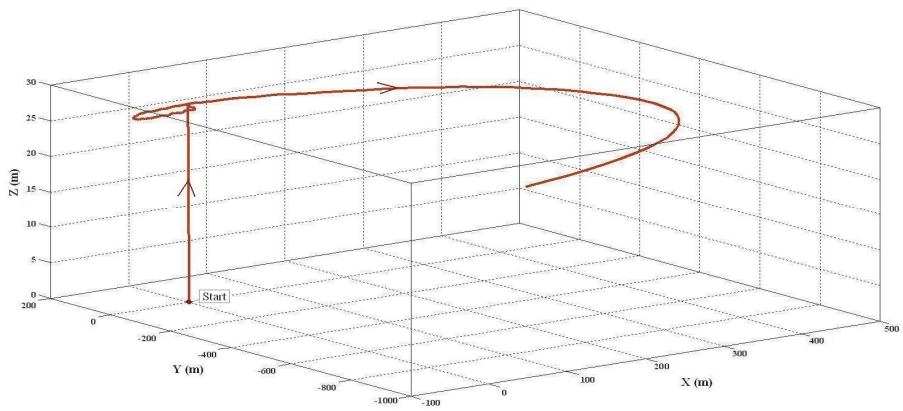


Fig. 4. 3D presentation of takeoff and hovering trajectory at height 25 m in the case of single-rate UAV control.

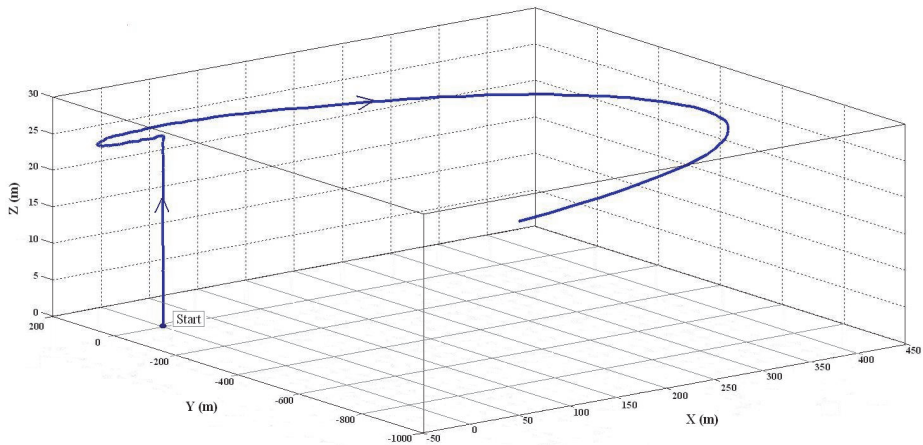


Fig. 5. 3D-presentation of takeoff and hovering trajectory at height 25 m in the case of three-rate UAV control.

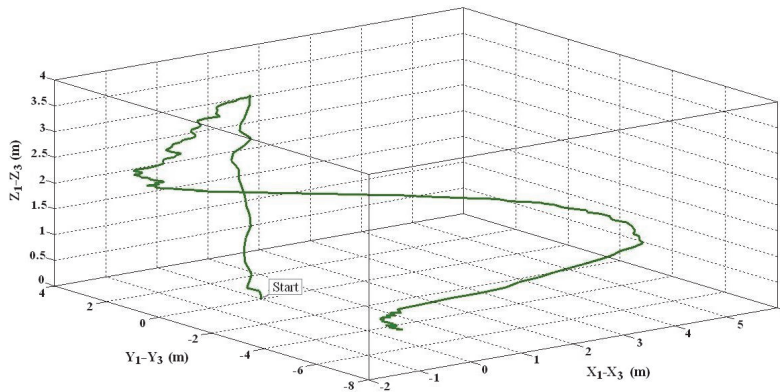


Fig. 6. 3D-presentation of the trajectories difference between the cases of single-rate and three-rate TUAV control.

V. CONCLUSIONS

A process speed based decomposed modeling and simulation technique is discussed and tested in this paper for a coaxial rotor ducted fan VTOL TUAV.

The research methodology of this paper is based on the methods of mathematical modeling, neural control, multi-rate control, computational mathematics, differential and integral calculus. The proposed methodology may be used as an example for improvement of model-based design on UAVs dedicated for different application fields including the different situation surveillance and situation awareness systems.

For stable and smooth flight maneuvers, we proposed a three-rate decomposition of the initial control task. By following the proposed methodology, the TUAV model of 9th order is decomposed into three subsystems: the “fast” subsystem of 3rd order used in the initial phase of trajectory (takeoff motion), the “intermediate” subsystem of 4th order used in the middle phase of trajectory (approach motion), and the “slow” subsystem of 2nd order used in the final phase of trajectory (hovering motion).

The effectiveness of the proposed control strategy has been verified by simulation tests for chosen model of TUAV using realistic simulator of Math Works software. Simulation results confirm the effectiveness of the three-rate control over the single-rate control yielding the higher accuracy of the tracking and correspondingly better energy efficiency indicators. In particular, the settling time is reduced by the factor of 2.2 and the height overshoot by factor of 2.9. From the applications viewpoint, we believe that the modeled and simulated flight control strategy may offer a reasonable possibility to improve VTOL class UAVs flight characteristics needed for

information collection in sophisticated situation awareness systems.

It is supposed to continue improving the synthesized three-rate approach in the future for the functioning of similar UAVs in conditions of uncertainty, unknown parameters and external disturbing effects.

REFERENCES

- [1] K. Nonami, F. Kendoul, S. Suzuki, W. Wang, and D. Nakazawa, *Autonomous Flying Robots: Unmanned Aerial Vehicles and Micro Aerial Vehicles*. New York: Springer, 2010.
- [2] M. R. Endsley, “Toward a theory of situation awareness in dynamic systems,” *Human Factors*, vol. 37, pp. 32–64, March 1995.
- [3] J. Gorman, N. Cooke, and J. Winner, “Measuring team situation awareness in decentralized command and control environments,” *Ergonomics*, vol. 49, pp. 1312–1325, October 2006.
- [4] S. D. Prior, S. T. Shen, A. S. White, S. Odedra, M. Karamanoglu, M. A. Erbil, and T. Foran, “Development of a novel platform for greater situational awareness in the urban military terrain,” *Proc. 8th International Conf. Engineering Psychology and Cognitive Ergonomics*, San Diego, USA, pp. 120–125, 2009.
- [5] S. Shouzhao, A. A. Mian, Z. Chao, and J. Bin, “Autonomous takeoff and landing control for a prototype unmanned helicopter,” *Control Engineering Practice*, vol. 18, pp. 1053–1059, September 2010.
- [6] I. Astrov and A. Pedai, “Control of hovering manoeuvres in unmanned helicopter for enhanced situational awareness,” *Proc. International Conf. Industrial Mechatronics and Automation*, Chengdu, China, pp. 143–146, 2009.
- [7] I. Astrov and A. Pedai, “Enhanced situational awareness for AUV’s stochastic model by multirate neural control,” *Proc 2010 IEEE International Systems Conf.*, San Diego, USA, pp. 66–70, 2010.
- [8] I. Astrov, *Multirate Approaches for Engineering Applications: Computational Strategies*. Saarbrücken: Scholars’ Press, 2015.
- [9] K. S. Narendra and S. Mukhopadhyay, “Adaptive control using neural networks and approximate models,” *IEEE Trans. Neural Networks*, vol. 8, pp. 475–485, May 1997.

Publication V

Astrov, I.; Udal, A.; Pedai, A.; Sell, R. (2019). Simulink/MATLAB based comparison of neural and basic tracking control for an autonomous surface vessel for situation awareness applications. CINTI-MACRo 2019 Proceedings: IEEE Joint 19th International Symposium on Computational Intelligence and Informatics and 7th IEEE International Conference on Recent Achievements in Mechatronics, Automation, Computer Sciences and Robotics (CINTI-MACRo 2019, Szeged, Hungary, November 14-16, 2019). IEEE, 105-110.

Simulink/MATLAB based Comparison of Neural and Basic Tracking Control for an Autonomous Surface Vessel for Situation Awareness Applications

Igor Astrov, Andres Udal, Andrus Pedai, and Raivo Sell

Department of Mechanical and Industrial Engineering and Department of Software Sciences
Tallinn University of Technology
Tallinn, Estonia

igor.astrov@ieee.org, andres.udal@taltech.ee, andrus.pedai@gmail.com, raivo.sell@taltech.ee

Abstract—The intelligent control of autonomous vehicles has become one of the high priority tasks in development of Cyber-Physical Systems (CPS) for Industry 4.0 and Situation Awareness (SA) applications. Moving of an Autonomous Surface Vessel (ASV) to the desired area of sea is a challenging task to achieve high level of autonomy under adverse conditions. Paper focuses on the development of methodology of model-based modeling and simulation of cyber-physical nonlinear system of ASV in Simulink/MATLAB software environment. The comparison between predictive neural control and basic tracking feedback control has been presented for two maneuvers: the turn at different angles and the circular motion at final destination. Simulation results confirm the necessity and superiority of neural controller approach.

Keywords—autonomous surface vessels, feedback control, predictive neurocontrollers, situational awareness.

I. INTRODUCTION

The unmanned autonomous vehicles are gaining rapidly increasing importance in different types of modern cyber-physical systems (CPSs) where reliable monitoring in different physical environment situations is needed [1]. In military, public security and rescue service fields the trustworthy positioning of autonomous vehicles is used to acquire necessary information to assure Situation Awareness (SA) that means “perception of elements in the environment within a volume of time and space, the comprehension of their meaning, and the projection of their status in the near future” [2-4].

In particular, considered here autonomous surface vessels (ASVs) application missions for SA may include [5]:

- Autonomous search and rescue, track and trail;
- Support of special operations, port and border security;
- Intelligence surveillance and reconnaissance;
- Communications relay (space, air, ground, sea surface, underwater);
- Detection and neutralization of dangerous objects.

With moving towards smarter CPS, the application of artificial intelligence elements and, in particular, the neural network control blocks is a fast rising trend also in the field of ASVs [6-8]. Reason for this is that often the traditional proportional or proportional-integral-derivative (PID) feedback tracking controller technologies cannot yield the desired control quality and more sophisticated controller realizations that take into account information about the

physical model of the vehicle under control are needed. To accomplish this advanced control system development task, the general approach is application of model-based methodology in design environment like Simulink/MATLAB where different options for neural network controllers and sophisticated possibilities description of linear or nonlinear physical object models exist. Below we demonstrate definition of an Autonomous Surface Vessel neural network assisted control modeling task in Simulink/MATLAB environment and study of control quality via simulation of different control scheme tasks in this environment.

In [9], a preliminary methodology of modeling of an ASV in Simulink/MATLAB environment was developed and tested. This study used some ideas offered in [10,11] for an under actuated unmanned surface vehicle (USV): a practical adaptive sliding mode control scheme applying backstepping technique; sliding mode control; radial basis neural network and auxiliary dynamic system. The present paper continues efficiency studies of the ideas applied in work [6] and offers direct modeling and simulation based comparison of sophisticated control with Neural Network (NN) Predictive Controller against simple proportional feedback tracking control approach for certain ASV localization task missions.

II. MODEL OF ASV

Let us take into consideration the model of an under actuated surface vessel (see Fig. 1). The vessel has two propellers which are responsible for the surge force and the yaw control torque. Fig. 1 shows the system variable definitions where heading angle ψ represents the orientation of the vessel's body-fixed frame relative to the North-East-Down (NED) frame. The instantaneous vessel heading angle ψ , is measured in anticlockwise direction from the global X axis.

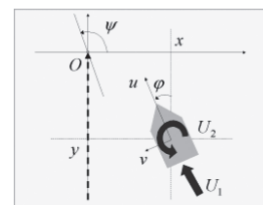


Fig. 1. Coordinate and variable definitions of an ASV [8].

Angle φ is connected to the angle ψ by $\varphi = \psi - \frac{\pi}{2}$.

The kinematics of this system can be presented as [12]

$$\begin{bmatrix} \dot{x} \\ \dot{y} \\ \dot{\psi} \end{bmatrix} = \begin{bmatrix} \cos \psi & -\sin \psi & 0 \\ \sin \psi & \cos \psi & 0 \\ 0 & 0 & 1 \end{bmatrix} \begin{bmatrix} u \\ v \\ r \end{bmatrix}, \quad (1)$$

where (x, y) denote the coordinates of the center of mass of the vessel in the earth-fixed frame, ψ is the heading angle of the vessel, and u, v, r are the velocities of surge, sway and yaw, respectively.

In present study we assume that:

- the disturbing environment forces due to wind, currents and waves can be neglected;
- the inertia matrices, added mass matrices and hydrodynamic damping matrices are diagonal.

The simplified mechanical model for of the analyzed ASV can be presented by the following equations [13]

$$\dot{u} = \frac{m_{22}}{m_{11}}vr - \frac{d_{11}}{m_{11}}u + \frac{1}{m_{11}}t_1 \quad (2)$$

$$\dot{v} = -\frac{m_{11}}{m_{22}}ur - \frac{d_{22}}{m_{22}}v \quad (3)$$

$$\dot{r} = \frac{m_{11} - m_{22}}{m_{33}}uv - \frac{d_{33}}{m_{33}}r + \frac{1}{m_{33}}t_2 \quad (4)$$

where $m_{ii} > 0, i=1,2,3$ model the vessel inertia and the added mass effects, $d_{ii} > 0, i=1,2,3$ describe the hydrodynamic damping, m_{ii} and d_{ii} are assumed to be constant, and t_1, t_2 specify the surge control force and the yaw control moment, respectively.

The parameters m_{11} through m_{33} and d_{11} through d_{33} in (2)-(4) have the following values [11]:

$$m_{11} = 200\text{kg}, m_{22} = 250\text{kg}, m_{33} = 80\text{kg};$$

$$d_{11} = 70\text{kg/s}, d_{22} = 100\text{kg/s}, d_{33} = 50\text{kg/s}.$$

Next, the center of mass coordinates and heading angle are obtained by the integration

$$x(\tau) = \int_0^\tau \dot{x}(t)dt, y(\tau) = \int_0^\tau \dot{y}(t)dt, \psi(\tau) = \int_0^\tau \dot{\psi}(t)dt, \quad (5)$$

where initial state $x(0) = 0, y(0) = 0, \psi(0) = 0$.

We can see from (1)-(5) that the position coordinates and the heading angle of the ASV $(x, y, \psi)^T$ can be

computed on the basis of given set of equations and initial conditions.

III. SIMULATION RESULTS

Below the simulation results of the ASV are analyzed for 2-part trajectories consisting of initial approach motion towards desired angle and following circular motion.

The predictive NN control method follows the approach offered in [14]. This controller uses a NN model to predict future plant (i.e. ASV) responses to potential control signals. Inside the model, an optimization algorithm computes the control signals that optimize future plant performance. To train the control system containing NN Predictive Controller block for the particular ASV, the tuning tools of Simulink were used.

The Simulink-style block-scheme, allowing simultaneously compare the predictive neural control and simple proportional feedback control methods, is presented in Fig. 2. For the initial parts of trajectories the constant surge control force $t_1 = 50N$ and feedback-controlled control moment t_2 were applied in order to achieve the desired heading angle. For the final circular motion phases the constant yaw control moment $t_2 = 5Nm$ was applied.

Simulation results for the two control methods and the main input and output signals for two desired heading angles are shown in Figs. 3, 4, 6 and 7 below. The resulting trajectories of ASV for two control methods and two heading angles are presented in Figs. 5 and 8. The main control quality parameters for basic and advanced control methods are summarized in Tables I and II.

TABLE I. COMPARISON OF CONTROL SYSTEM PERFORMANCE PARAMETERS FOR SIMPLE PROPORTIONAL FEEDBACK AND NEURAL CONTROL APPROACHES AT 45-DEGREE HEADING ANGLE

Systems	Rise Time (t_r)	Time to First Peak (t_p)	Settling Time (t_s)	Overshoot (O)	Decay Ratio (DR)
Feedback Control	23 s	45 s	670 s	78%	77%
Neural Control	17 s	25 s	100 s	33%	26%

TABLE II. COMPARISON OF CONTROL SYSTEM PERFORMANCE PARAMETERS FOR SIMPLE PROPORTIONAL FEEDBACK AND NEURAL CONTROL APPROACHES AT 135-DEGREE HEADING ANGLE

Systems	Rise Time (t_r)	Time to First Peak (t_p)	Settling Time (t_s)	Overshoot (O)	Decay Ratio (DR)
Feedback Control	27 s	46 s	580 s	44%	61%
Neural Control	31 s	45 s	120 s	20%	18%

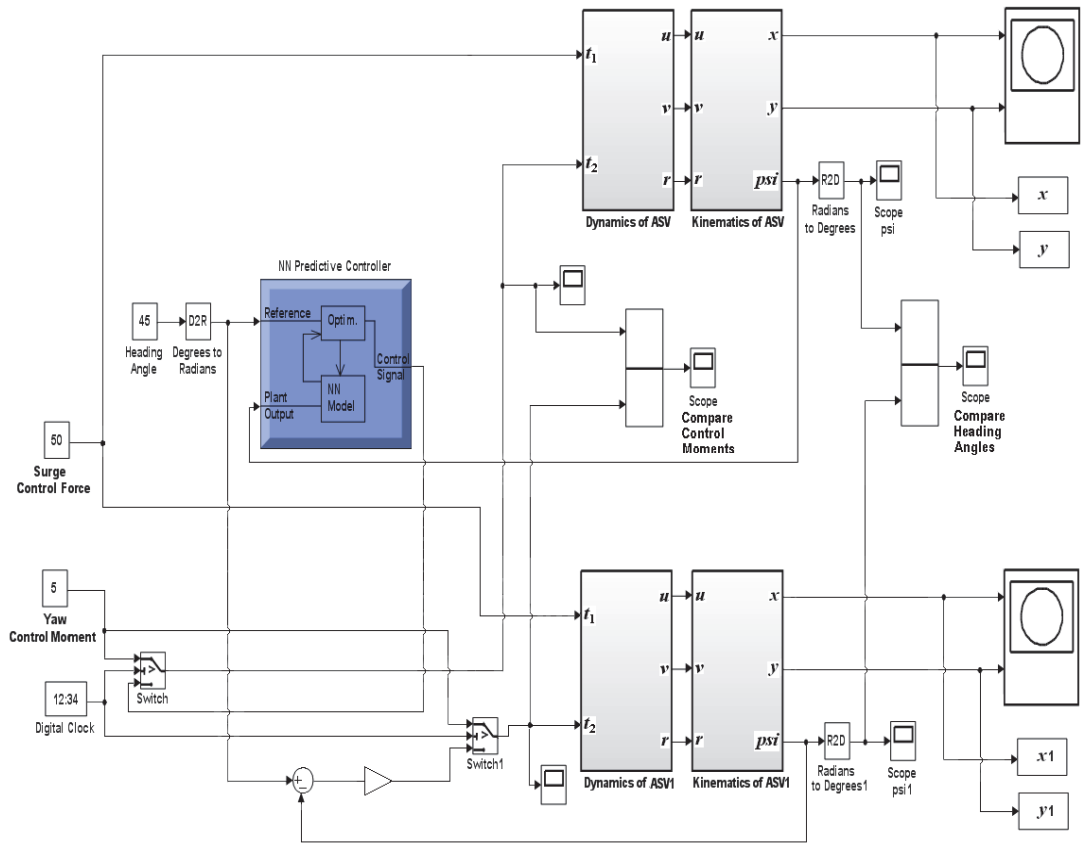


Fig. 2. Simulink-style block diagram allowing simultaneously investigate the behavior of Autonomous Surface Vessel with neural controller (upper part) and with simple proportional tracking controller (lower part) in feedback loop.

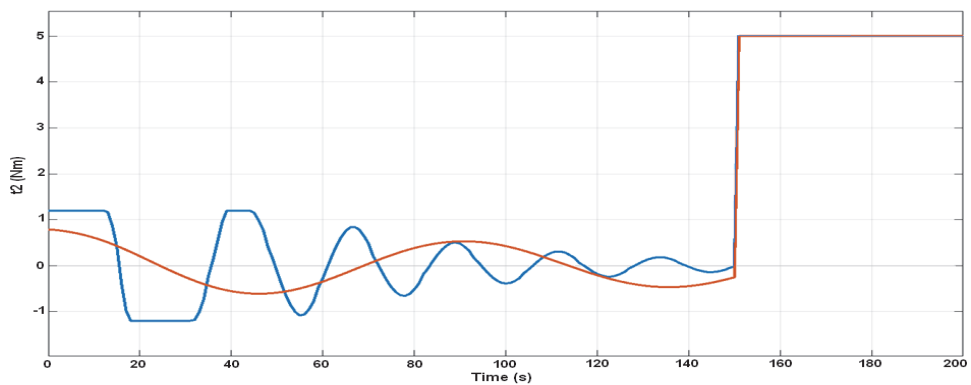


Fig. 3. Comparison of input control signals (yaw moment) of ASV in cases of simple proportional feedback control (red) and neural control (blue) for desired 45-degree heading angle. One can see that the trained neural tracking control uses intensive predictive control while the simple proportional approach is constantly late in influencing.

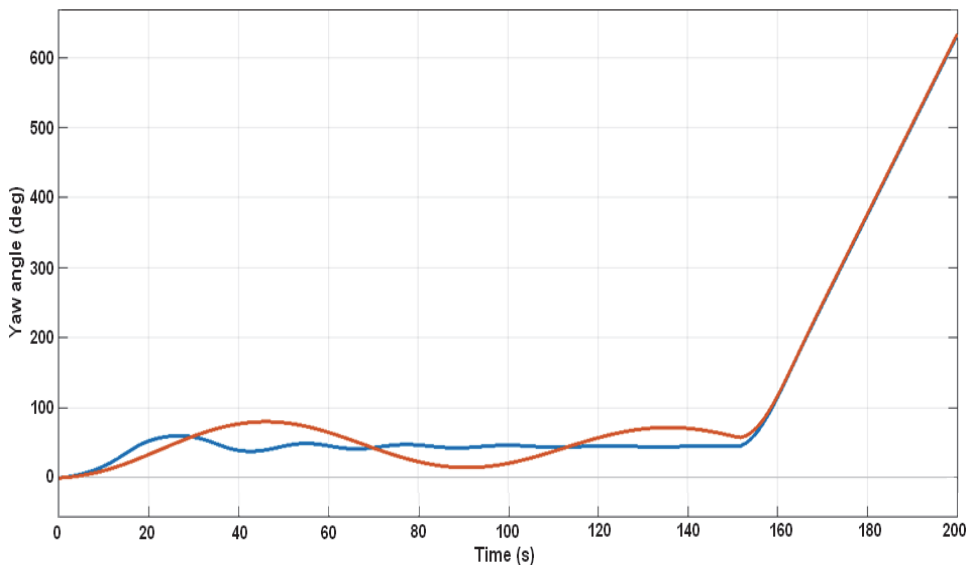


Fig. 4. Comparison of main output values (yaw angles of ASV) in cases of simple proportional feedback control (red) and neural control (blue) for desired 45-degree heading angle.

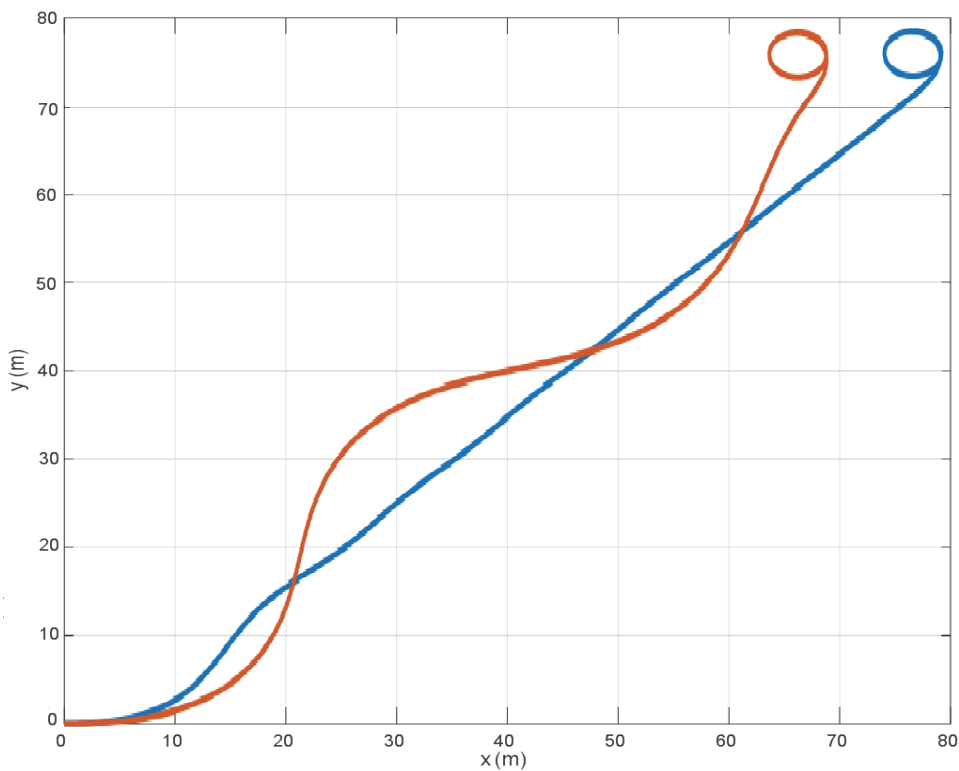


Fig. 5. Comparison of ASV trajectories for simple proportional feedback control (red) and neural control cases (blue) for desired 45-degree heading angle. Comparison of two trajectories confirms the fact that only predictive neural network approach assures the necessary stability of ASV moving direction while the traditional proportional feedback approach is constantly lagging behind in making the necessary changes in yaw control signal.

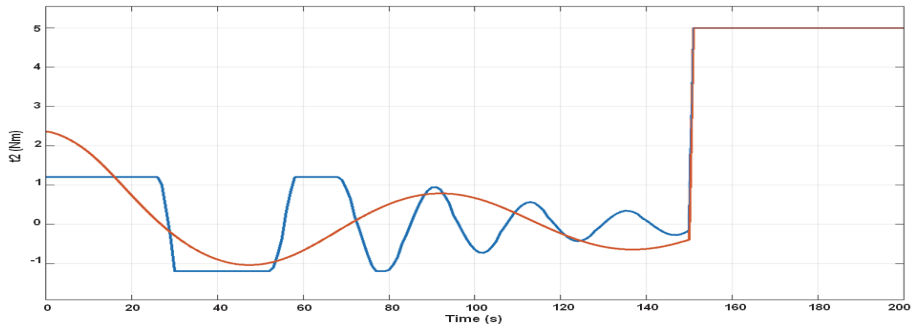


Fig. 6. Comparison of input control signals (yaw moment) of ASV in cases of simple proportional feedback control (red) and neural control (blue) for desired 135-degree heading angle.

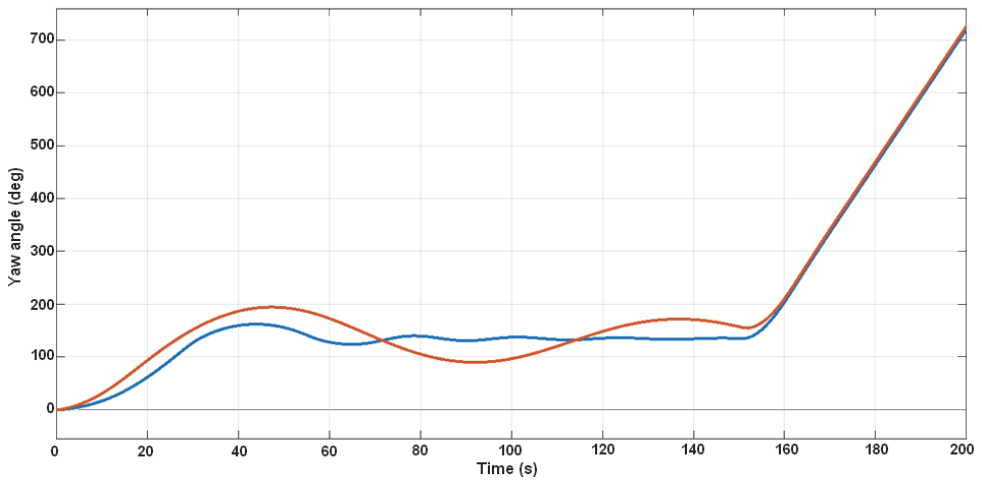


Fig. 7. Comparison of main output values (yaw angles of ASV) in cases of simple proportional feedback control (red) and neural control (blue) for desired 135-degree heading angle.

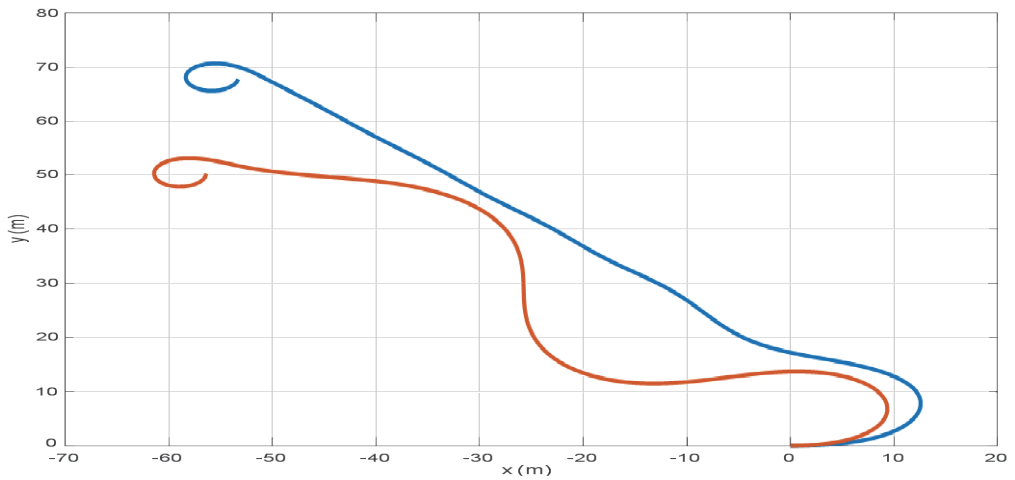


Fig. 8. Comparison of ASV trajectories for simple proportional feedback control (red) and neural control (blue) cases for desired 135-degree heading angle.

IV. CONCLUSIONS

A modeling and simulation technique in Simulink/MATLAB environment is presented and analyzed for an autonomous surface vessel. The proposed methodology may be used for improvement of model-based design on ASVs dedicated for different application fields including the different situation awareness tasks demanding reliable positioning of monitoring devices.

The simulation results clearly confirm the superiority of the predictive neural network control approach over the basic proportional feedback tracking method in order to assure the smoothness, fast response, and accuracy of control. Strictly speaking, demonstrated results even indicate that the traditional proportional feedback method cannot guarantee satisfactory quality of management at all, as it is constantly lagging behind in applying the necessary influences. Necessity of application of neural control approaches with predictive ability may be also formulated as a necessity of introduction of artificial intelligence methods into control of waterborne vehicles.

From the applications viewpoint, we believe that the proposed methodology may offer a reasonable possibility to improve the motion characteristics of ASVs used for environment monitoring in sophisticated cyber-physical and/or situation awareness systems. Although many details of this study is associated with the actual ASV model, the proposed model-based research approach may be extended to other types of surface vessels.

REFERENCES

- [1] V. Tsiatsis, S. Karnouskos, J. Holler, D. Boyle, and C. Mulligan, "Autonomous vehicles and systems of cyber-physical systems," in *Internet of Things: Technologies and Applications for a New Age of Intelligence*, 2nd ed., London: Academic Press, 2019, pp. 209-305.
- [2] M. R. Endsley, "Toward a theory of situation awareness in dynamic systems," *Human Factors*, vol. 37, March 1995, pp. 32-64.
- [3] J. Gorman, N. Cooke, and J. Winner, "Measuring team situation awareness in decentralized command and control environments," *Ergonomics*, vol. 49, October 2006, pp. 1312-1325.
- [4] Interim Brigade Combat Team Newsletter. [Online]. Available from: http://www.globalsecurity.org/military/library/report/call/call_01-18_toc.htm [Accessed on 14 August 2019].
- [5] Unmanned Surface Vessels. [Online]. Available from: www.bluebirdelectric.net/artificial_intelligence_autonomous_robotics/general_dynamics_robotic_systems_anti_submarine_warfare_usv_mission.htm [Accessed on 14 August 2019].
- [6] C.-Z. Pan, X.-Z. Lai, S. X. Yang, and M. Wu, "An efficient neural network approach to tracking control of an autonomous surface vehicle with unknown dynamics," *Expert Systems with Applications*, vol. 40, April 2013, pp. 1629-1635.
- [7] Z. Peng, J. Wang, and D. Wang, "Distributed maneuvering of autonomous surface vehicles based on neurodynamic optimization and fuzzy approximation," vol. 26, May 2018, pp. 1083-1090.
- [8] R. Polvara, S. Sharma, J. Wan, A. Manning, and R. Sutton, "Obstacle avoidance approaches for autonomous navigation of unmanned surface vehicles," *Journal of Navigation*, vol. 71, January 2018, pp. 241-256.
- [9] I. Astrov, M. Pikkov, and R. Paluoja, "Motion control of an autonomous surface vessel for enhanced situational awareness," *International Journal of Mechanical, Aerospace, Industrial and Mechatronics Engineering*, vol.7, November 2013, pp. 1178-1183.
- [10] B. Qiu, G. Wang, Y. Fan, D. Mu, and X. Sun, "Adaptive sliding mode trajectory tracking control for unmanned surface vehicle with modeling uncertainties and input saturation," *Applied. Sciences*, vol. 9, March 2019, pp. 1-18.
- [11] T.-H. Kim, T. Basar, and I.-J. Ha, "Asymptotic stabilization of an underactuated surface vessel via logic-based control," *Proc. 2002 American Control Conf.*, Anchorage, USA, 2002, pp. 4678-4683.
- [12] W. Dong and Y. Guo, "Nonlinear tracking control of underactuated surface vessel," *Proc. 2005 American Control Conf.*, Portland, USA, 2005, pp. 4351-4356.
- [13] K. Liang, J. Ai, Z. Lei, and G. Liu, "Sliding-mode trajectory tracking control of autonomous surface vessel," *Advances in Intelligent Systems Research*, vol. 145, July 2017, pp. 251-254.
- [14] J. M. Maciejowski, *Predictive Control with Constraints*. London: Prentice Hall, 2002.

Publication VI

I. Astrov, A. Pedai (2010). Flight control of a trirotor mini-UAV for enhanced situational awareness. Volume [2010-376X] of Proceedings of World Acad. Science, Engineering and Technology (Extended papers of Int. Conf. on Aeronautical and Astronautical Engineering ICAAE 2010, Amsterdam, Netherlands), volume 70, pp. 271-277, 2010 (referenced in Scopus, www.etis.ee classification 1.1 paper).

Flight Control of a Trirotor Mini-UAV for Enhanced Situational Awareness

Igor Astrov and Andrus Pedai

Abstract—This paper focuses on a critical component of the situational awareness (SA), the control of autonomous vertical flight for an unmanned aerial vehicle (UAV). Autonomous vertical flight is a challenging but important task for tactical UAVs to achieve high level of autonomy under adverse conditions. With the SA strategy, we proposed a two stage flight control procedure using two autonomous control subsystems to address the dynamics variation and performance requirement difference in initial and final stages of flight trajectory for a nontrivial nonlinear trirotor mini-UAV model. This control strategy for chosen mini-UAV model has been verified by simulation of hovering maneuvers using software package Simulink and demonstrated good performance for fast SA in real-time search-and-rescue operations.

Keywords—Flight control, trirotor aircraft, situational awareness, unmanned aerial vehicle.

I. INTRODUCTION

SITUATION awareness has been formally defined as “the perception of elements in the environment within a volume of time and space, the comprehension of their meaning, and the projection of their status in the near future” [1]. As the term implies, situation awareness refers to awareness of the situation. Grammatically, situational awareness (SA) refers to awareness that only happens sometimes in certain situations.

SA has been recognized as a critical, yet often elusive, foundation for successful decision-making across a broad range of complex and dynamic systems, including emergency response and military command and control operations [2].

The term SA have become commonplace for the doctrine and tactics, and techniques in the U.S. Army [3]. SA is defined as “the ability to maintain a constant, clear mental picture of relevant information and the tactical situation including friendly and threat situations as well as terrain”. SA allows leaders to avoid surprise, make rapid decisions, and choose when and where to conduct engagements, and achieve decisive outcomes.

Manuscript received April 26, 2010. This work was supported in part by the Ministry of Education and Research of Estonia under Project SF0140113As08.

I. Astrov is with the Department of Computer Control, Tallinn University of Technology, Tallinn 19086, Estonia (corresponding author to provide phone: 372-620-2113, fax: 372-620-2101; e-mail: igor.astrov@dcc.ttu.ee).

A. Pedai is with the Department of Computer Control, Tallinn University of Technology, Tallinn 19086, Estonia (e-mail: andrus.pedai@dcc.ttu.ee).

The tactical unmanned aerial vehicle (TUAV) is one of the key tools to gather the information to build SA for all leaders. The TUAV is the ground maneuver commander's primary day and night system. The TUAV provides the commander with a number of capabilities including:

- Enhanced SA.
- Target acquisition.
- Battle damage assessment.
- Enhanced battle management capabilities (friendly situation and battlefield visualization).

The combination of these benefits contributes to the commander's dominant SA allowing him to shape the battlefield to ensure mission success and to maneuver to points of positional advantage with speed and precision to conduct decisive operations. Some conditions for conducting aerial reconnaissance with TUAVs are as follows.

- Time is limited or information is required quickly.
- Detailed reconnaissance is not required.
- Extended duration surveillance is not required.
- Target is at extended range.
- Threat conditions are known; also the risk to ground assets is high.
- Verification of a target is needed.
- Terrain restricts approach by ground units.

A mini-TUAV offers many advantages, including low cost, the ability to fly within a narrow space and the unique hovering and vertical take-off and landing (VTOL) flying characteristics.

The current state of TUAVs throughout the world is outlined [4]. A novel design of a multiple rotary wing platform which provide for greater SA in the urban terrain is then presented.

Autonomous vertical flight is a challenging but important task for TUAVs to achieve high level of autonomy under adverse conditions. The fundamental requirement for vertical flight is the knowledge of the height above the ground, and a properly designed controller to govern the process.

In [5], a three stage flight control procedure using three autonomous control subsystems for a nontrivial nonlinear helicopter model on the basis of equations of vertical motion for the center of mass of helicopter was proposed. The proposed control strategy has been verified by simulation of hovering maneuvers using software package Simulink and demonstrated good performance for fast SA.

This paper concentrates on issues related to the area of [5], but demonstrates another field for application of these ideas, i.e., research technique using control system modeling and simulation on the basis of equations of motion for the center of mass of small trirotor TUAV for fast SA.

In this paper our research results in the study of vertical flight (take-off and hovering cases) control of small trirotor TUAV which make such SA task scenario as "go-search-find-return" possible are presented.

The contribution of the paper is twofold: to develop new schemes appropriate for SA enhancement using TUAVs by hybrid control of vertical flight of small trirotor TUAVs in real-time search-and-rescue operations, and to present the results of hovering maneuvers for chosen model of a trirotor TUAV for fast SA in simulation form using the MATLAB/Simulink environment.

II. TRIROTOR TUAV MODEL

The trirotor TUAV is composed of three rotors. It is clear that one of the advantages of trirotors with respect to quadrotors is that they require one motor less which can lead to a reduction in weight, volume and energy consumption. The two main rotors in the forward part of the trirotor rotate in opposite directions and are fixed to the aircraft frame. The tail rotor can be tilted using a servomechanism.

The dynamics of the trirotor TUAV for the case of low speeds of motion can be represented by the following equations [6]-[7]

$$\ddot{x} = -\tau_4 \frac{\sin \theta}{m} \quad (1)$$

$$\ddot{y} = \tau_4 \frac{\cos \theta \sin \phi}{m} \quad (2)$$

$$\ddot{z} = \tau_4 \frac{\cos \theta \cos \phi}{m} - g \quad (3)$$

$$JW\ddot{\eta} + J\dot{W}\dot{\eta} + W\dot{\eta} \times JW\dot{\eta} = \tau \quad (4)$$

where

$$\eta = (\psi \quad \theta \quad \phi)^T, \quad (5)$$

$$W = \begin{bmatrix} 0 & -\sin \psi & \cos \psi \cos \theta \\ 0 & \cos \psi & \sin \psi \cos \theta \\ 1 & 0 & -\sin \theta \end{bmatrix}, \quad (6)$$

$$\dot{W} = \begin{bmatrix} 0 & -\cos \psi & -\cos \psi \sin \theta - \cos \theta \sin \psi \\ 0 & -\sin \psi & -\sin \psi \sin \theta + \cos \theta \cos \psi \\ 0 & 0 & -\cos \theta \end{bmatrix}, \quad (7)$$

$$\tau = (\tau_1 \quad \tau_2 \quad \tau_3)^T, \quad (8)$$

$$\tau_1 = l_2(f_1 - f_2), \quad (9)$$

$$\tau_2 = -l_1(f_1 + f_2) + l_3 f_3 \cos \alpha, \quad (10)$$

$$\tau_3 = -l_3 f_3 \sin \alpha, \quad (11)$$

$$\tau_4 = f_1 + f_2 + f_3 \cos \alpha, \quad (12)$$

x, y, z are coordinates of center of mass in the earth-frame;

ψ, θ, ϕ are yaw, pitch and roll angles;

α is the tilting angle of third rotor;

$f_i (i = 1, 2, 3)$ is the thrust generated by the i -th rotor;

l_1 is the distance from the centre of mass to the centre of line between the first and second rotors;

$2l_2$ is the distance between the first and second rotors;

l_3 is the distance from the centre of mass to the third rotor;

J is the inertia matrix;

g is the gravity constant;

m is the mass of the TUAV.

The inputs in (9)-(11) then can be represented in matrix form as

$$\begin{bmatrix} \tau_1 \\ \tau_2 \\ \tau_3 \end{bmatrix} = \begin{bmatrix} l_2 & -l_2 & 0 \\ -l_1 & -l_1 & l_3 \cos \alpha \\ 0 & 0 & -l_3 \sin \alpha \end{bmatrix} \begin{bmatrix} f_1 \\ f_2 \\ f_3 \end{bmatrix} \quad (13)$$

Then the individual forces in (13) will be

$$\begin{bmatrix} f_1 \\ f_2 \\ f_3 \end{bmatrix} = -\frac{1}{2} \begin{bmatrix} -\frac{1}{l_2} & \frac{1}{l_1} & \frac{ctg \alpha}{l_1} \\ \frac{1}{l_2} & \frac{1}{l_1} & \frac{ctg \alpha}{l_1} \\ 0 & 0 & \frac{l_1}{l_3 \sin \alpha} \end{bmatrix} \begin{bmatrix} \tau_1 \\ \tau_2 \\ \tau_3 \end{bmatrix} \quad (14)$$

Note that exists an orientation of body frame in which the inertia matrix in (4) simplifies to:

$$J = \text{diag}(I_x, I_y, I_z) \quad (15)$$

For simplicity we consider the matrix J in (15) as unit matrix, i.e.

$$J = \text{diag}(1, 1, 1), \quad (16)$$

where $I_x = I_y = I_z = 1 \text{kgm}^2$.

Substituting (16) into (4), we obtain

$$W\ddot{\eta} + \dot{W}\dot{\eta} + W\dot{\eta} \times W\dot{\eta} = \tau \quad (17)$$

If we apply the properties of vector product to (17), we obtain

$$W\ddot{\eta} + \dot{W}\dot{\eta} = \tau \quad (18)$$

From (18), we have

$$\ddot{j} = W^{-1}\tau - W^{-1}\dot{W}\dot{j} \tag{19}$$

where

$$W^{-1} = \frac{1}{\cos \theta} \begin{bmatrix} \cos \psi \sin \theta & \sin \psi \sin \theta & \cos \theta \\ -\sin \psi \cos \theta & \cos \psi \cos \theta & 0 \\ \cos \psi & \sin \psi & 0 \end{bmatrix}. \tag{20}$$

We can regroup the three dynamics in (5), (7), (8), (19) and (20) as:

$$\ddot{\psi} = \dot{\theta}g\theta + \dot{\phi}\sec\theta + \tau_1tg\theta\cos\psi + \tau_2tg\theta\sin\psi + \tau_3 \tag{21}$$

$$\ddot{\theta} = -\dot{\phi}\cos\theta - \tau_1\sin\psi + \tau_2\cos\psi \tag{22}$$

$$\ddot{\phi} = \dot{\theta}\sec\theta + \dot{\psi}g\theta + \tau_1\sec\theta\cos\psi + \tau_2\sec\theta\sin\psi \tag{23}$$

From (1)-(3), (12), and (21)-(23) we can see that the attitude vector $(x \ y \ z)^T$ for given model of UAV can be computed.

The numerical values for trirotor UAV's constant parameters of (1)-(4) for a case of small elevation above sea level are given by [6]:

$$m = 0.5kg, l_1 = 0.07m, l_2 = 0.24m, l_3 = 0.33m, g = 9.81m/s^2.$$

III. CONTROL SYSTEM

It is possible to consider the thrusts f_1 and f_2 in (9) as constant functions of time with one value. Hence, we have

$$f_1 = f_2 = const \tag{24}$$

Hence

$$\tau_1 = 0 \tag{25}$$

Combining (10), (12) and (24), we can write

$$\tau_2 = -2f_1(l_1 + l_3) + l_3\tau_4 \tag{26}$$

Then, from (11), (12) and (24), it follows that

$$\tau_3 = l_3tg\alpha(2f_1 - \tau_4) \tag{27}$$

It is possible to consider the tilting angle α in (10)-(12) as a constant angle. Here, we take

$$\alpha = const \tag{28}$$

With selection of (24)-(28), a complex control problem is now turned into a control problem with using only one

collective thrust τ_4 as control input for controlling the coordinate z of altitude with respect to reference input z^0 .

The control system configuration to regulate the input variable τ_4 is thus designed, to have the next structure (see Fig. 1)

$$\dot{\tau}_4 = K(t_1(z^0 - z) - t_2\dot{z} - \ddot{z}) \tag{29}$$

where t_1, t_2 are constants to be determined.

It is possible to consider the variable τ_4 as a "fast" function of time. Hence, assuming that $\dot{\tau}_4 \approx 0$, from (29), we find

$$\ddot{z} + t_2\dot{z} + t_1z = t_1z^0 \tag{30}$$

The following coefficients of (30) are obtained from [8], for overshooting with value of $\sigma \approx 5\%$

$$t_1 \approx \frac{9}{t_{d_z}^2}, t_2 \approx \frac{3\sqrt{2}}{t_{d_z}} \tag{31}$$

where t_{d_z} is desired transition time of coordinate z .

For a hovering flight, angles of roll, pitch, and yaw must be zeros. Therefore, it follows from (3) that

$$\ddot{z}(t) = b\tau_4(t) - g, \tag{32}$$

where

$$b \approx \frac{1}{m}. \tag{33}$$

Differentiating both sides of (32) with respect to time, we obtain

$$\ddot{\tau}_4(t) = b\dot{\tau}_4(t) \tag{34}$$

Combining (29) and (34), we have

$$\ddot{\tau}_4(t) = bK(i_3(t) - \ddot{z}(t)), \tag{35}$$

where

$$i_3(t) = t_1(z^0 - z(t)) - t_2\dot{z}(t). \tag{36}$$

Defining $\ddot{z}(t) = a(t)$ in (35), we obtain

$$\dot{a}(t) = bKi_3(t) - bKa(t) \tag{37}$$

The variable $a(t)$ in (37) can be described in a common way through next expression as indicated in [9]

$$a(t) = (a_0 + \int_0^t e^{-A(\tau)} bKi_3(\tau) d\tau) e^{A(t)}, \tag{38}$$

where

$$A(t) = -\int_0^t bKd\tau \tag{39}$$

Let us consider the behavior of the considered control system (see Fig. 1) for the time t of time interval $t \geq t_{dz}$ during the hovering.

Hence, assuming that $a_0 = 0$, $z^0 - z(t) \approx \Delta z^0$, $\Delta = 0.05$, $\dot{z}(t) \approx 0$, from (38)-(39), we find

$$a(t) = i_3(1 - e^{-bk t}) \tag{40}$$

where

$$i_3(t) \approx t_1 \Delta z^0 \approx const. \tag{41}$$

Assume now that for the desired transition time for control of acceleration $a(t)$ lies in the zone of overshooting with value of $\sigma \approx 5\%$, then, from (40)-(41), it follows that

$$t_{d_z} \approx -\frac{\ln(\Delta)}{bK} \tag{42}$$

Therefore, using (33) and (42), and the ratio of coordinate-to-acceleration transition times $N = \frac{t_{d_z}}{t_{d_z}}$ and that $\ln(\Delta) \approx -3$,

we obtain

$$K \approx \frac{3Nm}{t_{d_z}} \tag{43}$$

IV. SIMULATION RESULTS

Consider the control of trirotor TUAV model (1)-(3), (21)-(23) for the case of take-off and hovering maneuvers by hybrid constrained system of two control subsystems.

The goal of the following simulations is twofold. First, we verify that these control subsystems are able to control the take-off and hovering trajectories. Second, we observed the effect of enhancing SA because the variety of such trajectory parameters as desired transition times, ratios of coordinate-to-acceleration transition times and heights of hovering easily can be changed the possible take-off and hovering trajectories of trirotor TUAV.

Constant thrust forces of the first and second rotors, constant tilting angle of the third rotor, initial conditions, desired height positions, ratios of coordinate-to-acceleration transition times and desired transition times for control subsystems are chosen to be:

$$f_1 = f_2 = 2.4N, \alpha = 89 \text{ deg}, x(0) = y(0) = z(0) = 0m, \\ z_1^0 = 3m, z_2^0 = 8m, N_1 = 40, N_2 = 15, t_{d1} = 3s, t_{d2} = 12s.$$

Simulation results of the offered block scheme with two control subsystems (see Fig. 1) are shown in Figs. 3-6.

Fig. 2 shows the height trajectory of flight control.

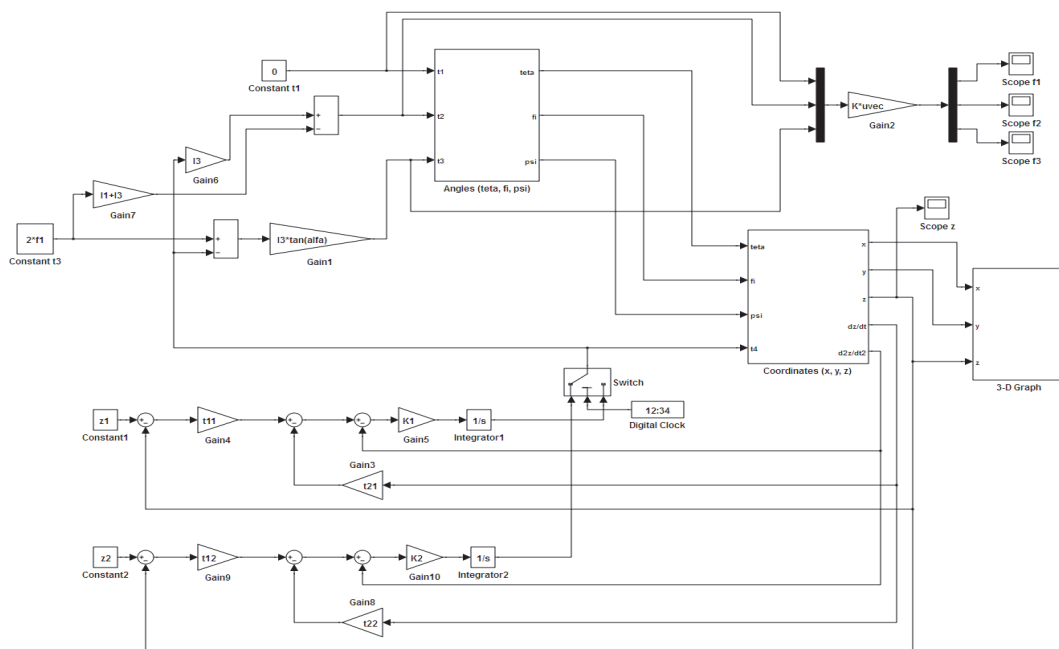


Fig. 1. Block diagram of hybrid control system.

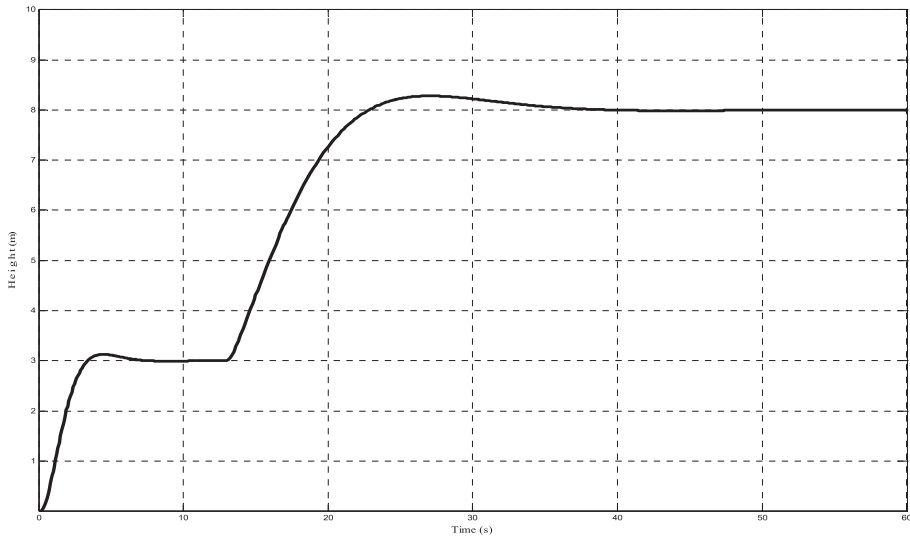


Fig. 2. Trirotor UAV's height trajectory.

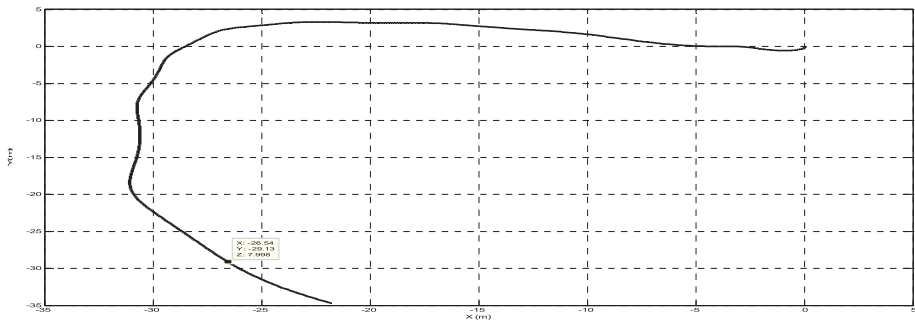


Fig. 3. X-Y view of trirotor UAV's trajectory.

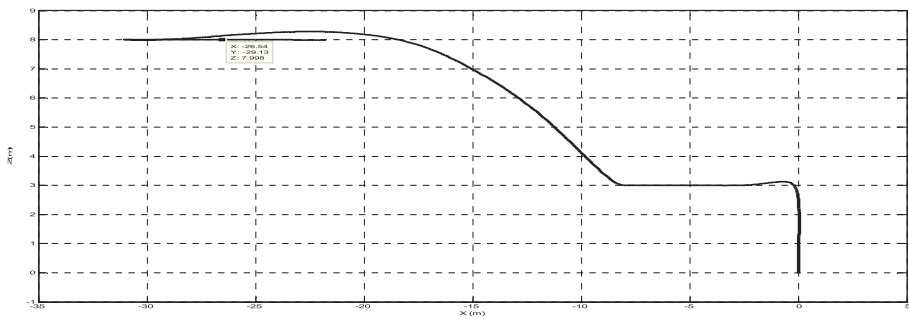


Fig. 4. X-Z view of trirotor TUAV's trajectory.

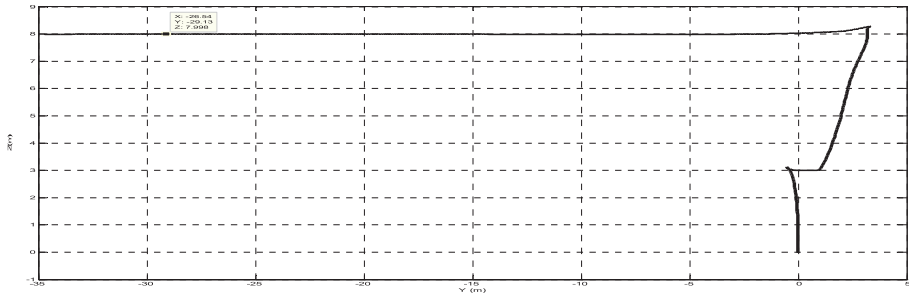


Fig. 5. Y-Z view of trirotor TUAV's trajectory.

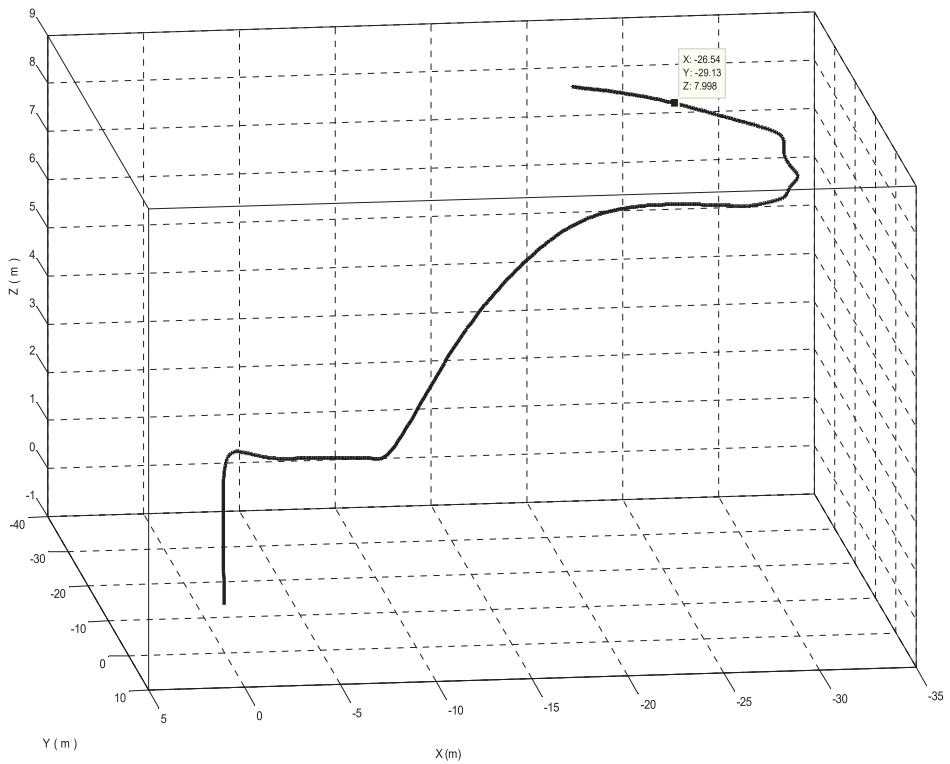


Fig. 6. 3-D motion of the trirotor TUAV.

We simulated the block diagrams of subsystems as parts of hybrid control system and take into account that the full take-off and hovering trajectories were separated into initial and final phases with boundary point in the first lag position. Some advantages of this example are as follows.

- Possibility to consider a terrain restriction in the places of hovering.
- Smooth trajectory of flight and possibility of lag in two different selected height positions.
- Using of two control subsystems to control the take-off and hovering trajectories of flight.

These results support the theoretical predictions well and demonstrate that this research technique would work in real-time flight conditions.

V. CONCLUSIONS

A new research technique is presented in this paper for enhanced SA in possible TUAV's missions.

The need for highly reliable and stable hovering for VTOL class TUAVs has increased morbidly for critical situations in real-time search-and-rescue operations for fast SA.

For fast, stable and smooth hovering maneuvers, we proposed a two stage flight strategy, which separates the flight process into initial and final phases. Two control schemes are designed for this flight strategy. The effectiveness of the proposed two stage flight strategy has been verified in field of flight simulation tests for chosen model of the trirotor TUAV using software package Simulink.

From the simulation studies of flight tests, the following can be observed:

- The block diagram of flight control is very useful for graphic representation of the flight trajectory.
- The received control subsystems are autonomous and completely shared in time.
- The trajectory tracking display forms give a researcher an immediate view of a trirotor TUAV motion with a range of such trajectory parameters as transition times, ratios of coordinate-to-acceleration transition times and heights of hovering. This allows us to investigate the sensitivity of the hybrid control system, providing a medium for such development and evaluation and enhancing the researcher's understanding of hovering maneuvers.

Although many of the details inevitably relate with this particular system, there is sufficient generality for this research technique to be applied to others models of TUAVs during hovering maneuvers.

From the applications viewpoint, we believe that this two stage flight strategy using flexible and effective hybrid control furnish a powerful approach for enhancing SA in applications to VTOL class TUAVs.

Future work will involve further validation of the performance of the proposed research technique and exploring other relevant and interesting TUAV's missions.

REFERENCES

- [1] M. R. Endsley, "Toward a theory of situation awareness in dynamic systems," *Human Factors*, vol. 37, pp. 32-64, March 1995.
- [2] J. Gorman, N. Cooke, and J. Winner, "Measuring team situation awareness in decentralized command and control environments," *Ergonomics*, vol. 49, pp. 1312-1325, October 2006.
- [3] Interim Brigade Combat Team Newsletter. [Online]. Available: http://www.globalsecurity.org/military/library/report/call/call_01-18_toc.htm
- [4] S.D. Prior, S.-T. Shen, A.S. White, S. Odedra, M. Karamanoglu, M.A. Erbil, and T. Foran, "Development of a novel platform for greater situational awareness in the urban military terrain," in *Proc. 8th International Conf. Engineering Psychology and Cognitive Ergonomics*, San Diego, USA, 2009, pp. 120-125.
- [5] I. Astrov and A. Pedai, "Control of hovering manoeuvres in unmanned helicopter for enhanced situational awareness," in *Proc. International Conf. Industrial Mechatronics and Automation*, Chengdu, China, 2009, pp. 143-146.
- [6] S. Salazar-Cruz, F.Kendoul, R. Lozano, and I. Fantoni, "Real-time control of a small-scale helicopter having three rotors," in *Proc. 2006 IEEE/RSJ International Conf. Intelligent Robots and Systems*, Beijing, China, 2006, pp. 2924-2929.
- [7] S. Salazar-Cruz, F.Kendoul, R. Lozano, and I. Fantoni, "Real-time stabilization of a small three-rotor aircraft," *IEEE Trans. Aerospace and Electronic Systems*, vol. 44, pp. 783-794, April 2008.
- [8] D. Krutko, *Inverse Problems of Control System Dynamics: Nonlinear Models*. Moscow: Nauka, 1989.
- [9] L.S. Pontryagin, *Ordinary Differential Equations*. Moscow: Nauka, 1974.

Curriculum vitae

Personal data

Name: Andrus Pedai
Date of birth: 09.03.1972
Place of birth: Tallinn, Estonia
Citizenship: Estonian

Contact data

E-mail: Andrus.Pedai@gmail.com

Education

2012–..... Tallinn University of Technology – PhD
2000–2002 MSC, Tallinn University of Technology
1992–1999 Diploma Engineer, Tallinn University of Technology
1979–1989 High school, Tallinn 37 Secondary School

Language competence

English Fluent
Estonian Fluent
Finnish Fluent
Russian Average
German Basic

Professional employment

2016–present Berry Global Inc. (www.berryglobal.com)
Berry Promens Vehicle Engineering
Sales and Business Development Manager
2009–2016 PKC Group (www.pkcgroup.com)
Global Account Manager for VOLVO Group
2005–2013 Tallinn University of Technology (www.ttu.ee)
Research Scientist
2007–2009 Enics AG (www.enics.com)
Key Account Manager for Schneider Electric and Telenor
2003–2007 Elcoteq SE (<https://en.wikipedia.org/wiki/Elcoteq>)
Senior Account Manager for Nokia Mobile Phones Europe
2001–2003 Elcoteq Tallinn AS
Product Line Manager for NOKIA Mobile Phones
2000–2001 Elcoteq Tallinn AS
Product Engineer for NOKIA Mobile Phones

R&D Related Managerial and Administrative Work

2012–present AFCEA Tallinn Chapter (www.afcea.org/site/)
The Armed Forces Communications and Electronics
Association

Scientific publications

55 scientific publications on above topics. Estonian Research IS (<https://www.etis.ee>)

Elulookirjeldus

Isikuandmed

Nimi: Andrus Pedai
Sünniaeg: 09.03.1972
Sünnikoht: Tallinn, Eesti
Kodakondsus: Eesti

Kontaktandmed

E-post: Andrus.Pedai@gmail.com

Hariduskäik

2012–..... Tallinna Tehnikaülikool – PhD
2000–2002 Tehnika Teaduste Magister, Tallinna Tehnikaülikool
1992–1999 Dipl. Insener, Tallinna Tehnikaülikool
1979–1999 Keskkool, Tallinna 37 Keskkool

Keelteoskus

Inglise keel kõrgtase
Eesti keel kõrgtase
Soome keel kõrgtase
Vene keel kesktase
Saksa keel algtase

Teenistuskäik

2016–... Berry Global Inc. (www.berryglobal.com)
Berry Promens Vehicle Engineering
Müügi- ja Äriarenduse Juht
2009–2016 PKC Group (www.pkcgroup.com)
Globaalne Müügijuht VOLVO Group
2005–2013 Tallinna Tehnikaülikool (www.ttu.ee)
Teadur
2007–2009 Enics AG (www.enics.com)
Võtmekliendihaldur Schneider Electric ja Telenor
2003–2007 Elcoteq SE (<https://en.wikipedia.org/wiki/Elcoteq>)
Võtmekliendihaldur Nokia Mobile Phones Europe
2001–2003 Elcoteq Tallinn AS
Tooteliini Juht NOKIA Mobiiltelefonid
2000–2001 Elcoteq Tallinn AS
Tooteinsener NOKIA Mobiiltelefonid

Teadusorganisatsiooniline ja -administratiivne tegevus

2012–... AFCEA Tallinn Chapter (www.afcea.org/site/)
The Armed Forces Communications and Electronics
Association

Teaduspublikatsioonid

55 publikatsiooni. Eesti Teadusinfosüsteem (<https://www.etis.ee>)

ISSN 2585-6901 (PDF)
ISBN 978-9949-83-642-0 (PDF)